Vanessa Fernandes Gomes Correia

Mestre em Biotecnologia

Oxazoline-based Antimicrobial Platforms for Water Treatment

Dissertação para obtenção do Grau de Doutor em

Química Sustentável

Orientador: Doutora Ana Isabel Aguiar-Ricardo

Professora Catedrática da FCT-UNL

FACULDADE DE CIÊNCIAS E TECNOLOGIA
UNIVERSIDADE NOVA DE LISBOA

Dezembro 2015

Oxazoline-based Antimicrobial Platforms for Water Treatment

Vanessa Fernandes Gomes Correia

Faculdade de Ciências e Tecnologia

Universidade Nova de Lisboa

Acknowledgments

The success of this work is also due to the people that were around me and gave me all the support, help and bright advices that I needed at the right time.

First of all, I would like to thank to my supervisor, Prof. Ana Aguiar Ricardo, who introduced me to the supercritical technology and alternative solvents and that later gave me the opportunity of working in the Polymer Synthesis and Processing Laboratory. Thank you for providing me such an interesting and multidisciplinary work and for all the precious orientations and advices throughout the last years! I will certainly miss the 5 a.m. emails in my mailbox!

I also want to acknowledge Drª Mariana Gomes de Pinho for receiving me in the Bacterial Cell Biology lab at ITQB, for all the scientific suggestions and for helping me in a completely new research area. Without your precious orientations, this work wouldn't have surely followed this path.

To Drª Teresa Casimiro, for the always bright advices in the supercritical part of the work and for the positive, enthusiastic and crucial supervision that helped us to move forward to submit a patent.

To Drª Guilhermina Fragoso also my acknowledgments for receiving me at Instituto Superior de Ciências da Saúde Egas Moniz and for all the help. To Dr. Vasco Bonifácio, thank you for the help in the beginning of my work in the lab.

To Prof. Susana Barreiros, I would like to thank the opportunity to be in this Master and in FCT. Without your precious help I wouldn't be here today. Also, a special thank for Professor Manuel Nunes da Ponte for teaching me all about green chemistry and for the opportunity to be present in the long life learning course in Budapeste.

Now, I would like to thank the Polymer Synthesis and Processing Group (FCT,UNL) and to Bacterial Cell Biology Group (ITQB,UNL).

To FCT's 510 lab team, thank you! To Mara (for the support, funny moments and pranks), Telma (for all the hilarious moments and time together), Eunice (for all the support and for the partnership at "fittings.ltd"), Rita (for your presence throughout all these years), Patrícia (thank you for the friendship, confidence and support), Anita (thank you for the friendship. I really enjoyed working together with you, we made a great team), Sofia (for all the joy and laughs), Gosia (I will miss our bus meetings, I will not miss your energy because I will still get it outside FCT!), Vanessa Almeida (thank you for all the help in the lab, you also made part of this story! My finger is still scared of you Vanessa-San!) and Márcia Tavares (thank you for the good

moments, I surely miss our lunch break together twin). To all, thank you for the companionship, sushi nights and good moments!

To ITQB's lab team: a special thank to Ana Jorge and Pedro Matos. Both had a relevant role in the initial part of my microbiology work, always answering to my questions! Also, I would like to acknowledge João Monteiro (for the help in the chapter 6), Pedro Fernandes (for clarifying my doubts all the time and for the funny moments with millions of pranks), Teresa (for the good moments and help), Gonçalo and Raquel for all the help.

I would like to thank to Dr. Vivek Raje for the synthesis of bisoxazoline monomer, to Dr. João C. Lima for the advices in photoluminescence assays. I would like to aknowlegde also professor Dr. Ana Maria Rego and Dr. Ana Ferraria for all the XPS discussions. A special thanks to Maria José, Idalina and Conceição for your sympathy and kindness. I want also to acknowledge the Analytical Services Laboratory of REQUIMTE, LabRMN at FCT/UNL and Rede Nacional de RMN, CENIMAT and CICS-UBI for the access to the facilities and the help in the products characterization. Also, I would like to acknowledge the financial support from Fundação para a Ciência e Tecnologia (FCT-Lisbon) through doctoral grant SFRH/BD/74730/2010.

Finally, I also would like to thank the people I carry in my heart, friends and family! To my parents Manuel and Paula, my sisters Nadine and Nádia, my brothers Manuel and Pedro, I would like to express my gratitude and love for all the support. And, of course, thank you Pedro for all the support and love!

In memory of my grandparents

Manuel António and Ilda Maria,

Guilhermino Joaquim and Maria de Lurdes.

Resumo

O desenvolvimento de novos materiais sustentáveis capazes de matar por contacto os microorganismos presentes em águas, sem comprometer a qualidade das mesmas e a saúde do consumidor, é uma necessidade urgente.

Uma biblioteca de oligómeros derivados de 2-oxazolina (OOXs) foi sintetizada utilizando dióxido de carbono supercrítico ($scCO_2$) e funcionalizada com diferentes aminas ou grupo hidroxilo, como controlo. Os oligómeros com menor valor de concentração mínima inibitória (MIC) apresentaram baixa citotoxicidade, taxas de morte rápidas e actividade de largo espectro.

A síntese em $scCO_2$ permitiu a inserção de unidades de ácido carbâmico na extremidade da cadeia conferindo assim propriedades de fluorescência aos oligómeros. As OOXs terminadas com *N*,*N*-dimetildodecilamina marcaram com sucesso *S. aureus*. Deste modo, OOXs antimicrobianas, quando em concentrações sub-inibitórias, podem ser usadas como marcadores fluorescentes azuis para ensaios de imagiologia.

Os oligómeros mais promissores foram incorporados numa rede polimérica 3D composta por quitosano (CHT) produzida por liofilização. OOXs antimicrobianas foram fisicamente misturadas em diferentes proporções com CHT. O monólito enriquecido com oligo(2-bisoxazolina) antimicrobiana (20 % w/w, CB8020) diminuiu 70 % a adsorção de BSA, sendo que 1 mg de CB8020 foi capaz de matar por contacto *E. coli*. Para alargar a actividade antimicrobiana contra a bactéria Gram-positiva *S. aureus*, imobilizaram-se OOXs na superfície de CHT utilizando uma tecnologia de plasma combinada com $scCO_2$. Produziram-se, pela primeira vez, superfícies bioactivas contendo OOXs antimicrobianas. CHT-OMetOx-DDA matou > 99.999 % de *S. aureus* e *E. coli* após 3 minutos de contacto. Finalmente, CHT-OMetOx-DDA demonstrou ser adequado para purificação de água, tendo sido testado utilizando diferentes amostras de água, sem ocorrer lixiviação e podendo ser reutilizado durante 10 ciclos.

Além disso, foi proposto um novo método para distinguir entre os dois mecanismos de acção de superfícies bioactivas: por contacto ou sistemas de libertação.

Finalmente, foram investigados os mecanismos de acção das oligo(2-oxazolina)s antimicrobianas em células bacterianas.

Palavras-chave: oxazolina, tratamento de água, antimicrobiana, dióxido de carbono supercrítico, superfície bioactiva, tecnologia de plasma.

Abstract

The development of new, green and sustainable platforms able to kill microorganisms present in water, without compromising water quality and consumer's health, is an urgent demand.

A library of 2-oxazoline-based oligomers (OOXs) was synthesized in supercritical carbon dioxide ($scCO_2$) and end-chain terminated with different amines or hydroxyl group as a control. The oligomers with the lowest minimum inhibitory concentration (MIC) values have shown low cytotoxicity, fast killing rates and broad-spectrum antimicrobial activity.

Oligomers synthesized in $scCO_2$ were enriched with satellite carbamic acid starting-end which confers light-emission properties to the oligomers. By end-capping OOXs with *N,N*-dimethyldodecylamine, successful labelling of *S. aureus* cells was attained. Therefore, the use of antimicrobial OOXs, in sub-inhibitory concentrations, is promising as blue fluorescent markers for imaging assays.

The promising oligomers were incorporated into a 3D polymeric network composed by chitosan (CHT) and produced by liophilization. Firstly, antimicrobial OOXs were physically blended in different ratios with CHT, where antimicrobial oligo(2-bisoxazoline)-enriched scaffolds (20 % w/w, CB8020) shut down 70 % of BSA adsorption and 1 mg of CB8020 was able to kill *E. coli* cells upon contact. Secondly, and to broaden scaffolds activity also against Gram-positive bacterium *S. aureus*, OOXs were grafted to the surface of CHT scaffolds using a solvent-free plasma technology in combination with $scCO_2$. Bioactive surfaces containing antimicrobial OOXs were produced for the first time. CHT-OMetOx-DDA killed > 99.999 % of *S. aureus* and *E. coli* cells within 3 minutes upon contact. Moreover, this scaffold was demonstrated to be suitable for water purification using different water samples without leaching to the water and to be reusable for 10 cycles. Additionally, it was proposed a new method to distinguish between the two mechanisms of action of bioactive surfaces: contact-active or releasing systems.
Finally, the mechanisms of action of antimicrobial oligo(2-oxazoline)s in bacterial cells was investigated.

Keywords: oxazoline, water treatment, antimicrobial, supercritical carbon dioxide, surface active, plasma technology.

Table of contents

Index of figures

Index of tables

Index of schemes

Acronyms and abbreviations

ATR-FTIR	Attenuated Total Reflectance Fourier Transform Infrared Spectroscopy
$BF_3.OEt_2$	Boron trifluoride diethyl etherate
BisOx	2-bisoxazoline
BSA	Bovine serum albumin
CB8020	80 % of CHT physically blended with 20 % of oligo(2-bisoxazoline) quaternized with *N*,*N*-dimethyldodecylamine
CB9010	90 % of CHT physically blended with 10 % of oligo(2-bisoxazoline) quaternized with *N*,*N*-dimethyldodecylamine
CE8020	80 % of CHT physically blended with 20 % of linear oligoethylenimine hydrochloride
CE9010	90 % of CHT physically blended with 10 % of linear oligoethylenimine hydrochloride
CF	Carboxyfluorescein
CFU	Colony forming units
CHT	Chitosan
CHT-OBisOx-DDA	CHT scaffold grafted with oligo(2-bisoxazoline) quaternized with *N*,*N*-dimethyldodecylamine
CHT-OEtOx-DDA	CHT scaffold grafted with oligo(2-ethyl-2-oxazoline) quaternized with *N*,*N*-dimethyldodecylamine
CHT-OMetOx-DDA	CHT scaffold grafted with oligo(2-methyl-2-oxazoline) quaternized with *N*,*N*-dimethyldodecylamine
CL	Cardiolipin
CM8020	80 % of CHT physically blended with 20 % of oligo(2-methyl-2-oxazoline) quaternized with *N*,*N*-dimethyldodecylamine
CM9010	90 % of CHT physically blended with 10 % of oligo(2-methyl-2-oxazoline) quaternized with *N*,*N*-dimethyldodecylamine
CO_2	Carbon dioxide
CROP	Cationic ring opening polymerization
DABCO	1,4-diazabicyclo[2.2.2]octane
DDA	*N*,*N*-dimethyldodecylamine
EtOx	2-ethyl-2-oxazoline

FBS	Fetal bovine serum
FTIR	Fourier transform infrared spectroscopy
GPC	Gel permeation chromatography
HPSCC	High pressure sapphire cylindrical cell
IsoOx	2-isopropenyl-2-oxazoline
LPEI	Linear oligoethylenimine hydrochloride
LPG	Lysylphosphatidylglycerol
LPS	Lipopolysaccharide
LUVs	Large unillamelar vesicles
MALDI-TOF	Matrix-assisted laser desorption/ionization with time-of-flight mass spectrometer
MBA	*N,N'*-methylenebisacrylamide
MeOTs	Methyl p-toluenesulfonate
MeOx	2-methyl-2-oxazoline
MHB	Mueller Hinton Broth medium
MIC	Minimum Inhibitory Concentration
MTT	3-(4.5-dimethylthiazol-2-yl)-2,5-diphenyltetrazolium bromide
M_w	Molecular weight
NMR	Nuclear Magnetic Resonance
OBisOx	Oligo(2-bisoxazoline)
OBisOx-DDA	Oligo(2-bisoxazoline) quaternized with *N*,*N*-dimethyldodecylamine
OD	Optical Density
OEtOx	Oligo(2-ethyl-2-oxazoline)
OEtOx-DDA	Oligo(2-ethyl-2-oxazoline) quaternized with *N*,*N*-dimethyldodecylamine
OMetOx	Oligo(2-methyl-2-oxazoline)
OMetOx-DDA	Oligo(2-methyl-2-oxazoline) quaternized with *N*,*N*-dimethyldodecylamine
OOXs	Oligo(2-oxazoline)s
OOXs-DDA	Quaternary-ammonium terminated OOXs
OPhOx-DDA	Oligo(2-phenyl-2-oxazoline) quaternized with *N*,*N*-dimethyldodecylamine
PBS	Phosphate Buffered Saline

Pc	Critical pressure
PEG	Poly(ethylene glycol)
PEtOx	Poly(2-ethyl-2-oxazoline)
PG	Phosphatidylglycerol
PhOx	2-phenyl-2-oxazoline
PI	Propidium iodide
PMeOx	Poly(2-methyl-2-oxazoline)
POXs	Polyoxazolines
POXs-DDA	Quaternary-ammonium terminated POXs
PSA or $(NH_4)_2S_2O_8$	Ammonium persulfate
RPMI-1640	Roswell Park Memorial Institute medium
$scCO_2$	Supercritical carbon dioxide
SCF	Supercritical fluids
SEM	Scanning Electron Microscopy
SR-SIM	Super - resolution structured illumination microscopy
Tc	Critical temperature
TEMED	*N*,*N*,*N*,*N*-tetramethylethlenediamine
UV	Ultraviolet-Visible Spectroscopy
Van-FL	BODIPY FL conjugate of vancomycin
XPS	X-Ray Photoelectron Spectroscopy

Chapter 1. Introduction

This chapter contains part of a manuscript published in

2015, Philosophical Transations A, 373
A Aguiar-Ricardo, VDB Bonifácio, T Casimiro, VG Correia
Supercritical carbon dioxide design strategies: from drug carriers to soft killers.

Personal contribution
VGC wrote the full chapter and included part of the manuscript that was written by herself.

1.1. Motivation

Water is essential to the survival of all organisms. It composes around 70 % of human body mass and has an important role in several metabolic processes. The adequate access to potable water with acceptable levels of toxins or suspended solids as well as with the total absence of pathogen bacteria is still a pressing problem around the globe. Contamination by microorganisms is of great concern in water purification systems specially when considering drinking usage and food preparation in order to avoid the widespread of waterborne diseases.[1] Therefore, it is essential to become conscious that drinking water treatment has now become an important issue and alternative technologies need to be developed.

The need to search for new materials and devices for water purification to overcome waterborne diseases, a foremost public health problem, is fully justified and represents a challenging research area. Therefore, this PhD project main goal is to develop and design new antimicrobial solutions able to improve human health by taking advantage of the unique properties of supercritical carbon dioxide as a processing solvent in the synthesis of these materials and of plasma technique as a process to modify surfaces homogeneously. The use of green technologies in this work will, undoubtedly, lead to a more environmental-friendly process.

1.2. Water Treatment

Water is commonly polluted with both chemical and biological contaminants (such as solids and certain bacterial species). The contaminants can be completely removed by a sequence of steps: coagulation–flocculation, filtration and disinfection.[2] In recent years, treatment of drinking water has become increasingly difficult due to limitations of ordinary water treatment processes – particularly, pathogen removal efficiency is affected by water conditions (such as turbidity, pH and temperature) or changes in water quality (pathogen type or concentration) and can often lead to the presence of disinfection resistant pathogens which could represent a pressing health hazard.[3]

In water treatment processes, the use of chlorine or water-soluble disinfectants is extremely common.[4] However, these approaches often lead to residual accumulation of toxic agents that will become concentrated in the environment (potentially carcinogenic disinfection by-products have been identified and associated with the chlorination of drinking water[5]) and later bring serious environmental consequences. To overcome this problem, the use of insoluble disinfectants can be

a suitable option that will not release any reactive agents to the bulk phase to be disinfected. Polymeric disinfectants are ideal for this application due to the versatility of their synthetic routes and ability to be easily produced in insoluble form.[4]

Other conventional water treatment systems, like advanced membrane filtration techniques (e.g. microfiltration, ultrafiltration, nanofiltration and reverse osmosis)[2] exhibit superior performance in treatment and removal of contaminants, although their use is still limited due to high operational requirements and costs.[6] Drinking water with highest quality standards can be, in fact, produced by advanced membrane filtration but for applications such as water treatment in distribution systems it is not guaranteed that the same potability standard is maintained before it reaches the consumer and the quality of treated water becomes highly questionable. Furthermore, the efficient removal of pathogenic bacteria is affected by water fouling potential and membrane integrity that could result in the leakage of pathogens in permeate water suggesting that membrane techniques still need to be improved.[3,7–9]

1.3. Water Treatment: Conventional and Alternative Processes

Reports comprising membrane techniques for water treatment significantly increased for the last decade.[10] The possibility to have biodegradable antimicrobial (AM) membranes is economically appealing when considering disposable elements for water purification. Porous membranes are often prepared by the wet phase inversion method, process that involves the use of organic solvents.[11] These solvents need afterwards to be removed from the membrane through an expensive process of purification in order to assure that it meets the required standards for the envisaged application.

More recently, supercritical carbon dioxide ($scCO_2$) has been investigated to induce phase separation of the polymer solution and has been successfully utilised in the production of membranes composed of different synthetic and natural polymers.[12,13] The use of $scCO_2$ has numerous advantages in membrane processing: it is not toxic, is cheap, can dry the polymeric membrane rapidly and totally, improves mass transfer and reduces solvent recovery costs and membrane morphology can be controlled by manipulating the pressure, temperature and depressurization rate.[14]

Alternatively, polymeric 3D structures with high porosity (the so-called scaffolds) can also represent a good alternative to the use of membranes as they have high permeability values and less fouling-associated problems. Scaffolds can be produced by lyophilisation of a polymeric

casting solution, where the commonly used organic solvent can be replaced by a green solvent (such as water). Herein, the focus of the work will be in polymeric 3D structures produced by lyophilisation.

1.4. Supercritical Carbon Dioxide

Supercritical fluids (SCF) have been investigated continuously in the last years to exploit their interesting physical properties in several areas of application.

The definition of a supercritical fluid usually begins with a phase diagram, which defines the critical temperature and pressure of a substance. For a pure substance, the critical point marks the end of the vapour-liquid coexistence curve. Above that critical point (with defined temperature and pressure), neither liquid or gas phases exist; instead, a poorly defined phase, known as a supercritical region, occurs. Then, a homogeneous and opalescent system without a phase separation takes place. Such fluids have the gas-like characteristic of compressibility, diffusivity and low viscosity, and the liquid-like characteristic of high density and solubilization power. Fascinatingly, the SCF characteristics can be tuned by simply changing the pressure or temperature, which is a great advantage in several processes.[15,16]

All pure substances become SCF above their respective critical points. However, the need to use high values of temperature and pressure to overpass the critical point can be an economical limitation in some processes. Therefore, the correct choice of what SCF should be used is of particular importance.

In particular, supercritical CO_2 ($scCO_2$) is the supercritical fluid more frequently used and is promoted as a green solvent with many advantages over conventional ones. $scCO_2$ is a non-flamable, non-toxic, chemically inert, readily accessible solvent and can be removed from a system by simple depressurization. In addition, its physical properties can be tuned by manipulation of the temperature and pressure.[17,18]

Supercritical carbon dioxide can be applied in different processes, such as the already mentioned phase inversion method for membrane production, but also as a solvent for polymerizations. $ScCO_2$ has been receiving increasing attention as a reaction medium in alternative to common and environmentally unattractive organic solvents. Although carbon dioxide is a greenhouse gas, it is an abundant material in the environment and can be extracted from the atmosphere, be used as an alternative solvent and later released again to the environment, completely clean from any chemicals used in the process. However, commercial CO_2 later on employed in a process is

usually not captured from the atmosphere, but in fact obtained as a byproduct of the commercial ammonia process. By this reason, this process can be considered as a process that prevents pollution once it avoids the emission of CO_2 to the atmosphere.[19]

1.4.1. Polymerization and polymer processing in $scCO_2$

Supercritical carbon dioxide and its distinctive properties allowed it to emerge as the most extensively studied supercritical fluid for polymerization reactions. $scCO_2$ have a great potential in polymer processing, providing some key advantages when compared to the conventional methods. Although there are significant costs associated with polymer processing under high pressures, the advantages of this type of polymerization add significant value to the final processed products.[15] As CO_2 is a gas at atmospheric conditions, the solvent can be simply separated from the reactional media. Additionally, polymerization reactions performed in $scCO_2$ have enhanced mass transfer rates due to high diffusivities and low viscosity of this SCF which significantly increase the yield and selectivity of a large range of chemical processes.[15]

Another advantage is the "solvent-free" nature of $scCO_2$ that makes it an ideal choice for the processing of pharmaceutical and biomedical materials, as these areas are under a strong control over product integrity and presence of harmful solvent residues. Moreover, and as industries are becoming increasingly more aware of environmental issues, research on $scCO_2$ field has intensified in the last years.[18]

Carbon dioxide is also a excelent solvent for most non-polar and some polar molecules of low molar mass but it is a poor solvent for most high molar mass polymers under mild conditions (<100 °C, <350 bar), being fluoropolymers and silicones the only polymers that show good solubility in supercritical CO_2.[20] This fact generally permits the precipitation of the polymer in high pressure reactor. Consequently, polymers can be isolated from the reaction media by simple depressurization (with removal of unreacted monomer and catalyst), resulting in a dry clean product.[20] This feature corresponds to a potential cost and energy saving in polymer manufacturing since it decreases the energy used and eliminates purification steps (drying and purification) required to remove the solvent.[20]

1.4.2. Classification of polymerization reactions

Polymerizations can be classified as chain growth and step-growth polymerizations. The main types of chain-growth polymerization include free-radical, cationic, anionic, and metal-catalyzed reactions. The majority of polymerizations in $scCO_2$ are focused on free-radical polymerizations, but there are a number of reports in the areas of cationic and metal-catalyzed reactions.[20,21]

In this work, it was used a chain growth polymerization through a cationic ring opening mechanism and, for that reason, this is the type in focus here.

Cationic polymerizations are a challenging area in polymer science.[22] *Living* cationic polymerization methods have been developed in order to produce polymers with a high control of molecular weight, molecular weight distribution, reactivity and end group functionalization by stabilization of the active carbocation through nucleophilic interactions. This stabilization is generally achieved by association of a nucleophilic counterion or with a Lewis base since it avoid side reactions.[23]

1.5. Oxazoline-Based Polymers

Among the alternative polymers for drug conjugation, oxazoline-based polymers are recognized as the most promising PEG substitutes, in particular, poly(2-methyl-2-oxazoline) (PMeOx) and poly(2-ethyl-2-oxazoline) (PEtOx) because of their demonstrated low toxicity, immunogenicity [56], biodegradability and water solubility. Their interesting characteristics, versatility and ability to form functional materials, turns this class of polymer interesting candidates for use in a large number of applications, such as smart materials, membrane structures, drug carriers, synthetic vectors for DNA or RNA delivery and antimicrobial agents.[24]

POXs are obtained through a cationic ring opening polymerization (CROP). The polymerization starts with a nucleophilic attack of the lone pair of the nitrogen of the 2-oxazoline ring onto an activated 2-oxazoline monomer (oxazolinium species formed by coordination of the 2-oxazoline monomer with the initiator). The nucleophilic attack of the second monomer unit onto the formed oxazolinium species leads to the ring opening by cleavage of the C–O bond. Due to the absence of chain-transfer or termination reactions under the appropriate conditions, the polymerization occurs in a *living* manner until all monomer is consumed or an end-capping agent is added.[25]

This challenging but also versatile type of polymerization allows the tuning of final polymer properties (such as hydrophilic, hydrophobic, fluorophilic) as it enables copolymerization with a variety of monomers and polymer chain end-capping. When the reaction is performed in $scCO_2$, oligo-oxazolines (OOXs) are obtained.[23] The schematic synthesis of OOXs and their structure are shown in Figure 1A. The structure of PEG is also shown for comparison (Figure 1B).

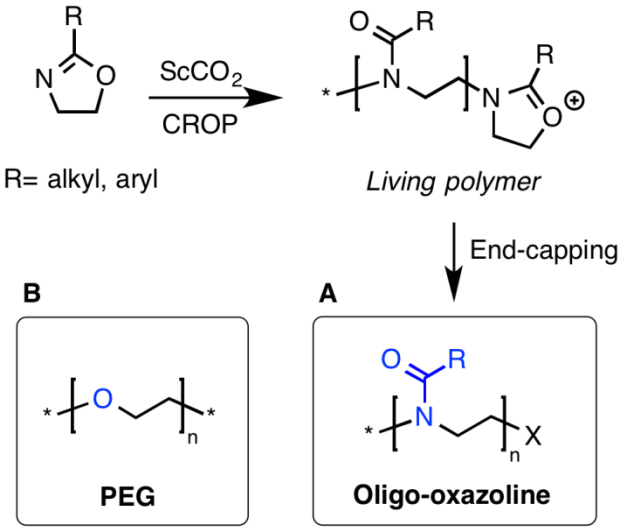

Figure 1.1 - Synthesis of oligo-oxazolines in supercritical carbon dioxide (A), and comparison of its molecular structure with poly(ethylene glycol) (PEG) (B).

However, 2-oxazoline-based polymers have not yet found widespread commercial application due, in part, to their polymerization times ranges (reactions times can vary from several hours to several days).[24] This disadvantage can be overcome with the use of supercritical fluid or microwave technologies. These alternative methods lead to less side reactions and maintain the *living* character of the reaction, using a higher temperature and pressure.

The synthesis of these polymers using conventional solvents,[26] microwave-assisted[27,28] or green $scCO_2$-assisted methodologies[23] has been previously described.

1.5.1. Conventional synthesis of 2-oxazoline-based polymers

Conventional polymerization of 2-substituted-2-oxazoline has been widely described in the literature. In a typical procedure, a solution containing 2-substituted-2-oxazoline in acetonitrile and the initiator methyl p-toluenesulfonate (MeOTs) is heated at 60 ºC with stirring. The polyoxazoline is obtained as white powder, after purification by precipitating again in diethyl ether and drying under vacuum.[26]

It is important to develop green alternatives to this process of synthesis mainly to reduce reaction time, avoid the use of organic solvents and purification steps.

1.5.2. Microwave-assisted synthesis of 2-oxazoline-based polymers

In the last decade, microwave irradiation has been developed to provide an effective alternative energy source for conventional reactions and processes, leading to an exponential increase of publications in this area.

Microwaves are electromagnetic radiation with frequencies between 300 GHz and 300 MHz (with a wavelength in the range of 1 mm to 1 m) and have been widely used in heating materials for industrial and domestic purposes.[28] Microwave irradiation, considered an environmentally-friend process, offers some advantages over conventional heating, such as instantaneous and rapid bulk heating, direct heating, high temperature homogeneity and energy saving. This technology can provide an improvement in reaction rate, yield and selectivity of a certain process and it is nowadays widely used in polymerizations and polymer processing. Microwave irradiation is then a fast and effective method for polymerization, being with no doubt an alternative methodology.[27]

This type of polymerization can be used to obtain polymers with a higher molecular weight, when compared to the supercritical technology, maintaining the *living* character of the reaction as well as the possibility of further functionalization.

1.5.3. Synthesis of 2-oxazoline-based polymers in $scCO_2$

The synthesis of 2-substituted-2-oxazolines in $scCO_2$ was already described in literature for three different monomers using boron trifluoride etherate ($BF_3.OEt_2$) as initiator. The effect of temperature, pressure and initial monomer/initiator molar ratio on the yield, average molecular weight and polydispersity of the synthesized polymers was also investigated. With this procedure it was obtained low molecular weight polymers in high yield (over 80 %) with narrow molecular weight distribution. 2-Methyl- and 2-ethyl-2-oxazolines oligomers were found to be water soluble while poly(2-phenyl-2-oxazoline) is only soluble in organic solvents.[23] This synthetic method was the one used throughout this project.

1.5.4. Comparison between classic and alternative methods for the synthesis of 2-oxazoline-based polymers

The different synthetic methods used to synthesize oligo(2-oxazoline) are compared in Table 1.1.

Table 1.1 - Synthesis of oxazoline-based polymers: classic methods *versus* supercritical CO_2

Method	Advantages	Disadvantages	Ref.
Conventional	Easy to reproduce.	Use of organic solvents. Several purification steps. High molecular weight polymers.	26
Microwaves	Fast reactions (minutes). High purity and yield.	Use of organic solvents. Several purification steps. High energy consumption (temperature range: 80 to 200 ºC)	27
Supercritical CO_2	Low molecular weight polymers. Low polydispersity. High purity and yield with less purification steps. Solvent recycling. Intrinsic blue fluorescence.	Expensive equipment. High pressure and associated hazards.	22,23,29

From Table 1.1 we can easily conclude that the supercritical CO_2 route is not only a viable alternative, but brings also additional advantages to the polymerization process. A particular feature observed for OOXs synthesized in $scCO_2$ is their intrinsic blue fluorescence, which is achieved by a carbamic acid insertion at the oligomer starting end during polymerization (Figure 1.2 - Blue emission of a carbamic acid oligo(2-methyl-2-oxazoline) synthesized by a cationic ring-opening polymerization in supercritical carbon dioxide.Figure 1.2 and chapter 2). This is contrary to the common assumption that CO_2 was inert in this type of polymerization.[29]

No matter which route is followed reported results demonstrate that OOXs and POXs can be prepared with different architectures and end-capped with selected functional groups for adequate functionalization.[30]

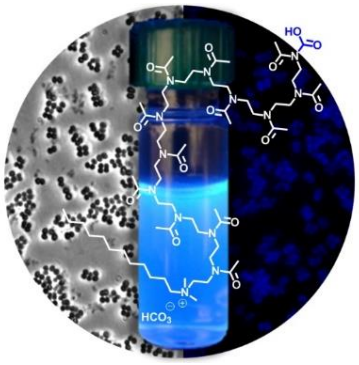

Figure 1.2 - Blue emission of a carbamic acid oligo(2-methyl-2-oxazoline) synthesized by a cationic ring-opening polymerization in supercritical carbon dioxide.[29]

1.6. Functionalized Polymers as Novel Antimicrobial Strategies

Microbial infections in humans and materials represent a critical health problem and economical challenge in modern society, aggravated by the appearance of new antibiotic resistant bacterial strains. Several approaches have been pointed out in the last years to control and ideally eradicate this problem, namely trough chemical disinfection or through the use of materials with antimicrobial properties.[31] The most common solution, chemical disinfection, is usually accomplished by the use of disinfectants that ultimately lead to environmental pollution and could also trigger the development of bacterial resistant strains. Antimicrobial polymers have been considered a new class of disinfectants, which have been recognised even as alternative antibiotics. The first polymer disinfectant that became commercially available was poly(hexamethylene biguanidinium hydrochloride), thoroughly investigated by Ikeda *et al*..[32]

Antimicrobial polymers widen up a whole new range of therapeutic solutions enabling the tuning of different properties by combining different polymer backbones and functionalities.[4] Interestingly, antimicrobial polymers can be used to modify surfaces, without losing their biological activity, which enables the design of surfaces that kill microbes without releasing biocides, solving numerous contaminations mainly in health care facilities.[31,33] In 1965, Cornell and Dunraruma reported, for the first time, antimicrobial polymers and copolymers based on 2-methacryloxytroponones.[34] Since then, different polymeric structures with antimicrobial properties have been reported in literature and the number of publications in this topic per year is growing fast. Just in the last decade, according to Web of Science, the number of publications has tripled.

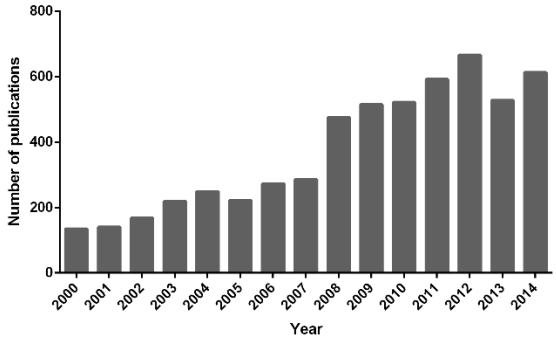

Figure 1.3- Number of publications per year (2000-2014) related to topic "antimicrobial polymer" (WEB Knowledge Thomson Reuters®).

Several studies have been reported towards the development of an ideal antimicrobial polymer. For that, some basic requirements should be taken in consideration: i) easy and inexpensive synthesis; ii) stability during usage and storage at the conditions of its intended application, do not lead to emission or generation of toxic products upon degradation; iii) biocompatibility; iv) easy recovery of activity, if lost; v) active against a broad spectrum of pathogenic microorganisms in brief times of contact.

Known antimicrobial polymers are commonly classified in three distinct groups depending on the mechanism of action of each one (Figure 4).[31]

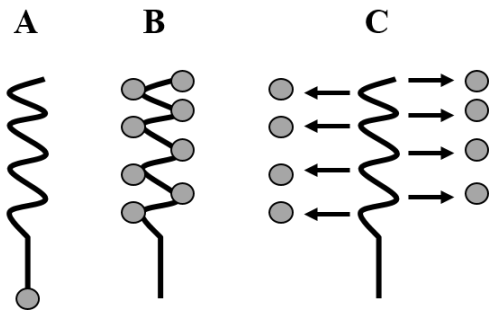

Figure 1.4 - Types of antimicrobial polymers: (A) biocidal polymers – the antimicrobial molecule is attached to the polymer; (B) polymeric biocides – the repeating unit in polymer backbone is a biocide; (C) biocide-releasing polymers – polymer act as a carrier that release the antimicrobial molecules.

Polymeric biocides are expected to be less active than their corresponding analogues to steric hindrance while biocide-releasing polymers could trigger the development of bacterial resistance and/or contamination of the surroundings. In contrast, biocidal polymers represent a good solution for the achievement of the basic requirements for an ideal antimicrobial polymer.[31] Interestingly, as bacterial cells carry a negative surface charge (due to the presence of membrane proteins, teichoic acids in Gram-positive bacteria and negatively charged phospholipids at the outer membrane in Gram-negative bacteria), positively charged polymers can be attracted to bacterial cell membrane and take their action.[35] For this reason, in the last decades, many efforts on the development of biocidal polymers relied on the use of antimicrobial polycations with quarternary ammonium and phosphonium. Table 3 highlights the common $scCO_2$-assisted methods used to synthesize antimicrobial agents and to confer antimicrobial properties to different materials.

Table 1.2 - Antimicrobial agent synthesis or processing using $scCO_2$-assisted methods.

Method	Active compound	Material	Application	Ref.
Impregnation	Cinnamaldehyde	Cassava starch biocomposite film	Food active packing	36
	Nanoparticulate silver metal	Silicone	Biomedical	37
	Silver ions	Polyamide	Industrial applications	38
	Silver ions	Reduced graphene powder	Industrial applications	39
	Thymol	Cotton gauze	Wound dressing	40
	Thymol	Linear low-density polyethylene	Food active packing	41
	Thymol	Cellulose acetate	Biomedical and food packing materials	42
	Thymol	Polypropylene and corona modified polypropylene non-woven material	Textiles, wound healing	43
Incorporation in solution	Enzyme	Cellulose acetate membranes	Food active packing	44
Adsorption	Quaternary ammonium salt silicone	Cellulose	Industrial applications	45
Synthesis and nano-encapsulation	Copper	Polystyrene particles	Variety of industrial applications	46
Synthesis	Sucrose and fructose fatty acid esters	-	Food additives	47
	Quaternary ammonium salt	2-alkyl-2-oxazoline oligomers	Variety of industrial applications	48

1.7. Biocidal Oxazoline-Based Polymers

Polymeric quaternary ammonium salts can be prepared using different approaches that will result in distinct polymeric architectures, exhibiting diverse antimicrobial activities and potential applications.[49] Interestingly, polymers bearing ammonium salts are cationic and their mechanism of action is believed to depend on the fundamental characteristic of negatively charged microbial cell membrane. This aspect suggests that the development of strains resistant to this class of compounds is impaired, as it would require bacteria to change membrane structure.[50]

Oxazoline based polymers (POXs) are an attractive class of compounds due to their biocompatibility and synthetic versatility[51] and represent a unique approach to the development of new antibiotics. Recently, they have been explored as strong candidates for the development of new polymer therapeutics.[52–55] Waschinski *et al*. reported the synthesis of a series of oxazoline-based polymers, terminated with quaternary ammonium groups, prepared via standard CROP by conventional synthesis.[54] The antimicrobial polymers activity was evaluated by determining the minimal inhibitory concentration (MIC) against *Staphylococcus aureus*. Only poly(2-oxazoline)-based polymers containing alkyl ammonium functions with alkyl chains of 12 carbon atoms or longer were found to be active. Correia *et al*. demonstrated that the synthesis of antimicrobial 2-substituted-2-oxazolines polymers can be successfully performed in $scCO_2$ in a more sustainable way. Several OOXs were synthesized by *living* CROP and later end-capped with a tertiary amine to produce quaternary-ammonium-terminated materials (OOXs-DDA). The synthesis and quaternization of branched oligo(2-bisoxazoline) was reported for the first time as well as its antimicrobial activity and cytotoxic effect, together with linear oligo(ethylenimine) hydrochloride quaternized, a polymer biocide, which was also synthesized by hydrolysis of a oligo(2-oxazoline).[48] Table 1.3 summarizes the reaction conditions used for the synthesis of POXs-DDA using either the conventional or the $scCO_2$ – assisted methods.

Table 1.3 – Methods for POXs-DDA synthesis.

	Reactional conditions	Type of POX	Ref.
Conventional synthesis	1. Inert atmosphere, monomer, initiator, chloroform, 70 °C, 48h 2. 10-fold excess of DDA, Na_2CO_3/H_2O, 70 °C, 24 h; 3. Re-precipitation with diethyl ether, dialysis, drying in vacuum.	PMeOx-DDA	53
	1. Inert atmosphere, monomer, initiator, chloroform, 0 ºC; 2. Reflux at 70 ºC, 48 h; 3. Monomer, 70 ºC, 48 h; 4. 10-fold excess of DDA, Na_2CO_3/H_2O, 70 °C, 24 h; 5. Re-precipitation with diethyl ether, dialysis, drying in vacuum.	X- PMeOx-DDA X-PEtOx-DDA X-PPhOX- PMeOx-DDA	54
$scCO_2$	1. monomer/$BF_3.Et_2O$/carbon dioxide, 60 ºC, 16-20MPa, 20 h; 2. 10-fold excess of DDA, 70 ºC, 24 h; 3. Purification by washing with fresh CO_2, extracting unreacted reagents. CO_2 is vented at the end.	OMeOx-DDA OEtOx-DDA OPhOx-DDA OBisOx-DDA	48

Comparing the syntheses (conventional versus $scCO_2$), it can be concluded that, following the supercritical route, a more sustainable protocol was achieved with a clear reduction of purification steps, solvents, and time (Table 1.4).

Table 1.4 - Comparison between POXs conventional and $scCO_2$ synthetic route from a green chemistry point of view.

Parameter	Conventional synthesis	$scCO_2$ synthesis	Green chemistry principles
Solvents involved	6	1	Safer solvents Less hazardous synthesis
Purification steps	3	0	Design for separation
Time consumption (h)	72-120	44	Time efficiency
Waste production	yes	no	Prevention

1.8. Bioactive POXylated Surfaces

Antimicrobial polymers can be effectively designed to improve the materials properties. The possibility to incorporate, combine or graft such versatile polymers (with tunable chemical and mechanical properties) into a surface broadens up the design of biocidal platforms. Antimicrobial surfaces can act by two ways: i) a biopassive surface coating or ii) an active bioactive-surface. The biopassive surface does not interact and kill bacteria but reduce the adsorption of proteins and, consequently, the adhesion of bacteria. This approach is mainly reported in literature trough the incorporation of hydrophilic polymers into surfaces, e.g. hydrogel coatings (mostly based on polyethylene glycol, PEG).[56] In contrast, bioactive surface coatings can kill bacteria on contact, either after the release of the biocide from the surface to the surroundings or after mere contact with the surface.[57]

Non-fouling poly(2-methyl-2-oxazoline) (PMOX)-based coatings have emerged as a promising alternative for the replacement of PEGs by more biocompatible analogues.[58] Essentially, PMOX-modified substrate is a biopassive approach to reduce biofouling and improve the ability to resist protein and bacterial adhesion (without killing) by enhancing materials hydrophilicity.

Importantly, bioactive materials that prevent biofouling should contain antimicrobial moieties attached onto polymeric backbones by covalent interactions to boost stability. Previous studies report the use of antimicrobial groups usually grafted to the polymer backbone or inserted in the main chain of polymers during synthesis by using monomers bearing antimicrobial moieties.[4] Many studies also show that biocidal end-capping is an effective strategy.[59,60] However, the

number of chemical steps and the use of organic solvents are not attractive from a sustainable point of view. Table 1.5 highlight the main methods used until now to immobilize POXs at a surface.

Table 1.5 - Methods for POXs surface immobilization.

Methods for POXs immobilization		Type of surface	Approach	Ref.
Grafting onto	Direct end-capping of the *living* polymer species	Silicon wafer, glass slide bearing silane coupling agents	Biopassive	61,62
	Quench the *living* oxazolinium species with an amine functionalized surface	APTES modified surfaces, inorganic fibers, ultrafine silica and carbon black, modified PAMAM with amine end groups	Biopassive	63–66
"Clicking" onto surface	Copper-catalyzed azide–alkyne cycloaddition	Azide modified surfaces	Biopassive	67
Grafting from	Initiator attached to the surface prior to the polymerization	Surfaces bearing OTos, OTf, ONs and bromine or iodine groups	Biopassive	68–72
	iPrEnOx attached to the surface prior to the polymerization, followed by CROP of another oxazoline	Surface bearing silane coupling agents	Biopassive	73
Photo-immobili-zation	Modifying the surface with a BP or PFPA derivatives	Silicon, silicon dioxide, glass or gold surfaces	Biopassive	74–79
Spontaneous self-assembly	Multiple electrostatic interactions between the negatively charged surface and the polycationic polymer	Nb_2O_5-coated silicon wafer	Biopassive	80
Blend	Cellulose-grafted-POX sprayed and air dried into surface	Glass slides	Bioactive upon release	59
	Physical blend with natural polymer	Chitosan scaffold	Bioactive upon contact	81

APTES: (3-aminopropyl)triethoxysilane; PAMAM: Poly(amido amine); OTos: tosylate; OTf: triflate; ONs: p-nitrobenzyl sulfonate; iPrEnOx: 2-isopropenyl-2-oxazoline; CROP: cationic ring opening polymerization; BP: benzophenone; PFPA: perfluorophenyl azide; PMMA: poly(methyl methacrylate); Nb2O5: Niobium pentoxide.

The immobilization of the antimicrobial polymers is a fundamental step in the overall process because it also requires the use of organic solvents in a common synthetic approach. In this PhD

project, bioactive surfaces will be designed by blending the antimicrobial polymers in the casting solution (physical immobilization, forming an entangled polymeric network, chapter 4)[81] or by covalently binding the antimicrobial polymers on the membrane surface by plasma technology (chapter 5). This last approach will defeat the use of organic solvents.[82] Plasma technology has been used in our group, with exciting preliminary results,[83] and will allow the activation of the 3D structure by introducing radicals on the 3D structure surface and the following immobilization of the antimicrobial polymer. The final structure is then obtained without any traces of organic contaminations and is ready-to-use.

Plasma technology will be applied to activate the 3D structures surface and that can be done with two different purposes: i) coating with polymers that act as spacers by injecting a monomer stream in the plasma chamber - followed by reaction with the biocidal agent; ii) activate the surface by creating specific radicals that will bind to predefined spacers (e.g. PEG).[82] Herein, we used plasma technology to create radicals and the activated 3D structures will then bind to the biocidal agents, synthesized in supercritical carbon dioxide.

The combination of supercritical fluid technology and plasma activation is a key innovation of this project.

1.9. Main Objectives and General Research Plan

This project seeks to develop a new, green and sustainable solution for drinking water treatment based on the use of biocidal polymeric 3D structures.

Herein, it is proposed the preparation of new, portable, polymeric, and low-cost biocidal 3D device using green technologies (supercritical carbon dioxide and plasma technology). This device will consist of a 3D biocidal structure with a morphology suitable for water permeation, which surface will bear synthesized antimicrobial oligomers trough surface functionalization. Produced and functionalized 3D porous structures in supercritical carbon dioxide will be designed to have minimal residual toxicity and prolonged lifetime, to have broad-spectrum antimicrobial activity, rapid bacteria killing rates (contact times of minutes), being also a strategy that avoids the development of bacteria drug resistance.

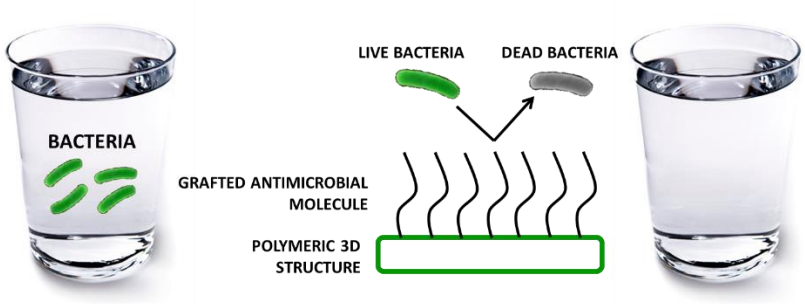

Figure 1.5 - Scheme of the project main idea: production and functionalization of 3D structures with antimicrobial activity for water bacterial purification.

The production of new and low-priced biocidal 3D structures with controlled morphology and structure will boost the use of sustainable technologies and alternative solvents in the area of water treatment. This project will culminate with the implementation of this technology to treat environmental water samples and provide drinking water with minimum production costs, separation capability, long-term use with minimum replacement costs and operational feasibility.

In order to pursue these general objectives, several studies were carried out to try to answer these specific research questions:

- Can oligo(2-oxazoline)s be functionalized successfully in $scCO_2$? Which are the best end-capping molecules to functionalize oxazoline-based oligomers in order to confer antimicrobial activity? Which is the impact of these end-capping molecules in the MIC value? How long do different oligomers take to kill *S. aureus* and *E. coli* cells? How cytotoxic are the most promising oligomers? (Chapter 2);

- What caused the unexpected blue emission of oligo(2-oxazoline)s? Can these oligomers label successfully *S. aureus* and be used as biotags? (Chapter 3);

- Can antimicrobial oligo(2-oxazoline)s be blended into a natural polymeric 3D network with success? What is the effect of the blending in the final 3D material properties? How different oligomers, while blended, influence the materials protein adsorption resistance and antimicrobial activity? (Chapter 4);

- Can antimicrobial oligo(2-oxazoline)s be grafted into a natural polymeric 3D network surface using green technologies with success? What is the effect of the grafting in the final 3D material properties? How different oligomers, while grafted, influence the materials protein adsorption resistance and antimicrobial activity? How will the material perform in the purification of environmental water samples? (Chapter 5);

- How do antimicrobial oligo(2-oxazoline)s kill the bacterial cells? Is the mechanism of action by carpeting or by the formation of pores? (Chapter 6).

Therefore, this PhD thesis is organized in seven chapters that try to elucidate each of the above mentioned specific research questions.

Chapter 1 highlights the motivation of this work and reviews the state of the art about oxazoline-based polymers synthethic methods and its incorporation into antimicrobial strategies and modified surfaces. Part of this chapter was already published in Philosophical Transactions of the Royal Society A ("Supercritical carbon dioxide design strategies: from drug carriers to soft killers", A. Aguiar-Ricardo, V.D.B. Bonifácio, T. Casimiro, V.G. Correia, Phil. Trans. R. Soc. A 2015, 373. DOI: 10.1098/rsta.2015.0009).

Chapter 2 describes the synthesis, characterization and biological evaluation of antimicrobial oxazoline-based oligomers in $scCO_2$. The work described in this chapter was already published in Macromolecular Bioscience ("Oxazoline-Based Antimicrobial Oligomers: Synthesis by CROP Using Supercritical CO_2", V. G. Correia, V. D.B. Bonifácio, V. P. Raje, T. Casimiro, G. Moutinho, C. L. da Silva, M. G. Pinho, A. Aguiar-Ricardo, Macromol. Biosci., 2011, 11 (8), 1128-37. DOI: 10.1002/mabi.201100126) and was highlighted in backcover of the issue. Also, this work was presented in an oral presentation ("Synthesis and characterization of 2-oxazoline-based polymers for anti-fouling and antimicrobial surface activity", V. G. Correia, T. Barroso, V. B. Bonifácio, C. Lobato da Silva, M. G. Pinho, and A. Aguiar-Ricardo, at the "12th European Meeting on Supercritical Fluids" at Graz University of Technology - Campus Inffeldgasse, Austria, 9th-12th May 2010) and in one poster presentation with proceeding ("Green synthesis of 2-oxazoline-based microbicidal polymers", V. G. Correia, V. D. B. Bonifácio, G. Moutinho-Fragoso, M. G. Pinho and A. Aguiar-Ricardo, Proceedings of the "II Iberoamerican Conference on Supercritical Fluids – Prosciba 2010" Natal, Brasil, 5th-9th April 2010).

Chapter 3 highlights the unexpected blue emission of oxazoline oligomers due to carbamic insertion during the synthetic procedure and their potential use as biotags. The work described in this chapter was already published in Matterials Letters ("Blue emission of carbamic acid oligooxazoline biotags", V.D.B. Bonifacio, V. G. Correia, M. G. Pinho, J. C. Lima, A. Aguiar-Ricardo, Mat. Lett., 2012, 81, 205-8. DOI: 10.1016/j.matlet.2012.04.134).

Chapter 4 describes the production of 3D structures with antimicrobial activity by blending the antimicrobial OOXs in the chitosan blend. The work described in this chapter was already published in Biofouling ("Anti-biofouling 3D porous systems: the blend effect of oxazoline-based oligomers on chitosan scaffolds", V. G. Correia, M. Coelho, T. Barroso, V. P. Raje, V. D. B. Bonifácio, T. Casimiro, M. G. Pinho and A. Aguiar-Ricardo, Biofouling, 2013, 29 (3), 273-82. DOI: 10.1080/08927014.2013.766172) and it was the subject of an oral presentation ("Antifouling and antimicrobial properties of oligo(2-oxazoline)s-based composites", V. G. Correia, M. Coelho, T. Barroso, V. P. Raje, V. D. B. Bonifácio, T. Casimiro, M. G. Pinho and A. Aguiar-Ricardo, at "II International Conference on Antimicrobial Research", Lisbon, 21st-23rd November 2012). Also, it was presented in two poster presentations ("Evaluation of fouling resistance on oligo(2-oxazoline)s modified chitosan-based devices", V. G. Correia, T. Barroso, M. Coelho, R. Domingues, V. P. Raje , V. D. B. Bonifácio, G. Moutinho, M. G. Pinho and A. Aguiar-Ricardo, 11th International Chemical and Biological Engineering Conference Chempor 2011 – FCT/UNL, Caparica, Portugal, 5th to 7th September 2011; "Antimicrobial surface coatings for water treatment using supercritical fluid technology", V. G. Correia, M. G. Pinho and A. Aguiar-Ricardo, at "II International Conference on Antimicrobial Research", Lisbon, 21st-23rd November 2012).

Chapter 5 describes the production of 3D structures coated with antimicrobial oxazoline-based oligomers by surface modification with plasma technology. It was described, for the first time, the design of a surface with grafted oxazoline-based oligomers able to kill bacteria upon contact. The work described in this chapter was already published in Biomacromolecules ("Antimicrobial contact-active oligo(2-oxazoline)s-grafted surfaces for fast water disinfection at the point-of-use", V. G. Correia, A. M. Ferraria, M. G. Pinho and A. Aguiar-Ricardo, Biomacromolecules, 2015, 16 (12), 3904-15. DOI: 10.1021/acs.biomac.5b01243) and it was the subject of an oral presentation (Fast disinfecting filters for water purification", V. G. Correia, M. G. Pinho and A. Aguiar-Ricardo, at "2nd EuCheMS Congress on Green and Sustainable Chemistry", Caparica, 4th-7th October 2015). Also, it was presented in five posters presentations ("Combining plasma activation and supercritical carbon dioxide to surface-graft antimicrobial coatings for water treatment", V. G. Correia, M. G. Pinho and A. Aguiar-Ricardo, at "11º Encontro Nacional de Química-Física", Oporto, 9th-10th May 2013; "Towards the ideal contact-active antimicrobial surface via grafting of oligo(2-oxazoline)s using $scCO_2$", V. G. Correia, M. G. Pinho and A. Aguiar-Ricardo, at 14th European Meeting on Supercritical Fluids, Marseille, 18th-21st May 2014; "Green route to graft antimicrobial oligo(2-oxazoline)s", V. G. Correia, M. G. Pinho and A. Aguiar-Ricardo, at Gordon Research Seminar and Gordon Research Conference on Green Chemistry, The Chinese University of Hong Kong, 26th-27th July 2014 and 27th July-1st August

2014; "Antimicrobial oligo(2-oxazoline)s surface immobilization by green technologies", V. G. Correia, M. G. Pinho and A. Aguiar-Ricardo, at XX Encontro Luso-Galego de Química, Complexo FFUP/ICBAS, Porto, 26th-28th November 2014; "Development of antimicrobial surfaces using green technologies", V. G. Correia, M. G. Pinho and A. Aguiar-Ricardo, at "XXIV Encontro Nacional da Sociedade Portuguesa de Química", Departamento de Química da Universidade de Coimbra, Coimbra, 1st-3rd July 2015).

Chapter 6 elucidates the mechanism of action of these antimicrobial oligomers in bacterial cells. The work described in this chapter is in preparation for submission.

Chapter 7 describes the main conclusions and future prospects.

1.10. Acknowledgments

The authors would like to thank the financial support from Fundação para a Ciência e Tecnologia (FCT—Lisbon) and COMPETE through Contracts UID/QUI/50006/2013 and SFRH/BD/74730/2010 (VGC).

Chapter 2. Oxazoline-Based Antimicrobial Oligomers: Synthesis by CROP Using Supercritical CO_2

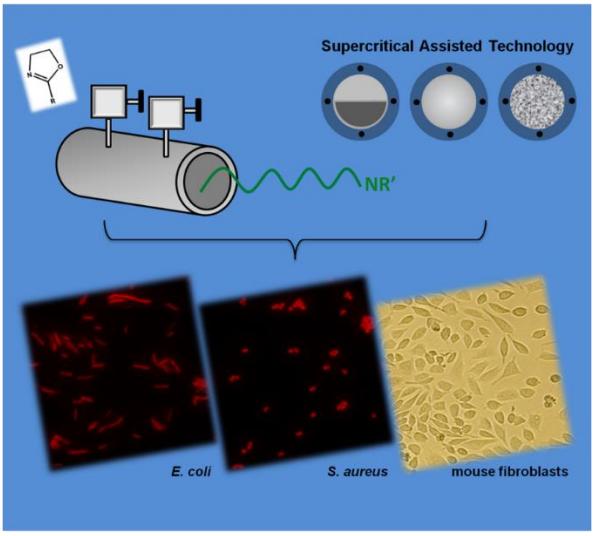

Article highlighted in journal's back cover

Manuscript published in

2011, Macromolecular Bioscience, 11, 1128-1137
VG Correia, VDB Bonifácio, VP Raje, T Casimiro, G Moutinho, CL da Silva, MG Pinho and A Aguiar-Ricardo
Oxazoline-based antimicrobial oligomers: synthesis by CROP using supercritical CO_2.

Personal contribution
VGC contributed to the design of the work, performed all the experimental work, interpreted the data and wrote part of the manuscript.

2.1. Abstract

A supercritical fluid assisted method was developed to obtain biocompatible 2-oxazoline-based oligomers quaternized with different amines. The synthesized oligo(2-oxazoline)s presented partial carbamic acid insertion at the starting end. Quaternized oligo(2-bisoxazoline) and linear oligo(ethylenimine) hydrochloride synthesis are reported for the first time. Oligo(2-methyl-2-oxazoline) and oligo(2-bisoxazoline) quaternized with *N*,*N*-dimethyldodecylamine were the most efficient biocidal agents showing fast killing rates against *S. aureus* and *E. coli*. Linear oligo(ethylenimine) hydrochloride had the lowest MIC values but higher killing times against both bacteria. Based on the antimicrobial activity studies, the cooperative action of carbamic acid with the ammonium end group is proposed.

2.2. Introduction

Due to public health concerns many modern materials are supposed to be equipped with antimicrobial properties. The use of antimicrobial polymers for rendering biomaterials resistant to microbial colonization is a very convenient way.[57] Polymeric antimicrobial agents have many advantages as they are chemically stable, reduced residual toxicity, nonvolatile, do not permeate though the skin and can have antimicrobial activity against different strains of bacteria and/or fungi. Significant advances have been made in the synthesis of antimicrobial polymers geared specifically for water treatment, for biomedical and food applications or for textile products.[4,84] Synthetic polymers are much easier to synthesize than peptides but the synthetic approaches still often involve multi-step synthesis including protection and deprotection steps. New synthetic approaches for the production of inherently antimicrobial and biocompatible polymers are required. Poly(2-oxazoline)s represent a unique approach to new antibiotics and are strong candidates for the development of new polymer therapeutics and its biocidal properties have been thoroughly explored in the last few years.[52–55] Oxazoline-based polymers with different architectures and chemical functionalities can be prepared in a *living* and controlled manner via cationic ring-opening polymerization (CROP), which results in well-defined degrees of polymerization and low polydispersity.[85–87] These polymers are biodegradable, relatively non-toxic, generally water soluble and, due to their versatility and ability to form functional materials, are interesting candidates for use in a large number of applications, such as drug delivery systems, smart materials and antimicrobial agents.[24,30,88] The synthesis of these polymers is well described in literature using conventional,[26] microwave-assisted[27,28] and green (synthesis in supercritical

carbon dioxide) methodologies.[23] The use of carbon dioxide as a polymerization reaction medium has been investigated continuously in recent years since it exhibits interesting physical properties, being promoted as a green solvent with many advantages over conventional solvents.[17,18] Poly(ethylenimine) is a polyamine which possesses a high number of advantages, such as being a chelating agent, having good water solubility, and good physical and chemical stability and that can be easily obtained by oxazoline-based polymers hydrolysis.[89,90]

Most of the studies of polymers with antimicrobial activity are based on compounds and materials possessing quaternary ammonium salts in their structure since its antimicrobial activity has been known for decades.[60,91,92] Waschinski and co-workers reported the synthesis of a series of oxazoline-based polymers, terminated with quarternary ammonium groups (using a series of *N*-alkyl-*N,N*-dimethyl amines but also pyridine), prepared via standard cationic ring-opening polymerization. Their antimicrobial properties were later evaluated by determining the minimal inhibitory concentration against *Staphylococcus aureus.* Only poly(2-oxazoline)-based polymers containing alkyl ammonium functions with alkyl chains of twelve carbon atoms or longer revealed to have antimicrobial activity and polymers with hydroxy or pyridyl functions at the chain end were found to be inactive. Moreover, Washinski et al.[52] showed that the antimicrobial activity of the polymers is believed to be polymer chain length independent and to be highly influenced by the polymers head group that are expected to cooperatively penetrate the cell wall at the same point as the quaternary ammonium group.[54] To the best of our knowledge, the antimicrobial effect of cyclic, aromatic and two branched linear amines to endcap poly(2-oxazoline)s was never investigated.

The mechanism of action of antimicrobial polymers remains largely unknown. However, poly(oxazoline)s resulting from CROP of 2-oxazolines can be considered as analogues of poly aminoacids[4] and the better studied mechanisms of action of antimicrobial peptides may be used as hypothetical models for the action of poly(oxazoline)s. Cationic antimicrobial peptides are attracted to the bacterial surfaces by electrostatic forces between the peptides and the anionic lipopolysaccharide (LPS) in outer membrane of gram-negative bacteria, or the negatively charged teichoic acids attached to the thick layer of peptidoglycan present in the surface of gram-positive bacteria.[35] Antimicrobial peptides therefore have some degree of selectivity towards negatively charged microbial cell envelopes and cytoplasmatic membranes in contrast with the generally neutral mammalian cytoplasmic membranes. After attachment to the bacterial surface, peptides must cross the outer membrane of gram-negative cells by a self promoted uptake[93] or the thick layer of peptidoglycan of gram-positive cells to reach the anionic surface of the cytoplasmic membrane. Peptides then disrupt it either by inserting perpendicularly to the membrane and forming pores (barrel-stave model or toroidal-pore model) or by accumulating on the bilayer

surface, covering it like a carpet and dissolving the membrane in a detergent-like manner (carpet model).[35]

The fact that the mechanism of action of cationic peptides or polymers depends on fundamental characteristics of the microbial cytoplasmic membrane suggests that development of resistance to these types of polymers would require bacteria to completely change their membrane structure. Therefore the development of antimicrobial polymers is envisaged as new and efficient alternative to conventional antimicrobial agents, less prone to the development of resistance.[94]

We have previously demonstrated that the polymerization of 2-substituted-2-oxazolines can be successfully performed in supercritical carbon dioxide. In this work, we synthesized several 2-oxazoline-based oligomers by the *living* CROP of 2-substituted oxazolines. After polymerization, the *living* oligomer was end-capped with water (**1a-3a**) or with different types of selected amines (linear, cyclic, and aromatic) (**1b**, **1c**, **2b-2f**, **3b**, **3c** and **4b**) in order to produce quaternary-ammonium-terminated materials. The synthesis and quaternization of branched oligo(2-bisoxazoline) 4b is reported for the first time as well as its antimicrobial activity and citotoxicity effect, together with oligo(hydrochloride quaternized ethylenimine) **5** wich was also synthesized by hydrolysis of a oligo(2-oxazoline) (Scheme 2.1). A detailed evaluation and description of the antimicrobial properties, comprising MIC and killing times determination, and cytotoxicity behaviour of novel ammonium quaternized oligomers (linear, cyclic, and aromatic) and oligo(hydrochloride quaternized ethylenimine) (5) are reported against six pathogenic bacteria and one fungi strains.

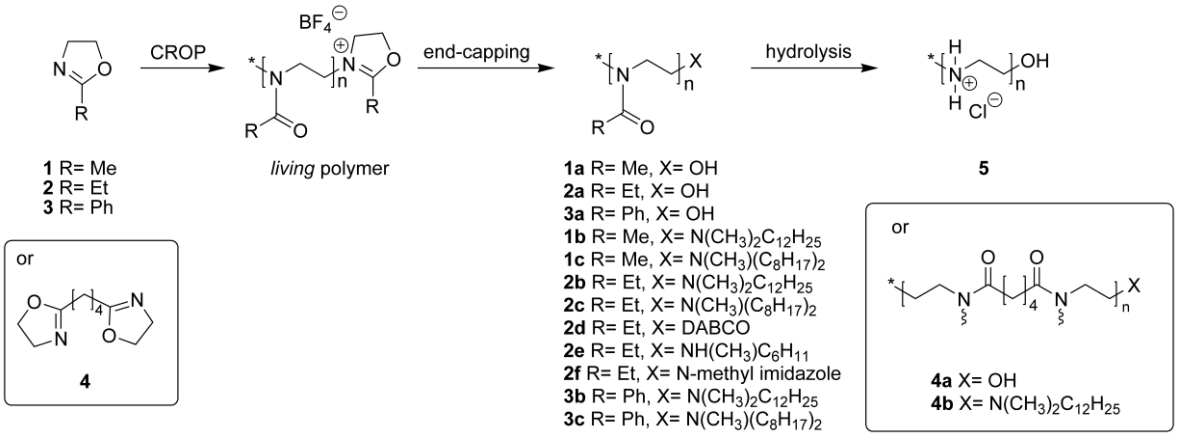

Scheme 2.1- General strategy to synthesize oligo(2-oxazoline)s (**1, 2** and **3),** oligo(2-bisoxazoline)s (**4**) and oligo(hydrochloride quaternized ethylenimine) (**5**).

2.3. Experimental Section

2.3.1. Materials

The monomers 2-methyl-2-oxazoline (MeOx), 2-ethyl-2-oxazoline (EtOx) and 2-phenyl-2-oxazoline (PhOx), the initiator boron trifluoride diethyl etherate ($BF_3.OEt_2$), methylimidazole, 1,4-diazabicyclo[2.2.2]octane (DABCO), accutase™ and Cell growth determination Kit MTT based were purchased from Sigma-Aldrich. *N*,*N*-dimethyldodecylamine and *N*-methylcyclohexylamine were purchased from Fluka. *N*-methyldioctylamine was purchased from Acros Organics. All the reagents were used without further purification. The monomer 2-bisoxazoline (BisOx) was synthesized as described in the literature.[95] Carbon dioxide was supplied by Air Liquide with a purity of 99.998 %. Mueller-Hinton broth medium was purchased from Oxoid. Propidium iodide was purchased from Molecular Probes, Invitrogen. RPMI-1640 (a Roswell Park Memorial Institute medium), trypan blue and fetal bovine serum (FBS) used in cell culture were purchased from Invitrogen. L929 cells were obtained from DSMZ, Germany and from Sigma.

2.3.2. Synthesis of *living* oligo(2-oxazoline)s

The polymerizations were carried out in a stainless-steel reactor, and four different 2-substituted oxazoline monomers were studied (MeOX, EtOx, PhOx and BisOx) and boron trifluoride etherate ($BF_3.Et_2O$) was used as the initiator. The monomer/initiator ratio used for each polymerization was, respectively: [M]/[I]=15 (MetOx), [M]/[I]=12 (EtOx), [M]/[I]=10 (PhOx) and [M]/[I]=7.5 (BisOx), according to our previous work.[23] Synthesis details as well as the end-capping of *living* oligo(2-oxazoline)s and the preparation of linear oligo(ethylenimine) hydrochloride are shown in the Supplementary Info.

2.3.3. Oligomers characterization

The infrared spectra were obtained using a FTIR Nicolet Nexus equipment. The ^{1}H and ^{13}C NMR spectra were acquired in a Bruker ARX 400 spectrometer. The MALDI-TOF mass spectrometry was performed on an AUTOFLEX Bruker apparatus using dithranol or α-cyano-4-hydroxycinnamic acid (CHCA) as the matrix. The samples were prepared by mixing aqueous

solutions of the oligomer (10^{-4} M) and matrix in a typical ratio of 1:1 (v/v). Due to very low solubility in common organic solvents and water we were unable to characterize the oligo(2-bisoxazoline) end-capped with water (**4a**).

2.3.4. Antimicrobial activity screening of synthesized materials by disc diffusion technique

Initial tests of antimicrobial activity were performed by disc diffusion technique for **1a**, **2a**, **1b**, **1c**, **2b-2f** and **4b** and **5**. These tests were performed using 7 different microorganisms: *Staphylococcus aureus* ATCC 25923, *Enterococcus faecalis* ATCC 29212 (both gram-positive bacteria), *Escherichia coli* ATCC 25922, *Proteus mirabilis*, *Pseudomonas aeruginosa* ATCC 27853, *Klebsiella oxytoca* (all gram-negative bacteria) and *Candida albicans* ATCC MYA-2876 (fungi). Cells were cultivated by plating 350 μL of bacterial or fungi cells stock solutions onto standard growth medium, Mueller-Hinton Agar. Papers disks (BBL no. 231039, BD) were impregnated with 15 μL of oligomers aqueous solutions at a concentration of 100 $mg.mL^{-1}$ and placed on the surface of the inoculated growth medium. Plates were incubated for 24 h at 37 ºC for bacterial strains and 48 h at 37 ºC for *Candida albicans* and the presence or absence of inhibition zones was evaluated. A negative control was set using a disc impregnated with water. Experiments were run in duplicate.

2.3.5. Bacterial strains, growth conditions and minimal inhibitory concentration (MIC) determination

Staphylococcus aureus NCTC8325-4 and *Escherichia coli AB1157* bacterial strains were grown in Mueller-Hinton broth medium. Cultures were grown overnight in broth at 37 ºC, diluted 1/200 and further incubated at 37 ºC, with aeration and vigorous shaking to an optical density at 600 nm of 0.5-0.6 for determination of killing curves and fluorescence microscopy. The MICs of the oligomers were measured using a broth microdilution method. 96-well plates containing in each well a volume of 100 μL of medium with a specific concentration of oligomer (sequential 2 fold dilutions) were prepared. Each well was inoculated with 5 μL of culture (5×10^5 cells) and plates were incubated at 37 ºC overnight. Controls of the medium, oligomer, monomers and amine were also carried out. MIC results were determined after 24 hours of incubation. The tests were performed in duplicate for both *S. aureus* and *E. coli* strains.

2.3.6. Killing curves

A solution of oligomer in growth medium was added to *S. aureus* and *E. coli* cultures in exponential growth phase (OD_{600nm}= 0.5-0.6) to achieve a final oligomer concentration of 5 times the MIC. Samples of the culture were taken before addition of oligomer and after the addition of **1b** and **4b** and **5**. Each sample was serially diluted to 10^{-2} and 10^{-4} in growth medium. 100 µL of each dilution were plated on Mueller Hinton agar and incubated at 37 ºC. After 24 hours, the number of viable colonies was determined. The minimum time to achieve 99.9 % killing of bacteria exposed to **1b**, **4b** and **5** was determined, except for *S. aureus* exposed to **5**, for which the minimum time to achieve 99 % killing was determined.

2.3.7. Fluorescence microscopy

A solution of oligomer in a growth medium was added to *S. aureus* and *E. coli* cultures in exponential phase (OD_{600nm}= 0.5-0.6) to achieve a final oligomer concentration of 5 times the MIC. The incubation time used for each oligomer solution was chosen according to the killing curve results obtained: **1b** (*E. coli*, 1 min.; *S. aureus*, 4 min.), **4b** (*E. coli*, 6 min.; *S. aureus*, 6 min.), **5** (*E. coli*, 75 min.; *S. aureus*, 240 min.). Cultures were then labeled with propidium iodide for 5 minutes at room temperature, with shaking. Cells were visualized by phase-contrast and fluorescence microscopy using a Leica DRMA2 microscope coupled to a CoolSNAP HQ Photometrics camera (Roper Scientific).

2.3.8. Cytotoxicity assays

Oligomers **1a**, **1b**, **4a**,**4b** and **5** were tested for cytotoxicity following the ISO 10993-5 guidelines. Briefly, triplicates of the oligomers were placed in polystyrene tubes at a concentration of 10 $mg.mL^{-1}$ in RPMI–1640 media with 10 % (v/v) of fetal bovine serum (FSB) and kept in an incubator (37 ºC, 5 % CO_2, fully humidified) for 1 day. The liquid extracts were diluted to 1 $mg.mL^{-1}$ and 0.1 $mg.mL^{-1}$ and used to culture L929 mouse fibroblasts (initial density 10^5 $cells.mL^{-1}$) in 24-well plates for 42 hours. The cell metabolic activity was determined by analyzing the conversion of 3-(4,5-dimethylthiazol-2-yl)-2,5-diphenyltetrazolium bromide (MTT) (yellowish color) to its formazan derivative (purple – absorbance at 570 nm after a 3 hour incubation at 37 ºC) using a MTT-based Cell growth determination kit. The results were normalized to the negative

control for cytotoxicity (fresh RPMI medium) and compared to the positive control (0.01 M phenol).

2.4. Results and Discussion

2.4.1. Synthesis of antimicrobial oligo(2-oxazoline)s (1b, 1c, 2b-2f, 3b, 3c), oligo(2-bisoxazoline) (4b) and oligo(hydrochloride quaternized ethylenimine) (5).

The oligomers were successfully synthesized *via* CROP using a two-steps green methodology: synthesis of the precursor *living* oligo(2-oxazoline)s and end-capping with selected terminating agents. The resultant materials were fully characterized by FT-IR, NMR, and MALDI-TOF confirming that low molecular weight and low polydispersity oligomers incorporating carbamic starting ends were obtained (Table 2.1). In order to establish its biocompatibility and antimicrobial profile the synthesized oligomers were end-functionalized either with water (in order to differentiate the role of the quaternization from the oligomer backbone) or tertiary amines giving the corresponding quaternary ammonium salts.

As previously mentioned many efforts have been made to synthesize novel quaternized ammonium polymers for the achievement of efficient biocidal materials.[4] The work developed so far has been focused on quaternization using linear amines with different chain lengths and also in obtaining polymers with telechelic functions. Since the antimicrobial activity does not depend on the polymer chain length, the exploitation of possible synergistic effects of the polyoxazoline starting end was studied for hydrogen, methyl, BOC-protected aromatic amine, free aromatic NH_2 groups, and it was shown that the functions at the starting end had a crucial effect to the bioactivity of the polymers.[52]

Oligo-oxazolines synthesized in $scCO_2$ are obtained as an enriched mixture of carbamic acid starting end enriched telechelic oligomers since carbon dioxide is partially incorporated (up to 35 %) in the starting end of the oligo-oxazoline chain.[23] Attempts to polymerize 2-bisoxazoline led to the formation of branched oligomer **4b,** which was further quaternized for the evaluation of branching on antimicrobial activity. The preparation of linear oligo(ethylenimine) from oligo(oxazoline) hydrolysis is well described in literature.[50] Therefore we prepared **5** by the acid hydrolysis of **1b**, with loss of the ammonium quaternization under these conditions. The investigation of the biocidal properties of **5** despite its simple preparation was never explored, to the best of our knowledge, although the complex preparation of crosslinked nanoparticles of

ammonium derivatives of **5** has been reported for the acquirement of antimicrobial dental resin composites.[96,97]

Table 2.1- Analytical data of synthesized oligo(2-oxazoline)s.

Oligomer	Yield (%)[a)]	M_n[b)] (Da)	D.P.[b)]	M_n[c)] (Da)	M_w/M_n[c)]	CO_2[d)] (%)	M_n[e)] (Da)	M_w/M_n[e)]
1a	43	-	-	840	1.2	22	851	1.3
2a	70	-	-	733	1.3	-	1082	1.2
3a	99	-	-	-	-	-	-	-
1b	68	1237	12	505	1.07	21	479	1.0
1c	66	1279	12	986	1.3	21	1169	1.3
2b	61	1504	13	897	1.5	28	1059	1.2
2c	66	1348	11	1237	1.3	30	929	1.3
2d	79	1304	12	1080	1.2	32	1118	1.1
2e	86	809	7	-	-	-	-	-
2f	85	778	7	860	1.2	35	997	1.2
3b	99	1097	6	-	-	-	-	-
3c	88	1287	7	-	-	-	-	-
4a	67	-	-	-	-	-	-	-
4b	67	812	3	459	1.0	21	505	1.0
5	74	-	-	558	1.0	-	-	-

[a)] Determined after purification. [b)] Determined by NMR. [c)] Data obtained by MALDI-TOF for the oligomer without CO_2 insertion. [d)] Percentage of CO_2 insertion in the oligomer determined by MALDI-TOF. [e)] Data obtained by MALDI-TOF for the oligomer with CO_2 insertion.

2.4.2. Antimicrobial activity of synthesized materials

The antimicrobial activity of **1a-c**, **2a-f, 4b** and **5** was initially screened against different gram-positive and gram-negative bacteria as well as fungi by disc diffusion technique. Only oligomers **1b**, **1c**, **2b**, **2c**, **4b** and **5** were active against all microorganisms tested (*Staphylococcus aureus* ATCC 25923, *Enterococcus faecalis* ATCC 29212, *Escherichia coli* ATCC 25922, *Proteus mirabilis*, *Pseudomonas aeruginosa* ATCC 27853, *Klebsiella oxytoca* and *Candida albicans* ATCC MYA-2876), indicated by a zone of growth inhibition of variable diameter around the disk containing the oligomers (Table 2.2). Oligomers **3a-c**, and **4a** were not tested due to its insolubility in water. Antimicrobial activity of the oligomers was further evaluated against the gram-positive bacteria *S. aureus NCTC8325-4* and the gram-negative bacteria *E. coli AB1157* by determining the minimal inhibitory concentration, the killing curves of exponentially growing cells upon addition of the oligomers and labeling by propidium iodide.

Table 2.2 - Antimicrobial activity of oligo(2-oxazoline)s screened against different gram-positive and gram-negative bacteria as well as fungi by disc diffusion.

Microorganism[a)]	Oligomer					
	1b	1c	2b	2c	4b	5
S. aureus	1.7	1.0	1.7	1.1	1.8	1.6
E. faecalis	1.5	1.2	1.8	1.0	2.0	1.3
E. coli	1.1	1.0	1.8	1.2	2.1	1.5
P. mirabilis	1.0	0.8	1.1	1.0	1.2	1.3
P. aeruginosa	0.8	0.7	0.8	0.9	0.9	1.8
K. oxytoca	1.2	0.9	1.5	1.0	2.5	1.3
C. albicans	3.6	1.4	6.6	1.3	5.2	1.9

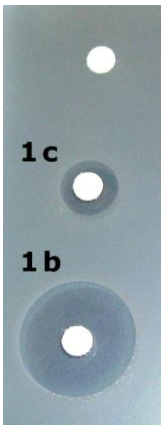

[a] Zone of growth inhibition around the disk shown in cm. The figure shows the disc diffusion assay for the fungi *C. albicans* in the presence of oligomers **1c** and **1b** (control experiment using water is shown on top).

2.4.3.Minimal inhibitory concentration (MIC) determination

Determination of MICs of oligomers **1-5** against *S. aureus* and *E. coli* showed that oligomers **1b**, **1c**, **2b**, **2c,4b** and **5** are the most efficient materials in terms of antimicrobial activity against both gram-positive and gram-negative bacteria (Table 2.3). Due to poor solubility in aqueous medium, the MIC values of oligomers **3a-c** and **4a** could not be measured. Oligomers terminated with water, which were synthesized as a control, showed no biocidal activity in the concentration range tested, a result in accordance with literature which states that the backbone of the polymer is not the primary determinant of its biocidal activity and that oligo(2-oxazoline) itself are not bioactive.[7] Analogous control tests were performed using either the amines or the monomers and no biocidal activity could be observed in the concentration range tested, as explained in the experimental procedure. This lack of activity of the amines can be explained with a lower binding affinity to the bacterial cell membrane due to the absence of a positive charge in the molecule.[52] We found that oligo-oxazolines end-capped with cyclic amines (**2d** and **2e**) and an aromatic amine (**2f**) showed higher MIC values for *S. aureus* and *E. coli* then oligomers end-capped with linear amines **1b**, **1c**, **2b** and **2c**. If we define oligomers with MICs higher than 10 $mg.mL^{-1}$ as antimicrobially ineffective,[52] we can consider that oligomers **2d-f** were not effective against both bacterial species tested. Assuming that the mechanism of action of oligomers **1b**, **1c**, **2b-f** and **4b** requires insertion in the cytoplasmic membrane, similarly to many antimicrobial peptides,[35] and that long alkyl chains are needed to penetrate the bacterial cell membrane, then it is possible that oligomers end-capped with cyclic amines are not as effective in penetrating the lipid bilayer as oligomers with a linear end-capping group or that the diffusion through the bacterial cell wall is hindered due to the non linearity of the amine group,[52] and therefore have higher MICs. Antimicrobial activity of oxazoline-based polymers functionalized with non-linear amines was never exploited in literature. In this work, oligomers **1c** and **2c** that are functionalized with *N*-methyldioctylamine, a two branched C8 amine, revealed to have biocidal activity contrarily to the reported non-biocidal behavior of poly(2-methyl-oxazoline) functionalized with octyldimethylamine, only one linear C8 amine.[52] The funcionalized oligomers with *N*,*N*-dimethyldodecylamine **1b**, **2b** and **4b** showed antimicrobial activity against both bacteria. Oligo(2-bisoxazoline) **4a** has a higher molar MIC value than **1b** (both terminated with the same linear amine) showing that branching influences the MIC values. This result can be possibly related with lower accessibility of both **4b** chain ends to the cell membrane, limiting the cooperative mehanism of action due to steric hindrance,[54] supporting the idea that not only the number of ammonium group in the terminal end of the chain has an impact in antimicrobial activity but also the possible conformational arrangement of the oligomers chain.

Data reported by Waschinski and co-workers[52,54] shows that the starting end group has a great influence on biocidal activity on poly(alkyloxazoline) with terminal quaternary ammonium groups. As reported by Veiga de Macedo *et al.* the 2-oxazoline polymer synthesis in $scCO_2$ leads to products with a percentage of carbamic acid insertion at the starting end (from 10 to 28 %, according to the 2-oxazoline monomer used).[23] Comparing the MIC value for *S. aureus* bacteria (although different strains) of **1b** (0.15 $\mu mol.mL^{-1}$ or 0.19 $mg.mL^{-1}$) (hydrogen and 21 % carbamic acid at the starting end) with the MIC value of analogous oligo(2-metyl-2-oxazoline) end-capped with *N*,*N*-dimethyldodecylamine reported in literature (1.0 $\mu mol.mL^{-1}$ or 2.5 $mg.mL^{-1}$) (only hydrogen at the starting end),[52] a positive impact of a low percentage of a carbamic acid satellite group on the oligomers biocidal activity was observed. The comparison of **1b** MIC value (0.15 $\mu mol.mL^{-1}$ or 0.19 $mg.mL^{-1}$) (only 21 % of carbamic acid content) with the reported[52] MIC value (0.08 $\mu mol.mL^{-1}$ or 0.2 $mg.mL^{-1}$) for analogous bitellechelic poly(oxazoline) having an end capped protected carbamic acid starting end (*tert*-butoxycarbonyl (BOC) group) shows a similar biocidal activity. Moreover, the antimicrobial activity of **1b** could be corrected by a factor of 5 taking in account the actual percentage of CO_2 insertion. The approach developed in this work and the ones from Waschinski *et al.*[52,54] indicate a possible synergic effect arising from carbamic-type and ammonium quaternized bistelechelic functions. Therefore increasing the percentage of carbamic acid insertion in oligo(2-oxazoline) should result in a significant enhancement of its antimicrobial activity. To verify this hypothesis, further studies with oligo(2-oxazoline)s with high percentages of CO_2 insertion (up to 80 %) will be performed. Polymer **5** is a oligo(ethylenimine) hydrochloride quaternized with 11 hydrochloride units (by MALDI-TOF analysis) and therefore with a high number of positive charges. The existence of positive charges may be an important requisite for the oligomers antimicrobial activity as the first step in their mechanism of action should be attraction to the predominant negatively charged bacterial surface. The lower MIC value obtained for **5** supports the strong correlation of antimicrobial activity and the initial binding to bacterial cell membrane.[52]

Despite the large differences between the surface of gram-positive and gram-negative bacteria, both have an anionic character, due mainly to the presence of LPS in the outer leaflet of the outer membrane of gram-negative bacteria and to the presence of teichoic acids in the surface of gram-positive bacteria.[98] Generally, oligomers showed a weaker antimicrobial activity for *E. coli*, when compared to *S. aureus*, what can be justified with the MIC values of quaternary ammonium salts itself, already reported in the literature (for dodecyltrimethylammonium chloride: $MIC_{E.\ coli}$ = 110 $\mu mol.L^{-1}$ and $MIC_{S.\ aureus}$ = 20 $\mu mol.L^{-1}$).[54]

Cationic polymers are believed to initiate electrostatic interactions with the negatively charged components of the bacterial surfaces, before killing the cells by disruption of the cellular membrane.

Table 2.3 - Minimum inhibitory concentrations obtained for 2-oxazoline-based oligomers using *E. coli* and *S. aureus* strains.

Oligomer	MIC *E. coli AB1157*		MIC *S. aureus NCTC8325-4*	
	$mg.mL^{-1}$	$\mu mol.mL^{-1}$	$mg.mL^{-1}$	$\mu mol.mL^{-1}$
1a	> 24		> 24	
2a	> 24		> 24	
1b	0.38	0.31	0.19	0.15
1c	1.50	1.15	0.75	0.58
2b	0.75	0.48	0.38	0.24
2c	1.50	1.09	0.75	0.55
2d	> 24		12	9.1
2e	24	29.2	12	14.6
2f	> 24		24	30.4
4b	0.75	0.92	1.5	1.85
5	0.09	0.18	0.19	0.39

2.4.4.Killing curves

Microbial killing by **1b**, **4b and 5** were studied in detail. Oligomer **1b**, with low MIC and which biocidal properties for higher molecular weights have been already reported,[52] was selected in order to evaluate the effect of a 21 % of insertion of a satellite carbamic acid on oligomer chain. Oligomer **4b**, quaternized with the same amine than **1b,** was chosen to evaluate the influence of branching on biocidal killing times. Polymer **5** has 11 hydrochloride quaternized units and was therefore chosen to evaluate the effect of the presence of a high number of positive charges per

oligomer. Killing curves for **1b, 4b** and **5** were determined as function of time, after addition of the oligomers at 5 times the MIC, to *E. coli* and *S. aureus* exponentially growing cultures (Figure 2.1).

After the addition of **1b**, the optical density of both cultures as well as the number of viable cells decreases after a few minutes (99.9 % killing is achieved after 4 minutes for *S. aureus* and in less than 1 minute for *E. coli*). After the addition of **4b**, the increase in optical density stops and 99.9 % of the cells are killed in 4-6 minutes for both *S. aureus* and *E. coli*. In contrast, after addition of **5**, optical density continues to slowly increase during the assay. However, the number of viable cells decreases, showing that although the cells are probably not being lysed immediately after the addition of the polymer, they are no longer viable. Although polymers **4a** and **5** have similar molar MIC values, polymer **5** took a much longer time to kill the bacterial cells, with 99 % killing achieved after 4 hours for *S. aureus* and 99.9 % killing achieved for *E. coli* after 75 minutes.

The low killing times observed for **1b** and **4b** could be justified by the synergistic effect of carbamic acid and linear amine telechelic functions. Antimicrobial polymers are suggested to disrupt the cytoplasmic membrane by two main mechanisms after the initial binding step: insertion of the polymer perpendicularly to the membrane with the formation of a either barrel-stave or toroidal transmembrane pores causing permeabilization and depolarization of the membrane or accumulation of the polymer at the membrane surface until a certain threshold concentration is reached causing subsequent disruption in a detergent like manner (carpet mechanism), with the consequent lysis of the bacterial cells.[92] It is possible that the different killing rates of **1b** and **4b** comparatively to **5** are due to different modes of action of these polymers. Polycation **5** is more effective in attaching to the bacterial cell surface due the higher positive charge per polymer chain, but less efficient in crossing the outer membrane of gram-negative bacteria and the thick peptidoglycan layer of the gram-positive bacteria and thus taking longer time to kill the bacteria. While growth of *E. coli* can be inhibited by just attacking the outer membrane, in *S. aureus* the polymer must firstly diffuse through the cell wall to be effective,[54] justifying longer times to kill *S. aureus*.

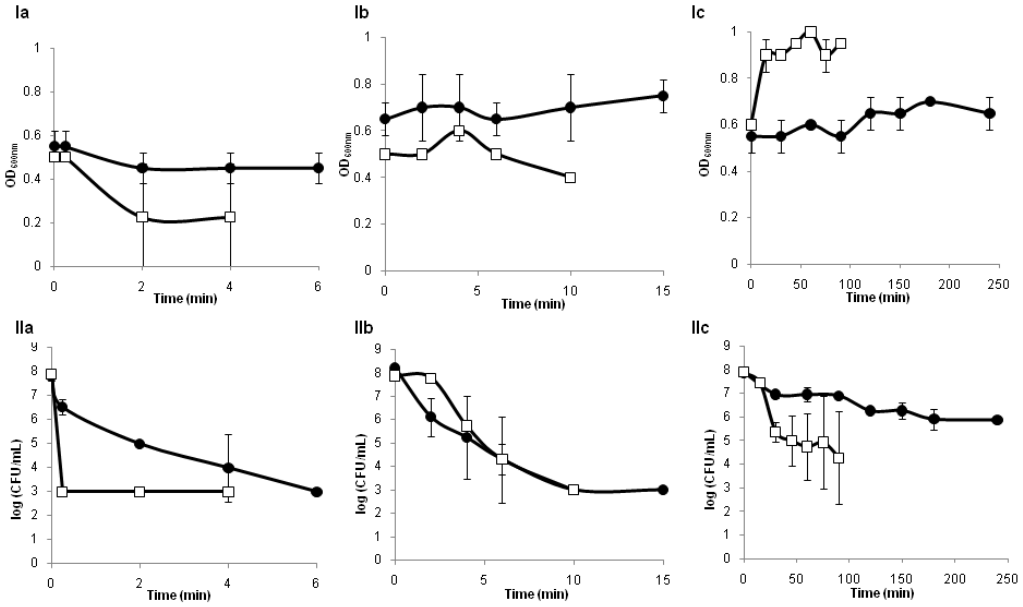

Figure 2.1- Oligo(2-oxazoline)s killing curves for *E. coli* and *S. aureus* strains: (I) Optical density at 600 nm (OD_{600nm}) and (II) colony-forming units per mL ($CFU.mL^{-1}$) as function of time for (●) *S. aureus* and (□) *E. coli* in the presence of (a) oligomer 1b, (b) oligomer 4b and (c) oligomer 5. Time t = 0 min. represents the sample taken before addition of the oligomer. All the assays were done in duplicate. Error bars represent the standard deviation

2.4.5.Fluorescence microscopy

The viability of *S. aureus* and *E. coli* in the presence of **1b**, **4b** and **5** was also assessed using propidium iodide fluorescent dye to label dead cells. Cells were incubated in the presence of the oligomers for variable times, chosen in agreement with the obtained killing curves for each oligomer (Figure 2.2).

Both *E. coli* and *S. aureus* become fluorescent after the addition of each oligomer, at times that are in accordance with the results obtained for the killing curves, indicating that fluorescence microscopy, a simple and reliable method, is a faster alternative to assess cell viability, with the advantage of viable cells not being underrepresented due to the formation of cell clusters.

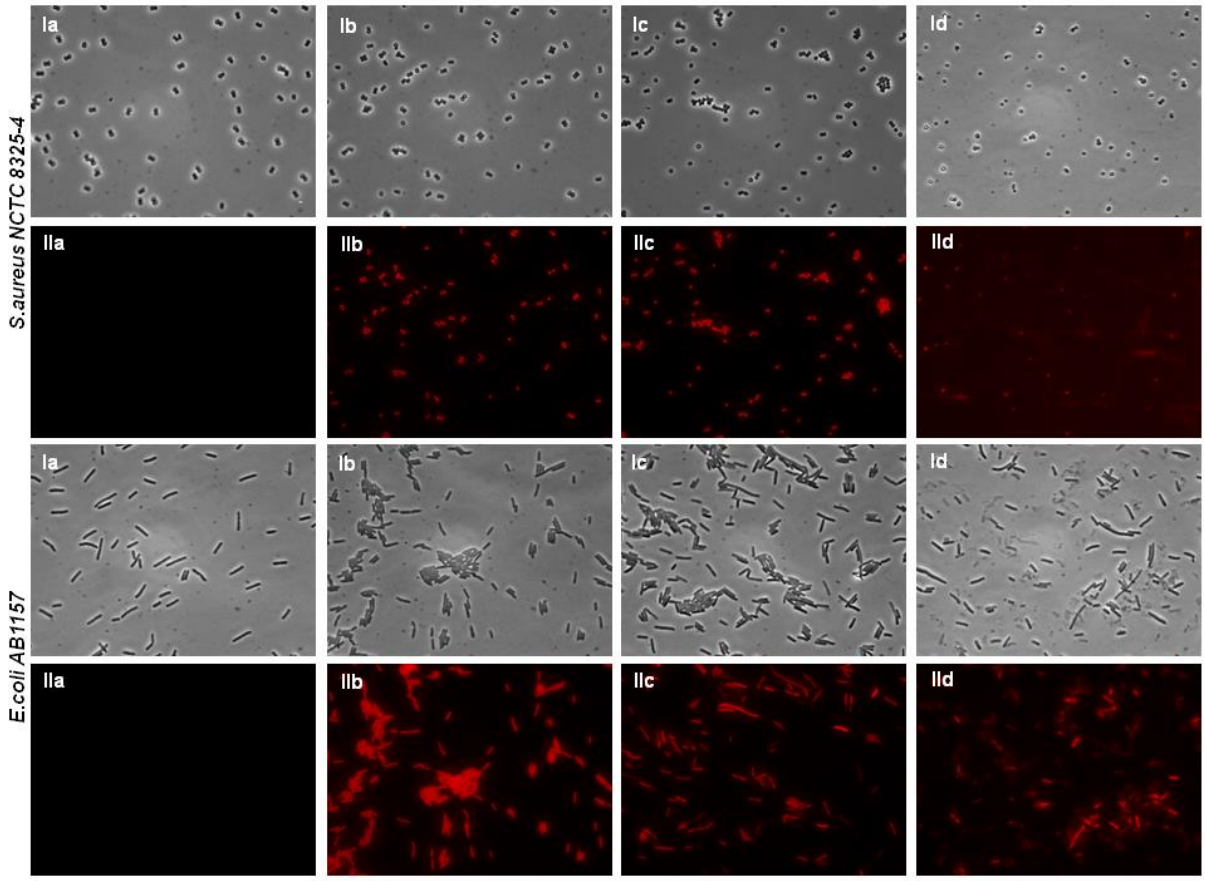

Figure 2.2 -. Fluorescence labeling using propidium iodide for the assessment of cell viability of *S. aureus NCTC 8325-4* and *E. coli AB1157* (a) cells in the absence of oligomer, (b) cells incubated with oligomer 1b, (c) cells incubated with oligomer 4b and (d) cells incubated with oligomer 5: (I) bacterial cells visualized by phase-contrast, and (II) cells visualized by fluorescence microscopy using Texas Red filter. Dead cells show red fluorescence.

2.4.6. Cytotoxicity assay

Prokaryotic and eukaryotic cells differ at the level of the membrane composition and lipids arrangement. Mammalian cytoplasmic membranes are generally neutral while bacterial cells tend to have a negatively charged surface. Therefore polymers with positive charges may bind selectively to prokaryotic membranes through electrostatic interactions.[99] This led us to investigate the cytotoxicity of these oligomers against mammalian cells (L929 mouse fibroblasts). Oligo-oxazolines were evaluated in terms of cytotoxicity following International Standard guidelines[100] with an incubation time of 42 hours. Table 2.4 shows the cell metabolic activity in the presence of each oligomer.

Cell number and cell metabolic activity in the presence of oligomer **1a,** in a concentration of 10 $mg.mL^{-1}$, were markedly decreased relatively to the control. For the lower concentrations of **1a** tested**,** 1 $mg.mL^{-1}$ and 0.1 $mg.mL^{-1}$, cells proliferated at the same extent as the control and remained viable, though higher cell metabolic activities were observed. This increased cell metabolic activity could potentially result from a cell stress response to oligomer **1a** present in the extracts. In the presence of 0.1 $mg.mL^{-1}$ of **1b** after 42 hours of incubation cells are still metabolically active. Comparing the bacterial killing rate of **1b** (4 minutes for *S. aureus* and in less than 1 minute for *E. coli*) we conclude that the bactericidal activity is much faster than their cytotoxic effect in mammalian cells, as cells are still metabolically active after 42 hours. At the same concentrations, cells in the presence of branched oligo(2-bisoxazoline) **4a** and **4b** and in the presence of oligomer **5** exhibited lower metabolic activities than in the presence of **1a** and **1b**. Additionally, ammonium quaternization of the oligomers results in increased cytotoxicity, as the cell metabolic activity decreases in the presence of these oligomers. These results suggest that all oligomers tested are promising for further biomedical or biotechnological applications as they combine low MIC values, fast killing rates and high biocompatibility.

Table 2.4 - Percentage[a)] of cell metabolic activity for different oligo(2-oxazoline)s concentrations ($mg.mL^{-1}$).

Oligomer	Cell metabolic activity (%)		
	10 $mg.mL^{-1}$	1 $mg.mL^{-1}$	0.1 $mg.mL^{-1}$
1a	8.2	195.9	209.6
1b	7.8	8.1	123.4
4a	-	25.0	83.3
4b	8.3	7.3	52.0
5	8.3	15.9	69.5

[a)] 100 % of cell metabolic activity was defined as the activity in RPMI medium.

2.5. Conclusions

A series of 2-oxazoline-based oligomers enriched with satellite carbamic acid starting end and ammonium quaternized terminated were successfully obtained using supercritical carbon dioxide via cationic ring-opening polymerization. The synthesis and quaternization of a branched oligo(2-bisoxazoline) and the synthesis of linear oligo(ethylenimine) hydrochloride quaternized, prepared by acid hydrolysis of a synthesized oligo(2-oxazoline), were reported for the first time. These materials were obtained with low molecular weight and low polydispersity and were fully

characterized by spectroscopic and microbiological techniques. This type of oligomers may have a mechanism of action similar to antimicrobial peptides as they may induce membrane permeation via membrane disintegration or pore formation, accompanied by a loss of bacterial membrane potential. Materials with fast killing rates against both *E. coli* and *S. aureus* were obtained for oligo(2-methyl-2-oxazoline) and oligo(2-bisoxazoline) both end-capped with *N*,*N*-dimethyldodecylamine. Linear oligo(ethylenimine) hydrochloride quaternized has a lower MIC value, is more effective in attaching to bacterial cell membrane, but required more time to kill bacteria. Our results suggest that oligo-oxazolines end-capped with cyclic amines are not able to insert efficiently in the cytoplasmic membrane and are therefore poor antimicrobial agents. Carbamic acid starting end of linear amine terminated oligo(2-oxazoline)s appears to enhance the antimicrobial activity of the materials. It should be stressed out that the reported oligomers are obtained by simple CO_2 insertion (used as solvent and C_1 feedstock) avoiding the synthesis of endcappers. Further carbamic acid starting end enrichment of the oligomers is being carried out.

The synthesized library provided good leading materials for the development of new antimicrobial agents with low cytotoxicity, fast killing rate and broad-spectrum biocidal activity, and represents a good strategy to avoid and overcome bacterial resistance. Further studies are being performed in order to elucidate the oligomers mechanisms of action.

2.6. Acknowledgments

We would like to acknowledge LabRMN at FCT-UNL and Rede Nacional de RMN for access to the facilities. Rede Nacional was supported with funds from FCT-Lisbon, Projecto de Re-equipamento Científico, Portugal. We thank the financial support from Fundação para a Ciência e Tecnologia (FCT), through contracts PTDC/QUI/73939/2006, MIT-Pt/BS-CTRM/0051/ 2008, doctoral grant SFRH/BD/74730/2010 (VGC), postdoctoral grant SFRH/BPD/38014/2007, FEDER, and FSE. VDBB was supported by the MIT-Portugal program (Bioengineering Systems Focus Area).

Chapter 3. Blue emission of carbamic acid oligooxazoline biotags

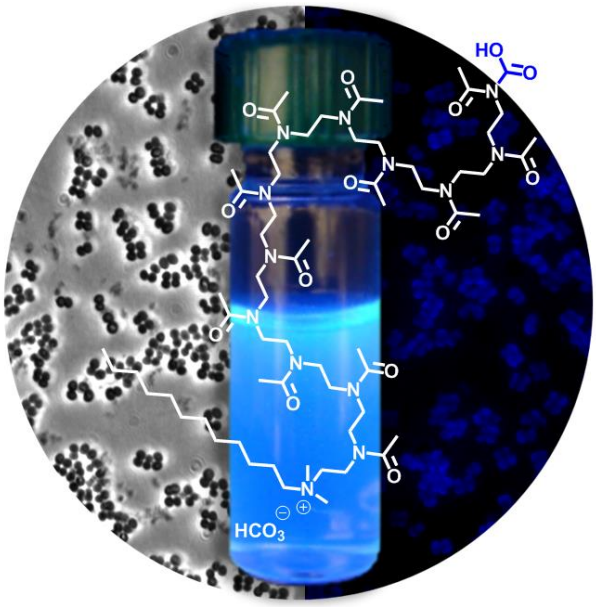

Manuscript published in

2012, Materials Letters, 81, 205-208
VDB Bonifácio, VG Correia, MG Pinho, JC Lima and A Aguiar-Ricardo
Blue emission of carbamic acid oligooxazoline biotags.

Personal contribution
VGC contributed to the design of the work, performed all the experimental work, interpreted the data and wrote part of the manuscript.

3.1. Abstract

The blue emission of a carbamic acid oligo(2-methyl-2-oxazoline) synthesized by a cationic ring-opening polymerization in supercritical carbon dioxide under controlled conditions is reported. The increase of the light- emission intensity of oligo(2-oxazoline)s was achieved by carbamic acid insertion at the oligomer starting end during the polymerization. Successful labeling of gram-positive *S. aureus* bacterial cells with carbamic acid ammonium-quaternized oligo(2-oxazoline)s turn these materials into promising blue fluorescent markers for imaging and bioanalytical assays.

3.2. Introduction

Bioluminescence staining is an attractive approach either to distinguish biological components,[101] detect pathogenic bacteria or track and quantify molecules and events in living cells with spatial and temporal resolution.[102] Pathogen recognition by polymer-based detection methods have become known in a variety of biological sensing applications,[103] but usually the polymeric-based sensors require pre- functionalization,[104] or addition of reagents. Ideally, a polymeric biosensor should comprise some requirements such as availability of varied range of monomer types, easy and direct detection, low detection limits, selectivity, precision, rapid assay time (5 up to 10 min) and be cost effective.[101]

The emergent interest in poly(2-oxazoline)s (POXs) is mainly related to their amphiphilic nature,[55,105] and high potential as antimicrobial materials.[52] While studying oligo(2-oxazoline)-based (OOX) architectures [23,26,28] we have found that all the synthesized polymers exhibit a blue fluorescence, which to the best of our knowledge, has not been previously described for POXs.[106] The intrinsic blue fluorescence of POXs is relevant for applications in the field of biocompatible tags (biotags) as there are only a few blue fluorescent bacterial cells membrane labels. Therefore, all efforts to rationalize the origin of the fluorescence in biocompatible polymers and design synthetic strategies to produce brighter materials is highly desirable. Previous reports have described the blue emission from hyperbranched polymers without pendant or on-chain fluorophores but very recently this puzzling emission has been fully understood.[107] Hence, all reports on blue emission from polymers having no fluorophores are, in general, due to oxidation triggered processes. Therefore, we first describe the purely intrinsic blue emission of OOXs, resulting from carbamic acid end-capping.

Accordingly to literature, ammonium terminated POXs have antimicrobial activity and are believed to initiate electrostatic interactions with the negatively charged components of the bacterial surface. Carbamic acid enriched OOXs quaternary-ammonium terminated proved to be effective in attaching to bacterial cells [48] thus enabling their application as fluorescent biotags. As a proof of concept, herein we report the synthesis of carbamic acid enriched oligo(oligo-2-methyl-2-oxazoline)s to elucidate the origin of the intrinsic fluorescence. Furthermore, oligomers were end-capped with *N,N*-dimethyldodecylamine (DDA) to assess its potential application as bacterial markers.

3.3. Experimental Section

3.3.1. Oligomer synthesis

Oligomerizations were carried out following a reported method [10] in the presence and in the absence of initiator (see Supplementary data). Using this procedure, oligo(2-methyl-2-oxazoline)s 1 and 1′,and carbamic acid starting end enriched oligo(2-methyl-2-oxazoline)s 2 and 2′ were obtained (Figure 3.1). Oligo(2-methyl-2-oxazoline) was further hydrolysed to oligo(ethylenimine) hydrochloride 3.[50] Oligo(2-methyl-2-oxazoline) was also synthesized under controlled experimental conditions using a high-pressure sapphire cylindrical cell (HPSCC) that was especially designed for spectroscopic measurements in supercritical fluids. The HPSCC apparatus used in these experiments is described in the Supplementary data.

3.3.2. Fluorescence microscopy

A solution of oligomer 1′ and 2′ in Mueller Hinton growth medium was added to *S. aureus* culture in exponential phase (OD_{600nm}=0.5– 0.6) to achieve a final oligomer concentration of 6 μM (4 % of minimum inhibitory concentration) for oligomer 1′ and a final concentration of 1mM (100 % of minimum inhibitory concentration) for oligomer 2′. Cultures were labeled individually with oligomer 1′ and 2′ for 5 min at room temperature, with shaking. Cells were centrifuged and washed with growth medium 3 times. Cells were visualized by phase-contrast and fluorescence microscopy (exposure time of 5000 msec) using a Leica DRMA2 microscope coupled to a CoolSNAP HQ Photometrics camera (Roper Scientific).

3.4. Results and Discussion

3.4.1. Synthesis of carbamate enriched oligo(2-methyl-2-oxazoline)s

Living cationic ring-opening polymerization (CROP) of 2-oxazolines using supercritical carbon dioxide ($scCO_2$)[48] was performed using a two-steps green methodology: synthesis of the precursor *living* OOXs and end-capping with selected terminating agents. Under these conditions CO_2 is partially incorporated in the starting end of the OOX chain (up to 35 %). Since there are no reports on fluorescent POXs prepared by conventional methodologies, the origin of OOXs fluorescence must be related to the synthetic route using $scCO_2$.As CO_2 can act as initiator of the *living* polymerization, even with low efficiency, the oligomerization was performed in the absence of $BF_3.OEt_2$, in order to force an increased incorporation of carbamic acid. End-capping of the *living* oligomers are achieved by addition of water (1 and 2) or DDA (1′ and 2′) (Figure 3.1). Using this methodology we obtained for the first time high carbamic acid enriched oligomers 2 and 2′. For comparison oligomers 1 and 1′ were synthesized in the presence of $BF_3.OEt_2$ as described.[23]

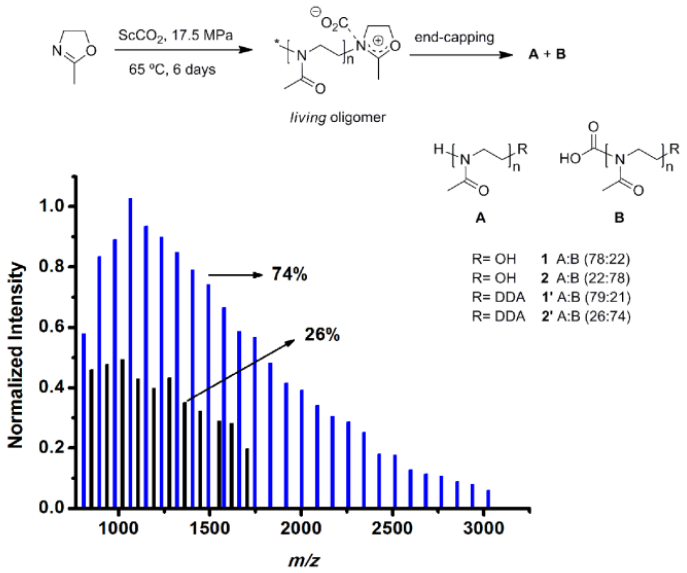

Figure 3.1 - Schematic synthesis of oligo(2-methyl-2-oxazoline)s 2 and 2' in supercritical carbon dioxide in the absence of initiator. The MALDI-TOF spectra show the molecular weight distribution for 2': mixture composed by 26 % of oligomer A (black lines) and 74 % of oligomer B (blue lines).

Subsequently, emission spectra of both oligomers 1 and 2 were acquired in order to compare oligomers with different carbamic acid percentages, and an increase of nearly 8 times in the emission intensity (due to increase in carbamic acid content) was observed (Figure 3.2).

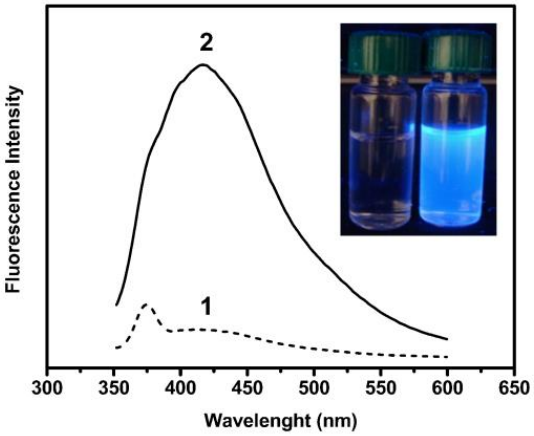

Figure 3.2 - Emission spectra λ_{ex}= 350 nm) of equimolar aqueous solutions of oligo(2-methyl-2 oxazoline)s synthesized in the absence (2) and in the presence of initiator (1). Inset: photograph of vials containing water (left) and an aqueous solution of 2 excited by a UV lamp (λ_{ex}= 366 nm).

The fluorescence apparent quantum yields (where apparent reflects the fact that the oligomers are always a mixture of carbamic acid terminated and hydrogen terminated oligomers) obtained for oligomers 1 (ϕ_f=0.013) and 2 (ϕ_f=0.092) at λ_{ex}=350 nm were determined using the coumarin 460 standard in methanol (ϕ_f=0.46). [108] The quantum yields of the polymers with intrinsic emission are very low (1–9 %), which is not significant, particularly when labeling such oligomers into bioorganisms.

3.4.2.Tagging of the membranes

Oligomers 1, 1′, 2 and 2′ were investigated as staining agents for bacterial membranes of gram-positive *S. aureus*. Hydroxyl end-capped oligomers (1 and 2) did not stain *S. aureus* in the tested concentrations and incubation times (data not shown). The presence of ammonium end-capping group of OOXs is crucial for the binding of the tag to the membrane leading to an effective bacterial staining. Solutions of both oligomers, 1′ and 2′,were individually used to incubate *S. aureus* bacterial cells, at room temperature for 5 min, and the results showed a successful staining in both cases (Figure 3.3).

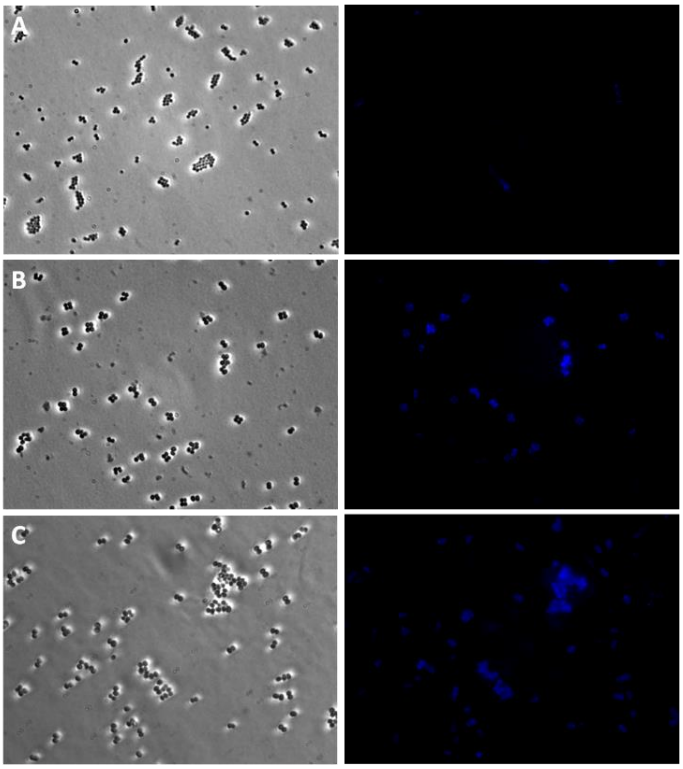

Figure 3.3 - Fluorescence labeling of *S. aureus* using oligo(2-methyl-2-oxazoline) terminated with *N*,*N*-dimethyldodecylamine (**1'** and **2'**). Bacterial cells visualized by phase-contrast (left panels) and cells visualized by fluorescence microscopy using DAPI filter (right panels). (A) cells in the absence of oligomer. (B) cells in the presence of oligomer **1'**. (C) cells in the presence of carbamic acid enriched oligomer **2'**.

As previously reported,[48] the antimicrobial activity of oligomer 1′ was evaluated and minimum inhibitory concentration (MIC) value for *S. aureus* determined (0.19 mg mL^{-1}). The MIC value of oligomer 2′ for the same bacteria was also obtained and the impact of carbamic acid enrichment on antimicrobial activity assessed. A higher MIC value (6.25 mg mL^{-1}) was obtained for oligomer 2′. As oligomer 2′ has a larger fraction of oligomer B, a satellite carbamic acid starting end ammonium-quaternized oligo(2-methyl-2-oxazoline), we can conclude that the biocidal effect arises from the non-fluorescent fraction of oligomer A, hydrogen starting end ammonium-quaternized oligo(2-methyl-2-oxazoline).

3.4.3. Origin of the intrinsic fluorescence

In order to discard any possible oxidation-triggered photoluminescence we have investigated the *living* polymerization and end-capping of OOXs in the total absence of oxygen using a High-Pressure Sapphire Cylindrical Cell (HPSCC) (supporting information). At the end of the polymerization reaction, emission spectra were recorded in total absence of oxygen using the HPSCC and an adapted high-pressure apparatus for luminescence measurements (supporting information). The oligomers obtained under these conditions, are identical to 1 and 1′, in all aspects, including fluorescence. We also investigated the addition of an oxidizing agent, ammonium persulfate $(NH_4)_2S_2O_8$, to aqueous solutions of 1 (48 h at rt), but no significant changes in the fluorescence were detected. Moreover, emission spectra of 1 at different pH values (pH=1, 6 and 13) were measured in order to evaluate a possible fluorescence pH dependence, but found that the oligomers emission is not pH sensitive. As observed in Figure 3.2, carbamic acid enriched oligomers showed enhanced fluorescence intensity. In addition, we performed the acid hydrolysis of 1, as firstly reported by us,[109] in order to obtain the corresponding linear oligoethylenimine hydrochloride (**3**). From FTIR, ^{1}H and ^{13}C NMR spectra analysis it was possible to conclude that complete hydrolysis of both oxazoline's acetyl and carbamic acid groups occurred. Oligomer 3 showed no fluorescence (data not shown). In order to finally confirm that the carbamic acid was in fact the primary agent responsible for OOXs fluorescence, we synthesized tris(2- aminoethyl)amine carbamic acid (**4**) from tris(2-aminoethyl)amine (**5**) using $scCO_2$ (see Supplementary data). While no emission was observed for 5, the carbamate derivative 4 showed a blue emission (Figure 3.4).

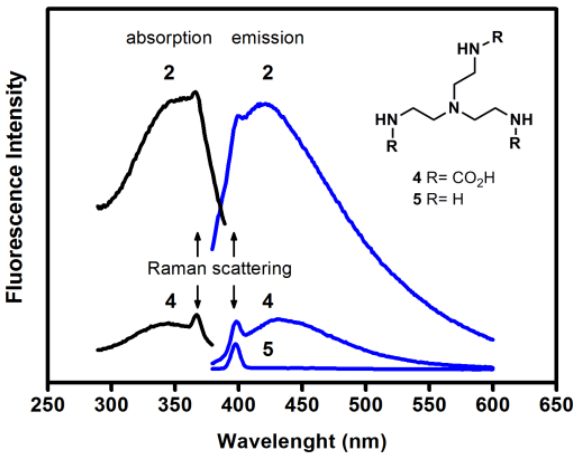

Figure 3.4 - . Excitation (λ_{em}= 420 nm; black lines) and emission (λ_{ex}= 350 nm; blue lines) spectra of oligo(2-methyl-2-oxazoline) (**2**) synthesized in $scCO_2$ and tris(2-aminoethyl)amine carbamic acid (**4**), taken in water. The emission spectra of tris(2-aminoethyl)amine (**5**) in water are also shown for comparison.

High intensity spectra correspond to **2** and medium intensity to **4**. Compound **5** only shows background emission. Same excitation and emission wavelength were observed for both oligomer **2** and reference compound **4**, showing undoubtedly that fluorescence is due to the same chemical group, carbamic acid.

3.5. Conclusions

The fluorescence of enriched carbamic acid linear oligooxazolines without on-chain fluorophores was reported for the first time. We have developed a versatile way to manipulate the light-emission properties of oligooxazolines through control of their starting end functionalization with a carbamic acid, achieved by a cationic ring-opening oligomerization of 2-oxazolines in supercritical carbon dioxide. The unexpected fluorescence of antimicrobial oligooxazolines was used in the labeling of gram-positive *S. aureus* cells. Our results show that ammonium-quaternized oligooxazolines with a satellite carbamic acid starting end are valuable non-toxic blue fluorescent biotags for biological sensing applications.

3.6. Acknowledgments

We acknowledge LabRMN at FCT-UNL and Rede Nacional de RMN for access to the facilities. Rede Nacional is supported with funds from FCT-Lisbon, Projecto de Re-equipamento Científico, Portugal. We thank the financial support fromFundação para a Ciência e a Tecnologia (FC&T), through contracts PTDC/QUI/73939/2006, MIT-Pt/BS-CTRM/0051/2008 and doctoral grant SFRH/BD/74730/2010, FEDER, FSE. VDBB is supported by the MIT-Portugal Program (Bioengineering Systems Focus Area). AAR is grateful to E Melo, S Abecasis, P Ricardo and C Mata for their help and technical support in the design of the HPSCC.

Chapter 4. Anti-biofouling 3D porous systems: the blend effect of oxazoline-based oligomers on chitosan scaffolds

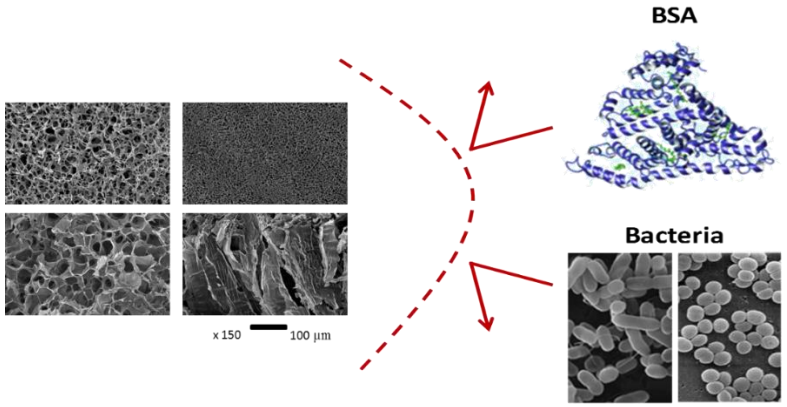

Manuscript published in

2013, Biofouling: The Journal of Bioadhesion and Biofilm Research, 29, 273-282
VG Correia, M Coelho, T Barroso, VP Raje, VDB Bonifácio, T Casimiro, MG Pinho and A Aguiar-Ricardo
Anti-biofouling 3D porous systems: the blend effect of oxazoline-based oligomers on chitosan scaffolds.

Personal contribution
VGC contributed to the design of the work, performed most of the experimental work, including all the bacterial cells assays, interpreted the data and wrote the manuscript.

4.1. Abstract

The production, characterization and anti-biofouling activity of 3D porous scaffolds combining different blends of chitosan and oxazoline-based antimicrobial oligomers is reported. The incorporation of ammonium quaternized oligo(2-oxazoline)s in the scaffold composition enhances the chitosan scaffold stability under physiological conditions as well as the ability to repel protein adsorption. The blended scaffolds showed mean pore sizes in the range of 18–32µm, a good pore interconnectivity and high porosity, as well as a large surface area, ultimate key features for anti-biofouling applications. The bovine serum albumin (BSA) adhesion profiles showed that the scaffolds composition plays a critical role in the chitosan-oligooxazoline system. Oligobisoxazoline enriched scaffolds (20 % w/w, CB8020) decreased protein adsorption (BSA) up to 70 %. Moreover, one mg of CB8020 was able to kill 99.9 % of *E. coli* bacteria upon contact, demonstrating its potential as promising material for production of tailored nonfouling 3D structures to be used in the construction of novel devices with applications in the biomedical field and water treatment processes.

4.2. Introduction

Biofouling, the non-specific surface adhesion of proteins, bacteria and higher organisms,[110,111] is a worldwide problem affecting a variety of areas such as industries, waterworks and medicine.[8] It affects devices performance, which can influence both water quality and consumer health;[112] it decreases product quality in pharmaceutical and food manufacturing industries[113] and it can result in the contamination of medical implants and surfaces in the hospital environment.[8] For these reasons, anti-biofouling strategies can have a large economic impact in many fields, increasing production and avoiding expensive remediation.

Biofouling is a multistage process that, when caused by bacteria, starts with the formation of a "conditioning biofilm" in which bacterial adhesion to a surface is an essential step.[114] Primary adhesion between bacteria and surfaces is generally mediated by nonspecific interactions, namely electrostatic forces. In this initial stage, bacterial adhesion is still reversible. In a second stage, the microorganism consolidates its adhesion through the production of extracellular proteins. Since these proteins are able to complex with surfaces, adhesion becomes irreversible and a maturation process is initiated. When a critical mass is reached, the biofilm outer layer starts to generate planktonic bacteria that can colonize other surfaces (Figure 4.1).[115]

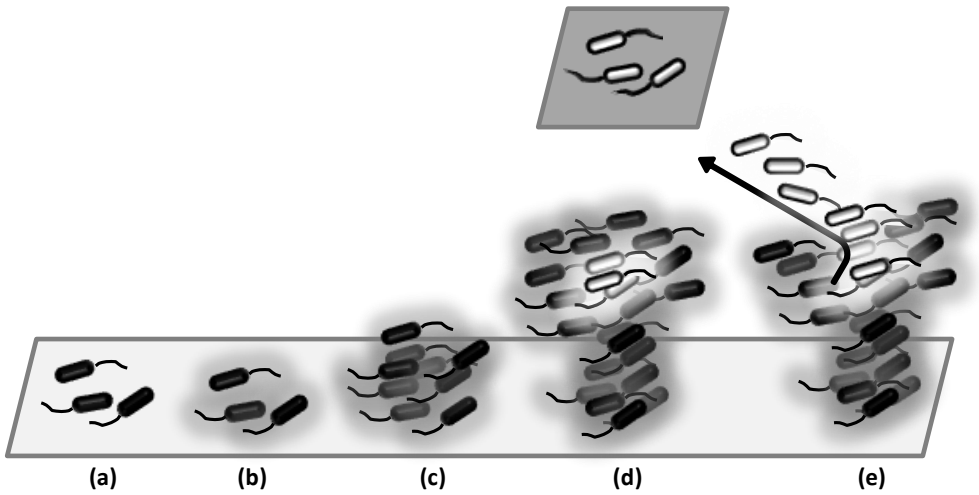

Figure 4.1 - A multistep process for biofilm formation: (a) reversible bacterial adhesion to the surface, mediated by electrostatic interactions; (b) the anchoring phase, where extracellular proteins are produced and complexed to the surface; (c) maturation; (d) bacterial population growth, with heterogeneous pattern within the biofilm; (e) generation of planktonic bacterial cells phenotypically adapted to the microenvironment conditions of the biofilm, and able to colonize other surfaces.

Currently, biocontamination is usually controlled by numerous disinfection processes which make use of common antimicrobials that act non-specifically against multiple microbial targets. Unfortunately, these chemicals are not always efficient against biofilms, leading to public health problems, since surface-bound cells are believed to be generally more resistant to antimicrobials than their planktonic counterparts. The mechanisms involved in biofilm resistance to disinfectants have been extensively studied[115,116] and are related to diffusion/reaction limitations of disinfectants in biofilms (the extracellular polymeric material produced by bacteria constitutes a barrier to the diffusion of biocides into the biofilm internal layers); or phenotypic adaptations of biofilm cells to sub-lethal concentrations of disinfectants which may result from the expression of specific genes in response to changes in micro-environmental conditions. In order to surpass biofilm resistance to disinfectants, the synergistic use of different treatments comprising different molecules and modes of action has been reported.[116] Diverse combinations of, for example, sodium hypochlorite, hydrogen peroxide, chlorhexidine, silver, surfactants, ultrasonic or sonic agitation, ultraviolet light and many others, have been described in the literature, referring the effectiveness of these compounds when used in association.[117–120] However, procedures involving these are time consuming, complex, environmentally unfriendly and do not always guarantee full biofilm eradication. Therefore, new strategies are needed to overcome bacterial adhesion to surfaces, particularly alternative solutions that make use of greener materials or environmentally friendly processes. Bioadhesion is known to be influenced by several factors and, consequently, the strategies to solve the biofouling problem may comprise: (1) mechanical detachment of

biofouling organisms and/or adsorbed molecules; (2) biofilm inactivation or killing by biocides and (3) surface modification to obtain low-adhesive and non-sticky materials. This last strategy, which leads to surfaces that prevent bacterial attachment, is accepted nowadays as the most promising and eco-friendly alternative to toxic biocides.[114] Since adhesion of bacteria to surfaces usually starts with protein adsorption, low protein adsorption is one of the most important requisites for a material to resist to biofouling. Proteins are versatile macromolecules that can have different adsorption mechanisms, which can be affected by various factors such as surface chemical composition, surface hydrophilic/hydrophobic charge and the mobility of surface functional groups. The biofouling resistance of a surface can be assessed by the adsorption profile of bovine serum albumin (BSA), an useful initial assay for the development of strongly low-adhesive, protein-repellent, bioinert materials and non-sticking fouling release surfaces.[114] Besides the ability to resist protein adhesion, good mechanical properties and materials wettability also play an important role in the development of surfaces that can resist biofilm formation.

Functional polymers represent a new class of antifouling and antimicrobial agents as alternative to antibiotics, for which tunable chemical and mechanical properties can be obtained through biomaterials engineering. Taking advantage of the available antimicrobial polymers and the possibility of incorporating and combining them into different 3D structures, it is now possible to design biocidal matrices with tuned biocidal efficiency. The incorporation of hydrophilic well-hydrated polymers into a surface, commonly designated by biopassive surface coatings, reduces the adsorption of proteins and thus the adhesion of bacteria, but does not actively interact with bacteria to kill them. In marked contrast, surface immobilized bioactive polymers can kill bacteria on contact. This mechanism is well reported for antimicrobial agents such as quaternary ammonium compounds, guanides, phosphonium salts, or antibiotics.[121] The first polymer that became a commercial disinfectant was poly(hexamethylene biguanidinium hydrochloride), thoroughly investigated by Ikeda et al..[32] The antimicrobial activity of protonated tertiary and primary amino groups has also been recently described, as well as that of different polymers and copolymers, such as poly(phenylene ethynylene)s and dimethylaminomethyl styrene,[122] and copolymers of dimethylaminoethylacrylamide and aminoethylacrylamide.[123] Hyperbranched polyethylenimine is another example of a strong antimicrobial due to a high density of antimicrobial groups per chain.[124] Surfaces which repel microbes were also achieved using hydrogel coatings (mostly based on polyethylene glycol, PEG),[56] obtained through the incorporation of negatively charged groups or through ultrahydrophobic modifications.[57] Non-fouling poly(2-methyl-2-oxazoline) (PMOXA)-based coatings have emerged as a promising alternative for the replacement of PEGs by more biocompatible analogues.[111] Importantly PMOXA-modified substrata constitute a biopassive approach to reduce biofouling and their ability to resist protein and bacteria adhesion (without killing) is mainly due to higher

hydrophilicity. In order to obtain stable bioactive substrata that prevent biofouling, antimicrobial moieties have to be attached onto polymeric backbones by covalent interactions. Previously reported approaches involve the use of antimicrobial groups that are usually grafted to the polymer backbone or inserted in the main-chain of polymers synthesized using monomers bearing antimicrobial moieties.[125] Several other studies have shown that biocidal endcapping is also an effective strategy.[48,59] Most of the reported approaches involve many chemical steps and the use of organic solvents and, for that reason, are not attractive from an economical point of view.

In this paper, the production of highly biocidal and biocompatible materials using a new strategy that combines the use of natural and greenly synthesized antimicrobial polymers. Chitosan (CHT) is the *N*-deacetylated derivative of chitin, a polycationic polysaccharide. This inexpensive, non-toxic, biodegradable and biocompatible biopolymer shows good water permeability and good chemical resistance.[126] CHT has been widely employed to develop suitable 3D supports for applications in tissue engineering[127,128] and controlled drug delivery.[129] Oligo(2-oxazoline)s, due to their biocompatibility and easy quaternization, represent a unique approach to the development of new antibiotics and have been explored in the last few years as strong candidates for the development of new polymer therapeutics.[24,52–55] The synthesis of these polymers using conventional,[26] microwave-assisted[27,130] and green (synthesis in supercritical carbon dioxide) methodologies[23] has been previously described. Recently, a series of 2-oxazoline-based oligomers enriched with satellite carbamic acid starting end and ammonium quaternized terminated were successfully obtained using supercritical carbon dioxide via cationic ring-opening polymerization (CROP), resulting in 2-oxazoline-based oligomers which were active against bacteria and fungi.[48] The synthesis and quaternization of branched oligo(2-bisoxazoline) and the synthesis of linear oligo(ethylenimine) hydrochloride, prepared by acid hydrolysis of oligo(2-oxazoline), were also reported for the first time by Correia et al..[48] This library of oligomers proved to have a broad spectrum activity against different micro-organisms comprising fungi and Gram-positive and Gram-negative bacteria, while being biocompatible to fibroblast cells. Therefore, the incorporation of the most effective cationic antimicrobial oligomers (oligo (2-methyl-2-oxazoline) quaternized with *N*,*N*-dimethyldodecylamine, oligo(2-bisoxazoline) quaternized with *N*,*N*-dimethyldodecylamine and linear oligoethylenimine hydrochloride) into a 3D structure might represent an efficient alternative to conventional strategies to prevent protein adsorption and subsequent bioadhesion.

Herein, a systematic study of the anti-biofouling profile of 3D macroporous biocomposites is presented, with controlled morphological and mechanical properties, obtained by cross-linking a blend of fully biocompatible oligo(2-oxazoline)s and chitosan. The performance of these devices as antifouling bioactive matrices was evaluated using BSA adhesion assays. The antimicrobial

activity was assessed by direct exposure of *Staphylococcus aureus* and *Escherichia coli* cells to the scaffolds.

4.3. Experimental Section

4.3.1. Materials

Chitosan (CHT) (75-85 % deacetylated, M_w = 190–310 kg.mol^{-1}), *N,N'*-methylenebisacrylamide (MBA), monomer 2-methyl-2-oxazoline (MeOx, purity > 98 %), initiator boron trifluoride diethyl etherate ($BF_3.OEt_2$, synthesis grade), ammonium persulfate (PSA), *N,N,N,N*-tetramethylethlenediamine (TEMED), glacial acetic acid (purity ≥ 99 %), phosphate buffered saline (PBS) and bovine serum albumin (BSA, purity ≥98 %) were purchased from Sigma-Aldrich. The monomer 2-bisoxazoline (BisOx) was synthesized following a procedure described by H. Witte et al..[95] *N,N*-dimethyldodecylamine was purchased from Fluka. Ethanol (p.a.) was purchased from Pancreac. Mueller-Hinton broth medium was purchased from Oxoid. Carbon dioxide was supplied by Air Liquide with a purity of 99.998 %. All materials and solvents were used as received without any further purification. Oligo(2-methyl-2-oxazoline) quaternized with *N,N*-dimethyldodecylamine (**M**), oligo(2-bisoxazoline) quaternized with *N,N*-dimethyldodecylamine (**B**), and linear oligoethylenimine hydrochloride (**E**) were synthesized as described previously.[48]

4.3.2. Scaffolds preparation

Scaffolds were prepared by the freeze-drying method.[131] Briefly, the casting solutions with concentrations of 3 % (w/v) were prepared by dissolving chitosan or a mixture of chitosan/oligo(2-oxazoline) in acetic acid 1 % (v/v) at room temperature under stirring. The casting solutions were prepared using 90 % or 80 % (w/w) of chitosan and 10 % or 20 % (w/w) of oligo(2-oxazoline), respectively. A cross-linking agent (MBA, 2% w/w) was also added to the mixture. The homogeneous solutions were cooled and 74 µL PSA solution (0.1 g.mL^{-1}) and 46 µL of TEMED were added to the mixtures and stirred overnight. The solutions were then placed in sample tubes with an inner diameter of 1.2 cm and 3 cm height. The sample tubes were freeze-dried at -20 ºC during 20 minutes. Afterwards, the scaffolds were washed with ethanol in order to remove remaining cross-linker.[132] Finally, the scaffolds were placed in a high pressure cell and

fully cleaned with a pure CO_2 flow during one hour. At the end of this operation, the system was depressurized and the scaffolds were collected.

4.3.3. Scaffolds characterization

The morphology of the scaffolds was recorded using scanning electron microscopy (SEM) in a Hitachi S-2400 equipment, with an accelerating voltage set to 15 kV. The scaffold samples were frozen and fractured in liquid nitrogen for cross-section analysis. All samples were coated with gold before analysis.

The compression modulus of the scaffolds was determined with a tensile testing equipment (*MINIMAT firm-ware* v.3.1). Samples with length of 1 cm and width of 1 cm were compressed until their deformation. The used speed of testing was 1 $mm.min^{-1}$. A full scale load of 20 N was used. The compression modulus was calculated from the slope of the linear portion of the stress-strain curve. All samples were tested in dry state at room temperature.

Load compression graphs were obtained during testing and converted to stress strain curves applying equations:

$$Stress = \sigma = \frac{F}{A} \qquad (1)$$

$$Strain = \varepsilon = \frac{\Delta l}{L} \qquad (2)$$

where F is the applied force, A the cross sectional area, Δl is the change in length and L is the length between clamps.

Scaffolds porosity and pore size distribution were determined by mercury porosimetry (micromeritics, autopore IV). The scaffolds stability in PBS solution (pH 7.4) was also evaluated. Scaffolds samples were immersed in 10 mL of PBS at 37 ºC during 63 days. Samples were removed from the medium periodically, freeze dried for 24 hours and then weighted. A new PBS solution was always used after each freeze-drying step.

The water fluxes were determined at 37 ºC and 1 atm. Due to the high porosity of the scaffold network no pressure was applied. Thus, Varian columns (with a capacity of 3 mL and an effective volume of 1.2 cm^3) were packed with antimicrobial scaffolds and charged with 1 mL of distilled water. The run time was registered and at least three measurements of distilled water flux were recorded.

4.3.4. Protein adsorption assays

A scaffold sample of approximately 45 mg was immersed in BSA solution (1 $mg.mL^{-1}$). Samples were withdrawn from the solution in order to evaluate the protein concentration in the medium after 48 h (loading step). At the end of the assays, the scaffolds were removed and washed with PBS in order to remove the BSA absorbed into the scaffold (recovery step). In parallel, and in order to evaluate the leaching of the antimicrobial polymer from the blend, the samples were placed in PBS solution (control). The absorbance at 280 nm was measured periodically. The protein percentage was normalized to the scaffold's weight.

4.3.5. Bacteria viability after direct exposure to scaffolds

S. aureus NCTC8325-4 and *E. coli AB1157* bacterial strains were grown in Mueller-Hinton broth medium. Cultures were grown overnight in broth at 37 ºC. Blended scaffolds were placed in the wells of 24-well plates containing, in each well, a volume of 1 mL of medium with a scaffold sample of approximately 4.5 mg. Each well was inoculated with 5 µL of culture (approximately $5x10^5$ cells) and plates were incubated at 37 ºC to assess the viability of bacterial cells. After incubation (1 h and 18 h), the medium with bacteria was plated on Muller Hinton Broth agar and incubated at 37 ºC for 24 h, and the number of bacterial colonies was determined. The influence of stirring (no stirring or stirring at 100 rpm) on bacterial viability was also tested. Experiments were performed in duplicate for both *S. aureus* and *E. coli* strains. The results were normalized per mg of scaffold.

4.4. Results and Discussion

4.4.1. Scaffolds preparation

Antimicrobial oligo(2-oxazoline)s enriched CHT scaffolds were prepared. In order to evaluate the impact of the addition of antimicrobial oligomers to a CHT native scaffold, CHT was blended with three different oligo(2-oxazoline)s synthesized in supercritical carbon dioxide.[48] The scaffolds were prepared by freeze-drying using different percentages (10 or 20 %) of oligo(2-oxazoline)s (Scheme 4.1). The blended materials were further characterized to evaluate the morphology as well as the mechanical, protein-repellent and antimicrobial properties.

CHT

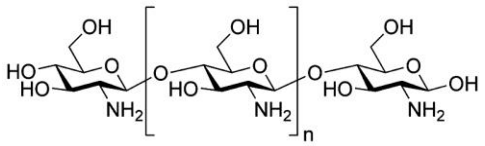

Oligomer M

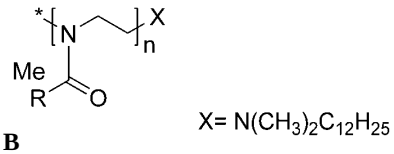

Oligomer B

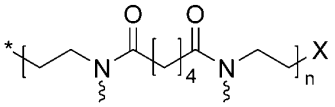

Oligomer E

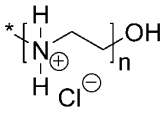

Scheme 4.1 - Polymeric compounds used in the preparation of 3D macroporous biocomposites: **CHT**-chitosan, **M**- Oligo(2-methyl-2-oxazoline) quaternized with *N*,*N*-dimethyldodecylamine, **B**- Oligo(2-bisoxazoline) quaternized with *N*,*N*-dimethyldodecylamine, and **E**- Linear oligoethylenimine hydrochloride.

CHT native scaffold stands for 100 % **CHT.** The scaffolds blended composition will be described hereinafter as: CM9010 – 90 % of **CHT** blended with 10 % of oligomer **M**; CM8020 – 80 % of **CHT** blended with 20 % of oligomer **M**; CB9010 – 90 % of **CHT** blended with 10 % of oligomer **B**; CB8020 – 80 % of **CHT** blended with 20 % of oligomer **B**; CE9010 – 90 % of **CHT** blended with 10 % of oligomer **E**; CE8020 – 80 % of **CHT** blended with 20 % of oligomer **E**.

4.4.2. Scaffolds characterization

The native CHT scaffold and antimicrobial oligo(2-oxazoline)s-enriched CHT scaffolds were characterized to assess their mechanical and morphological properties as well as water permeability. Mercury intrusion porosimetry data showed variations in average pore size diameter and the pore size distribution and water fluxes, depending on the oligo(2-oxazoline), and its content in the casting solution. The data obtained are summarized in Table 4.1and Figure 4.2.

Table 4.1 - Compression modulus, porosity, average pore size diameter and water permeability of the scaffolds produced.

Scaffold	Compression modulus (kPa)	Porosity (%)	Average pore size diameter (μm)	Water flux ($L.m^{-2}.h^{-1}$)
CHT	2.2±1.3	90±5	26 ± 5	3.0 ± 0.2
CM9010	2.0±0.6	91±5	27 ± 5	15.4 ± 3.9
CM8020	1.6±0.3	90±5	19 ± 5	4.4 ± 0.8
CB9010	3.9±1.1	90±5	25 ± 5	4.4 ± 0.9
CB8020	1.4±0.0	90±5	32 ± 5	110 ± 20
CE9010	1.4±0.8	90±5	21 ± 5	n.a.
CE8020	1.2±0.0	91±5	24 ± 5	n.a.

All the scaffolds produced were highly porous (~ 90 %) with an average pore size diameter in the range 18-32 μm. The mechanical properties were not greatly influenced by the presence of oligo(2-oxazoline) since all 3D matrices showed a similar compression modulus and, consequently, similar stiffness. Moreover, the incorporation of oligomer M in the scaffold composition did not significantly change the water flux. Contrarily, a high water flux can be observed for the CB8020 scaffold, 40 times higher than that obtained for the CHT native scaffold. The increase in the oligo(2-bisoxazoline) content of the scaffold composition increased the average pore size diameter leading to higher water permeability. Furthermore, oligo(2-substituted-2-oxazoline) are hydrophilic polymers that showed very promising properties in antifouling applications and its incorporation in the blend was expected to improve scaffolds hydrophilicity and consequently the water flux permeability.[133] However, this was only observed for oligomer B. The methodology used (cross-linking, solvent, purification) may influence the polarity and the physical arrangement of the hydrophilic oligo(2-oxazoline) chains in the cross-

linked network. Therefore, it is possible that the oligomer B chains in the blend were enriched in the surface pore walls and ultimately in the scaffold surface, providing extra hydrophilicity. The water flux permeability for scaffolds containing oligomer E could not be measured due to the poor stability of the supports.

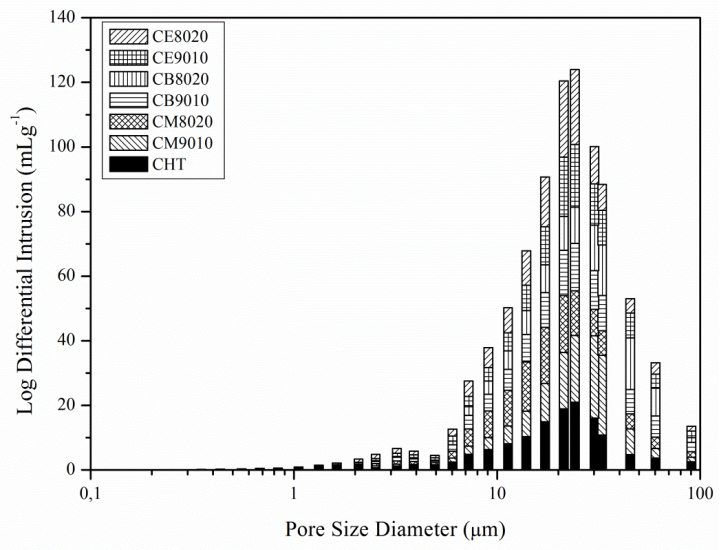

Figure 4.2 - Comparison of pore size distributions obtained for CHT native scaffold and for antimicrobial oligo(2-oxazoline)s-enriched CHT scaffolds: CM9010, CM8020, CB9010, CB8020, CE9010 and CE8020.

These results are in agreement with data collected from the SEM images (Figure 4.3). The SEM micrographs (see cross-sections) show that all scaffolds have elongated pores with high interconnectivity and porosity. This type of 3D structure, combining high porosity, interconnectivity and pore sizes (>18 μm) larger than bacterial cell diameter (<2 μm), is entirely suitable for applications that envisage the development of materials with strong biocidal activity. In addition, the large surface area is an important advantage to promote bacterial killing upon contact.

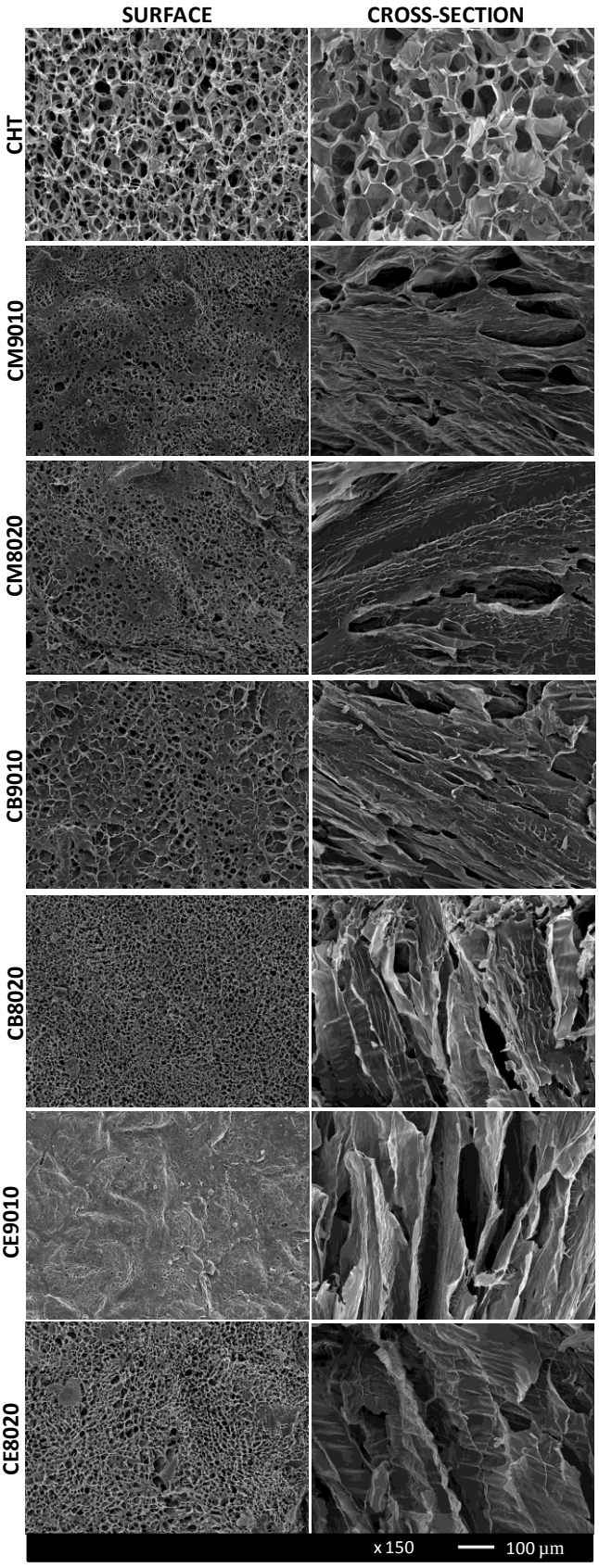

Figure 4.3- SEM micrographs of surface and cross-sections of the CHT native scaffold and antimicrobial oligo(2-oxazoline)s-enriched CHT scaffolds CM9010, CM8020, CB9010, CB8020, CE9010 and CE8020.

Figure 4.4 exhibits the stability of the scaffolds in PBS solution during 63 days. The addition of oligo(2-oxazoline)s to the blend clearly improved the stability of the materials when compared to a CHT native scaffold. The CHT native scaffold presented a higher swelling ratio than the antimicrobial oligo(2-oxazoline)s-enriched CHT scaffolds, and its expanded 3D structure was be the most fragile. After 63 days at 37 ºC, all antimicrobial oligo(2-oxazoline)s-enriched CHT scaffolds, except CE8020, proved to be highly stable, maintaining 90 % of the initial weight, suggesting that the scaffolds can be reused in antifouling applications. These results also show that the materials are physical blends where the antimicrobial oligomers are immobilized within the cross-linked CHT network. The fast degradation of the CE8020 scaffold can be correlated with the easier leaching of oligomer E from the network. Due to the linearity of oligomer E its diffusion through the network should be facilitated, comparated to oligomers M and B (oligomer M has pendant groups along the backbone and oligomer B is a branched oligomer).

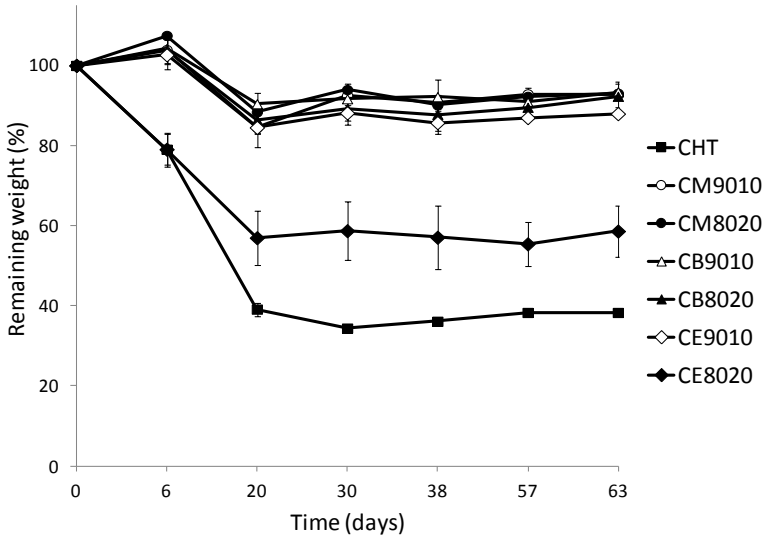

Figure 4.4 - Structure stability of the native CHT scaffold and the antimicrobial oligo(2-oxazoline)s-enriched CHT scaffolds in PBS solution (pH 7.4) during 63 days.

4.4.3.Protein adsorption assays

Specific proteins, namely adhesins, are necessary for the initial attachment that constitutes the first step of biofilm development, therefore protein adsorption assays can be used to assess the efficacy of the fouling resistance of materials.[134] Antifouling assays were performed by determining the adhesion profiles of BSA, a model protein. The BSA retained in the scaffold was calculated through the difference between BSA concentration in the initial solution and BSA quantified in both loading (BSA in the medium) and recovery step (BSA recovered – reversible fouling) (Figure 4.5).

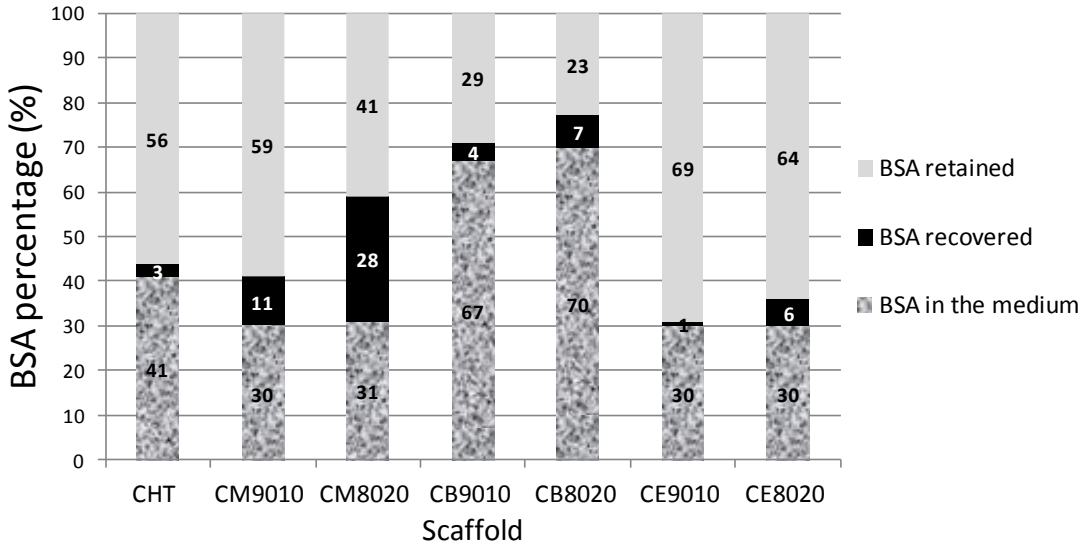

Figure 4.5 - BSA adhesion profiles (BSA in the medium, recovered and retained (%)) for the native CHT and the different antimicrobial oligo(2-oxazoline)s-enriched CHT scaffolds. Percentage values are indicated in the histogram. All protein percentage values were normalized to the weight of the scaffolds.

Figure 4.5 shows that addition of oligomers M and E to the scaffold led to a decrease in the BSA remaining in the medium while oligomer B led to an increase of BSA in the medium. This means that incorporation of oligomer B to CHT improved the protein repellent properties of the scaffold. Moreover, the increase of B ratio from 10 to 20 % in the scaffold composition resulted in a twofold increase in the recovery of adsorbed BSA. Since the addition of oligomer B allowed a better protein-repellent profile, CB8020 becomes the most promising of the tested scaffolds for anti-biofouling applications if bacterial adhesion can be precluded by the removal of the attachment platform.

4.4.4.Bacteria viability after direct exposure to scaffolds

To test the biological relevance of findings previously discussed and to characterize the ability of the scaffolds to kill bacteria upon contact, bacterial viability after direct exposure to antimicrobial oligo(2-oxazoline)s-enriched CHT surfaces was evaluated using *E. coli* and *S. aureus*.

The viability of bacterial cells was assessed by incubating the materials in medium containing approximately 10^5 cells. After incubation, the medium was plated and the number of colony forming units was counted to assess bacteria viability. Two assays were carried out in parallel to study the impact of stirring on bacterial killing (Figure 4.6(a)). Scaffolds containing antimicrobial oligomers that are only able to kill bacteria upon contact are expected to have an increased killing

activity when the medium containing bacteria is stirred, given that stirring ensures a homogeneous and continuous contact between bacteria and the 3D scaffold.

The leaching properties of antibacterial materials is of great relevance, as leached biocide will lead to a loss of biocidal activity, to additional problems related with cytotoxicity of the released agent, as well as to the possible development of resistance in the presence of sub-inhibitory concentrations of biocide in the medium. To evaluate the presence of leached biocide, medium that was in contact with the scaffold was collected and inoculated with bacteria. The ability to inhibit bacterial growth at 37 ºC was then assessed (Figure 4.6(b)).

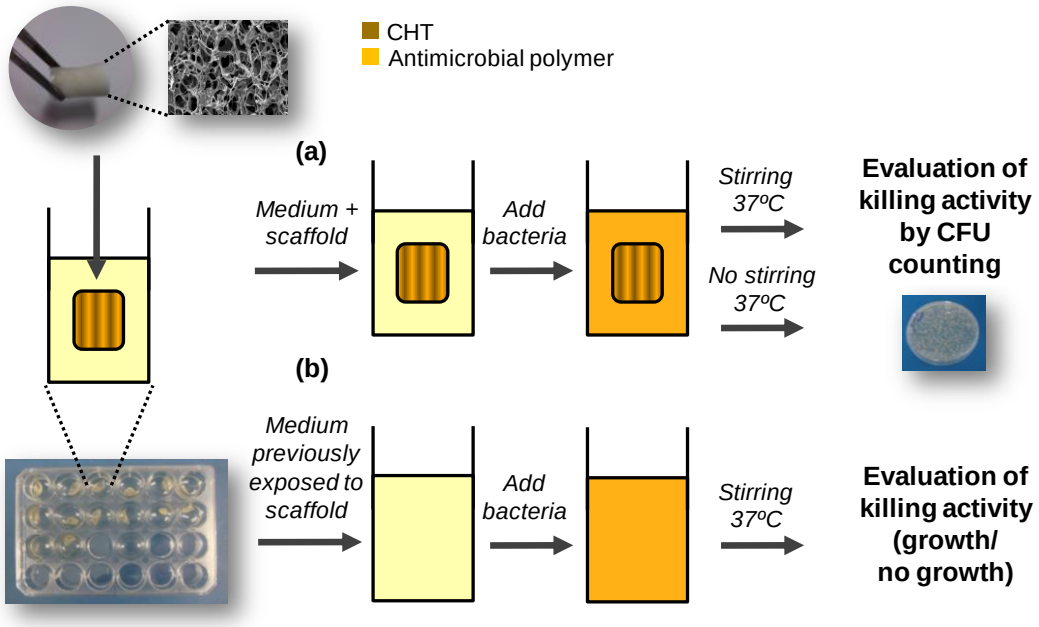

Figure 4.6 - Schematic representation of the methodology used to assess killing activity of scaffolds. (a) Bacterial viability after direct exposure to the scaffolds. The well containing the scaffold and culture medium was inoculated with bacteria (10^5 cells) and the influence of stirring on the reduction in bacterial viability was assessed after 1h and 18h by CFU counting. (b) Evaluation of the presence of leached biocide from the scaffold. The well containing the medium exposed to the scaffold was inoculated with bacteria (10^5 cells) and the presence of leached biocide in the medium was assessed by the presence or absence of bacterial growth.

In addition, in order to ensure that the scaffolds were not colonized with bacteria, the 3D structures were placed in medium at 37 ºC. No visible bacterial growth was observed after 24 hours, indicating that they are ready-to-use for bacterial assays.

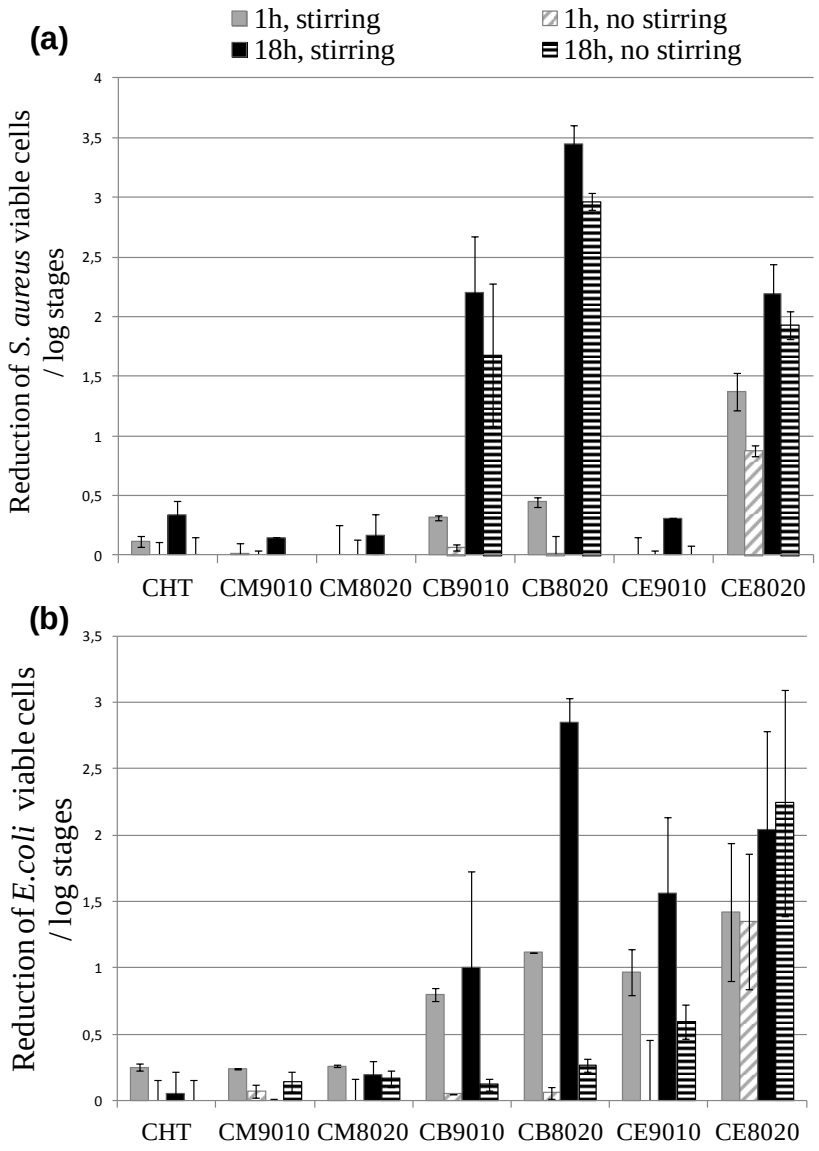

Figure 4.7 - Killing of (a) *S. aureus* and (b) *E. coli* by direct exposure to biocidal chitosan-based scaffolds. The results are presented in a logarithmic scale as the reduction in number of viable cells mg^{-1} of scaffold used (1 log stage = a reduction of 90 %, 2 log stages = a reduction of 99 %, 3 log stages = a reduction of 99.9 %).

Incubation of bacterial cells, with stirring, in the presence of the native CHT scaffold killed <50 % of *S. aureus* cells (<0.5 log reduction). Addition of oligomer M did not improve the antibacterial properties of the chitosan-based scaffold. In marked contrast, addition of oligomer B into the blend improved the material antibacterial performance. After 18 h, the scaffold reduced the viability of *S. aureus* cells by close to 99 % with or without stirring, indicating that stirring does not greatly increase the killing activity against these gram-positive bacteria. This could indicate that the killing activity observed was mainly due to the release of the antimicrobial agent to the medium. In accordance, we observed that medium previously incubated with this scaffold

had antimicrobial activity as it was shown to kill *S. aureus* cells. Importantly, this data does not determine the extent of leaching of oligomer B from the scaffold (which seems low, based on the stability tests) but they merely indicates that the amount of leached oligomer B is sufficient to kill planktonic bacteria in these experimental conditions. The increase in oligomer B content in the scaffold composition led to increased antimicrobial activity. Incorporation of oligomer E into the chitosan blend resulted in a scaffold whose killing activity was not significantly dependent on stirring, suggesting that the killing mechanism is not dependent on contact. The fact that >90 % of bacteria were killed within 1 hour could be due to the rapid release of this oligomer from the 3D matrix to the medium, in agreement with the data obtained in the stability tests in PBS. Additionally, the medium exposed to this scaffold had killing activity against *S. aureus* (Figure 4.7(a) and Table 4.2Table 4.2 - *S. aureus* and *E. coli g*rowth (+) or killing (-) in medium previously exposed to the scaffold.).

Killing of *E. coli* in the presence of native CHT and CHT-based scaffolds containing oligomer M was similar to that of *S. aureus*. However, the effect of the addition of oligomer B to the antimicrobial performance of the scaffolds was strongly influenced by the presence or absence of stirring. Upon stirring, 1 mg of scaffold containing 20 % of oligomer B was able to reduce viable *E. coli* by almost 99.9 %, while in the absence of stirring this reduction was <68 %, suggesting that scaffolds containing oligomer B killed the Gram-negative bacterium *E. coli* upon contact. As previously discussed in the scaffold characterization section, oligomer B should be preferentially positioned at the matrix interface, directing its chains to the surface of the pores thus being more accessible to the bacteria. This fact emphasizes the substantial killing ability upon contact with this scaffold compared to those containing oligomer M. Scaffolds containing oligomer E also decreased bacterial viability but the oligomer released to the medium had a major contribution to this effect, as confirmed by additional tests where medium exposed to the scaffolds had killing activity against *E. coli* (Figure 4.7(b) and Table 4.2).

Table 4.2 - *S. aureus* and *E. coli g*rowth (+) or killing (-) in medium previously exposed to the scaffold.

	S. aureus				*E. coli*			
Scaffold	1/1	1/2	1/4	1/8	1/1	1/2	1/4	1/8
CHT	+	+	+	+	+	+	+	+
CM9010	+	+	+	+	+	+	+	+
CM8020	+	+	+	+	+	+	+	+
CB9010	-	+	+	+	+	+	+	+
CB8020	-	+	+	+	+	+	+	+
CE9010	+	+	+	+	-	+	+	+
CE8020	-	-	-	-	-	-	-	+

Notes: Bacterial killing indicates the presence of leached biocide in the medium (dilution 1/1). Sequential twofold dilutions were performed (dilutions 1/2, 1/4 and 1/8) to assess the ability to kill bacteria.

The differences observed in the killing activity of 3D structures against different bacterial species can be justified by the different cell wall structure of Gram-negative and Gram-positive bacteria. In a previous work,[48] it was hypothesized that antimicrobial oligo(2-oxazoline)s can inhibit the growth of the Gram-negative bacteria *E. coli*, by acting at the outer membrane while for *S. aureus* the antimicrobial oligomer needs to difuse through the thicker peptidoglycan layer to be effective in the inner membrane. This diffusion would be impaired when the antimicrobial oligo(2-oxazoline)s are immobilized in the blended scaffolds. To overcome this problem, oligo(2-oxazoline)s should be located at the scaffold surface so that the antimicrobial group at the chain end can easily kill bacteria while covalently immobilized in the structure.

4.5. Conclusions

In order to develop 3D structures able to kill bacteria upon contact and prevent bacterial biofilm formation, oxazoline-based antimicrobial oligomers were blended into CHT scaffolds produced by a freeze-drying technique followed by a $scCO_2$-assisted process. By varying the antimicrobial polymer concentration in the casting solution, the hydrophilicity, permeability, BSA adhesion profiles and bacteria killing activity of CHT-based scaffolds could be tuned. CB8020 was the 3D structure with best performance in repelling protein and killing bacteria upon contact. Moreover,

1mg of CB8020 scaffold was sufficient to kill 99.9 % of an initial *E. coli* inoculum of $5x10^5$ CFU mL^{-1}.

For permanent antimicrobial effect, bacterial killing should occur upon contact. The development of new platforms is currently under study in order to improve mobile antimicrobial group density on the surfaces of materials, an important requisite for a highly active scaffold that kills different bacterial species upon contact. During recent years, several approaches have proposed for the removal or prevention of biofilm formation on surfaces. Some have had variable and short success, particularly so in biomedical field where the development of resistance by microorganisms after continued exposure to a specific antibiotic is a reality. Thus, the incorporation into a biomaterial of cationic oxazoline-based antimicrobial oligomers with proved broad-spectrum activity and rapid killing times represents an excellent anti-biofouling platform and a unique strategy to avoid the development of microorganism resistance in the context of biomedical applications and of water treatment processes.

4.6. Acknowledgments

The authors would like to thank the financial support from Fundação para a Ciência e Tecnologia (FCT-Lisbon) through contracts PEst-C/EQB/LA0006/2011, MIT-Pt/BS-CTRM/0051/ 2008, PTDC/EQU-EQU/116097/2009 and doctoral grants SFRH/BD/74730/2010 (VGC), SFRH/BD/75094/2010 (MC) and SFRH/BD/62475/2009 (TB). VDBB is supported by the MIT-Portugal Programme (Bioengineering Systems Focus Area). The authors also wish to thank the Analytical Services Laboratory of REQUIMTE, FCT/UNL.

Chapter 5. Antimicrobial contact-active oligo(2-oxazoline)s-grafted surfaces for fast water disinfection at the point-of-use

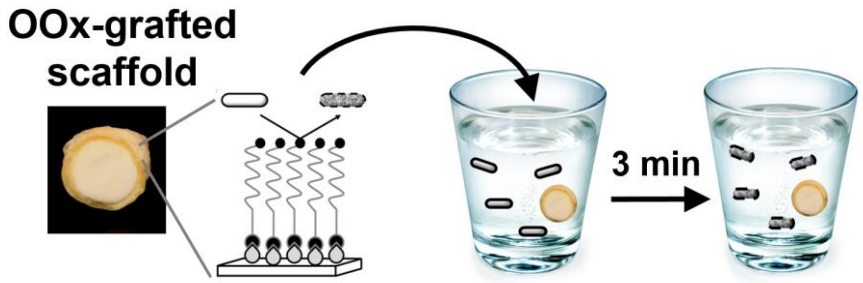

Manuscript published in

2015, Biomacromolecules, 16, 3904-3915
VG Correia, AM Ferraria, MG Pinho and A Aguiar-Ricardo
Antimicrobial contact-active oligo(2-oxazoline)s-grafted surfaces for fast water disinfection at the point-of-use.

Personal contribution
VGC contributed to the design of the work, performed all the experimental work except XPS analysis, SEM microscopy and water physico-chemical characterization, interpreted the data and wrote the manuscript.

5.1. Abstract

Water is one of the most valuable resources today and its purity is crucial to health and society well-being. The access to safe drinking water is decreasing in the world, which can have a huge socio-economic impact especially in developing countries, more prone to water-associated diseases. The goal of this work was to develop an innovative, fast and cost-effective 3D material capable of decontaminating water. We have used an eco-friendly strategy, combining plasma surface activation and supercritical fluid technology to produce, for the first time, a 2-oxazoline-grafted 3D surface with broad-spectrum contact-active antimicrobial properties. Oligo(2-methyl-2-oxazoline) quaternized with *N,N*-dimethyldodecylamine and grafted to a chitosan (CHT) scaffold (CHT-OMetOx-DDA) efficiently and quickly (<3 min) killed >99.999 % of *Staphylococcus aureus* and *Escherichia coli* cells upon direct contact and avoided bacterial adhesion to the materials surface, which is important for the prevention of biofilm formation. As a proof of concept, CHT-OMetOx-DDA scaffold was demonstrated to be suitable for water purification efficiently killing the microorganisms present in different water samples within minutes of contact and without leaching to the water. Additionally, we report for the first time a new method to clearly distinguish two mechanisms of action of bioactive surfaces: contact-active and releasing systems.

5.2. Introduction

Water biocontamination can severely influence human health. There is an urgent need of new and effective solutions able to achieve safe drinking water quality.[135] The Center for Disease Control and Prevention (CDC) from the United States reported 33 drinking water–associated outbreaks during 2009-2010, comprising 1040 cases of illness, 85 hospitalizations, and 9 deaths. These drinking water-associated diseases were related to the presence of Legionella in plumbing systems (57.6 %), untreated ground water (24.2 %), and deficiencies of the distribution system (12.1 %).[136]

Conventional chemical processes used in drinking water purification rely on the use of chemicals, such as free chlorine, to significantly reduce the microorganisms present in the source water to a level that represents a negligible risk to the general population. However, these processes usually represent low protection against some viruses and parasites, their effectiveness is dependent on the presence of certain organic and inorganic compounds, there is a potential long-term carcinogenic effect of chlorination by-products and the long-term effect of discharging

dechlorinated compounds to the environment is unknown.[137] Ineffective bacterial decontamination processes have a great impact especially in developing countries where microbial diseases transmitted by water or lack of hygiene facilities constitute a major health problem.

A second area requiring the development of new materials with antibacterial activity is the prevention of biofilm formation. The unspecific absorption of substances or adhesion of bacteria to surfaces can lead to the formation of biofilms, which are intrinsically more resistant to antimicrobial agents and can alter the performance of a material.[138–140] Frequently, development of resistant bacterial species implies the use of higher doses of chemicals to achieve disinfection.[141] Recently, the use of alternative solutions like bacteria repelling and antiadhesive surfaces, materials with intrinsic antibacterial properties, antibacterial coatings, nanostructured materials, and molecules interfering with bacterial biofilm has been the focus of important research.[142–149] When assessing the performance of these materials it is important to consider the ability of the modified surfaces to eliminate a microbial threat upon contact[57] without leaching[31,150] and without the accumulation of killed microbes on the coated surface, which reduces antimicrobial activity over time.[151] Therefore, reusable and biocompatible new materials that impair formation of toxic byproducts and biofilms should be developed for disinfection and large spectrum microbial control. Ideally, the new alternatives should meet the principles of green chemistry by avoiding the use of hazardous solvents or reagents.

Polyethylene glycol (PEG) is a widely used polymer for substrates modification to obtain biocompatible coatings.[140,152,153] Recently, polyoxazolines (POXs) were described as biocompatible alternatives to PEG[51,154] and as an attractive new class of compounds for potential applications in the biomaterial field.[155] Commonly, biocompatible and biodegradable polymers of this class are synthesized by *living* cationic ring opening polymerization (CROP), allowing an excellent control in terms of chain length, polymer architecture, polydispersity and end-chain functionality.[48] Over the last years, the impact of different start- and end-chain functionalities in POXs antimicrobial activity has been assessed.[48,52,53,156,157] More recently, coating and modification of different surfaces with POXs has started to be reported in the literature for antifouling applications. However, materials coated with POX do not actively kill the bacteria, but merely prevent bacterial adhesion by changing material properties such as hydrophobicity. This constitutes a so-called biopassive approach, where the coating has repellent and antiadhesive characteristics than prevent bacterial colonisation.[58,73,158,159] Biopassive coating with POXs has the advantage of being easy to accomplish; by the end of the CROP, a *living polymer* is obtained that can be put in contact with a surface with functional groups that will react with the POX *living* polymer in an inert atmosphere. Hence, immobilization of POXs has, for now, been reported mainly as a *grafting to* approach (Figure 5.1A).

Modification of surfaces with POXs, not only to repel bacteria and avoid biofilm formation, but also to actively kill microorganisms (a so-called bioactive approach, Figure 5.1C) would be a major contribution to the development of new antimicrobial surfaces. In fact, POX can be modified to acquire antimicrobial activity, for example through the introduction of an antimicrobial group, such as quaternary ammonium groups, at the end of POX chains.

We have previously synthesized a library of ammonium quaternized oligo(2-oxazoline)s (OOXs) and characterized their antimicrobial activity to select the most promising oligomers for antimicrobial applications.[48] OOXs are a class of oligomers which can be synthesized by a sustainable synthetic route using supercritical carbon dioxide ($scCO_2$). Accordingly, their syntheses avoid the use of organic solvents and the need of downstream purification steps, resulting in green and less pollutant processes. Antimicrobial OOXs are biocompatible, active against fungi and a broad spectrum of bacteria, have short killing times and are believed not to generate resistant bacteria,[48] making them suitable for biomedical and water treatment applications. We have previously blended antimicrobial oligomers within polymeric matrices.[81] These materials were active against Gram-negative bacteria but not against Gram-positive bacteria, such as *S. aureus*, possibly because of the type of immobilization and the homogeneous distribution of the antimicrobial OOXs across the material and not only at its surface. This type of immobilization impairs oligomers access to the *S. aureus* membrane due to the presence of a thick peptidoglycan layer. The main challenge therefore is to immobilize OOXs only at the surface of the scaffolds, using green technologies. For that purpose, OOXs should be grafted not through the reactive end-chain (the *living polymer*) but through the opposite end-chain, so that the *living polymer* can be later functionalized with the antimicrobial group. In this way, the antimicrobial group would be located at the exterior of the thin coating film so that it can access and kill bacteria in the surroundings of the coated material.

In this work, ammonium quaternized oligo(2-oxazoline)s were, for the first time, covalently grafted onto 3D shaped polymeric chitosan scaffolds using a *grafting from* approach (Figure 5.1B). The covalent immobilization was performed using only green procedures, namely $scCO_2$ and plasma treatment. [82,83,160] In order to clearly elucidate if the produced bioactive surfaces killed the bacteria by mere contact or by releasing the antimicrobial agent to the medium, a new method to distinguish both systems was used and it is herein reported for the first time. CHT-OMetOx-DDA efficiently killed *S. aureus* and *E. coli* cells upon direct contact, prevented bacterial adhesion in the materials surface and, in test with water samples from different sources, showed to be a suitable material for water purification over 10 cycles of reuse, within minutes of contact and without leaching to the water.

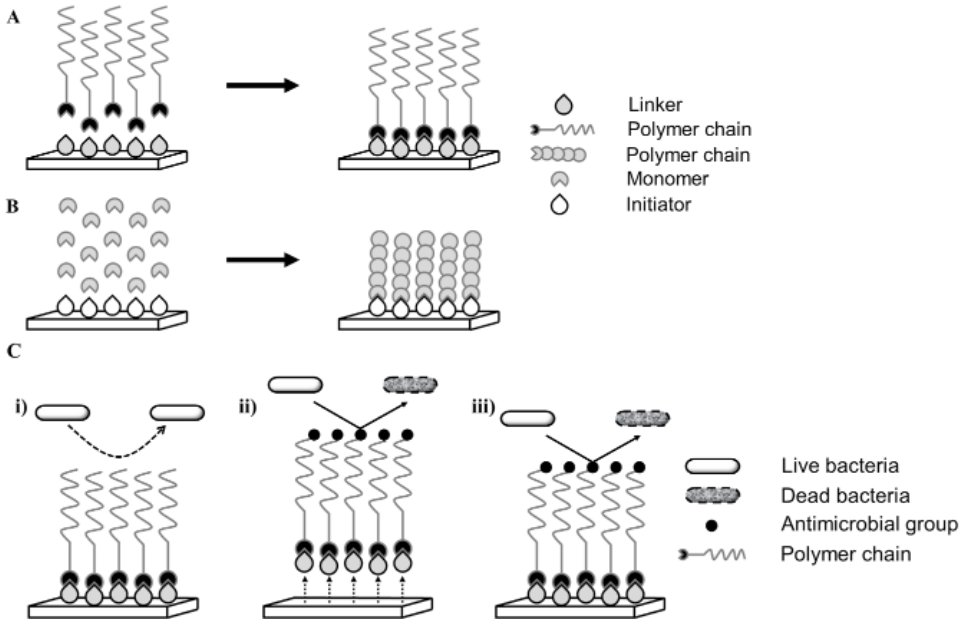

Figure 5.1 - Two different approaches to immobilize polymers to a surface: A) *grafting to* – involves a chemical reaction between a polymer chain and a complementary reactive group on a substrate surface; B) *grafting from* – involves a polymerization reaction initiated by a grafted molecule; C) classification of antimicrobial surfaces: i) biopassive approach - repelling system: the surface repels bacteria without killing them; ii) bioactive approach - releasing system: the antimicrobial polymer is released from the surface and kills bacteria; iii) bioactive approach - contact-active system: the bacteria are killed upon contact with the antimicrobial oligomer at the surface.

5.3. Experimental Section

5.3.1. Material

Chitosan (CHT) (75-85 % deacetylated, M_w = 190–310 kg.mol^{-1}), *N,N'*-methylenebisacrylamide (MBA), monomer 2-methyl-2-oxazoline (MeOx, purity>98 %), 2-ethyl-2-oxazoline (EtOx, purity >99 %), 2-isopropenyl-2-oxazoline (IsoOx, purity> 99 %), initiator boron trifluoride diethyl etherate ($BF_3.OEt_2$), ammonium persulfate (PSA), *N,N,N,N*-tetramethylethlenediamine (TEMED), glacial acetic acid (purity ≥ 99 %), phosphate buffered saline (PBS) and bovine serum albumin (BSA, purity ≥98 %) were purchased from Sigma-Aldrich. The monomer 2-bisoxazoline (BisOx) was synthesized following a procedure described by H. Witte *et al.*[95] *N,N*-dimethyldodecylamine was purchased from Fluka. Ethanol (p.a.) was purchased from Pancreac. Glutaraldehyde 25 % (v/v) was purchased from Carl Roth. Mueller-Hinton broth medium was purchased from Oxoid. Bacto yeast extract medium and Bacto agar were purchased from BD Bioscience. Carbon dioxide was supplied by Air Liquide with a purity of 99.998 %. All materials and solvents were used as received without any further purification.

5.3.2. Scaffolds preparation

Chitosan (CHT) scaffolds were prepared by the freeze-drying method.[131] Briefly, the casting solutions with concentrations of 3 % (w/v) were prepared by dissolving chitosan in acetic acid 1 % (v/v) at room temperature under stirring. A crosslinking agent (MBA, 2 % w/w) was also added to the mixture. The homogeneous solutions were cooled and 74 µL PSA solution (0.1 $g.mL^{-1}$) and 46 µL of TEMED were added to the mixtures and stirred overnight. The solutions were then placed in sample tubes with an inner diameter of 1.2 cm and 3 cm height. The sample tubes were freeze-dried at -20 ºC during 20 minutes. Afterwards, the scaffolds were washed with ethanol in order to remove remaining crosslinker.[132]

5.3.3. Scaffolds surface activation with plasma technology

CHT scaffolds were activated by argon plasma treatment for further grafting with OOXs in supercritical carbon dioxide. The plasma treatment was carried out in a radio frequency plasma reactor (Plasma system FEMTO, version 5). Polymeric structures were introduced in the plasma chamber which was thoroughly purged with a continuous flow of argon to reduce trace amounts of air and moisture. Samples were placed on the top of a porous network in order to assure a homogeneous activation of all surface area (from the top to the bottom). During the treatment, the argon flow was adjusted in order to keep a constant pressure of 0.1 MPa inside the chamber. A power of 60 W was applied during 10, 20 or 30 minutes. At the end of the experiment, the plasma chamber was ventilated and the samples were immediately introduced in the high pressure cell to be coated.

5.3.4. Scaffolds grafting with ammonium quaternized oligo(2-oxazoline)s

CHT scaffolds were placed inside the high pressure cell and $scCO_2$ was used as a solvent to carry the monomer to the activated polymeric substrates. The interior of the high pressure cell is divided in two parts with a porous structure in order to avoid any contact of polymeric structures (in the top compartment) with the monomer (placed in the bottom compartment). Weighted CHT scaffolds were coated in the presence of an excess of 2-isopropenyl-2-oxazoline in $scCO_2$ for 24 hours and 40 ºC, and then thoroughly washed with fresh CO_2 to remove unreacted monomer.

After that initial grafting step, another oxazoline monomer was added to the high pressure reactor (MeOx, EtOx or BisOx) together with the initiator. The reactions took place at 18 MPa, 65 ºC

during 20 hours. In the end, a tertiary amine was added to the reactor and the reaction occurred at 18 MPa, 40 ºC, 20 hours (Figure 5.2). In all the reactions, it was assumed that the yield was 100 % and monomer added in excess to assure that there was not any limiting step. Oligo(2-methyl-2-oxazoline) quaternized with *N,N*-dimethyldodecylamine (OMeOx-DDA), oligo(2-ethyl-2-oxazoline) quaternized with *N,N*-dimethyldodecylamine (OEtOx-DDA) and oligo(2-bisoxazoline) quaternized with *N,N*-dimethyldodecylamine (OBisOx-DDA) were synthesized as described previously.[48]

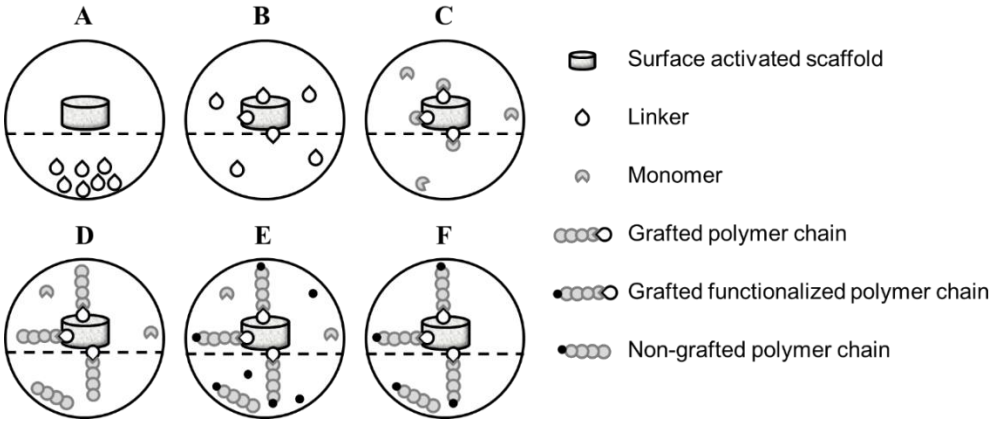

Figure 5.2 - Schematic illustration of the grafting procedure comprising oligomerization and functionalization in $scCO_2$. The high pressure cell is divided in two parts with a porous structure in the middle. A) activated polymeric structure (in the upper part) is separated of the linker molecule, 2-isopropenyl-2-oxazoline (placed in the lower part). B) $scCO_2$ is added to the high pressure cell, an homogeneous distribution of the linker molecule is attained in the reactor and the linker reacts with the activated surface; C) unreacted linker molecules are vented from the cell, 2-substituted-2-oxazoline monomer and initiator are added to the reactor and oligomerization takes place; D) oligomerization ends, and free oligomer is precipitated at the bottom of the reactor; E) functionalization molecule, *N,N*-dimethyldodecylamine, is added to the reactor and end-capps both grafted and free oligomer; F) unreacted monomer and functionalization molecule are washed out from the reactor and purified OOXs-DDA grafted scaffold and OOXs-DDA are obtained.

5.3.5. Scaffolds characterization

The surface composition was studied by X-Ray Photoelectron Spectroscopy (XPS) using the non-monochromatic Al Kα radiation (hυ = 1486.6 eV) from a Kratos XSAM800 spectrometer. Operating conditions and data treatment are described elsewhere.[161] Spectra were recorded by a Sun SPARC Station 4 with Vision software from KRATOS. Charge shift was corrected considering the binding energy (BE) of aliphatic carbon atoms, centred at 285 eV, as reference.[162]

Sensitivity factors used for quantitative analysis were as follows: 0.25 for C 1s, 0.42 for N 1s, 0.66 for O 1s, 1.00 for F 1s and 0.13 for B 1s.

ATR-FTIR spectra were recorded on a spectrometer BRUCKER - alpha. The Platinum ATR accessory contained a Ge ATR-crystal. All spectra (32 scans at 0.9 cm^{-1} resolution and rationed to the appropriate background spectra) were recorded at 25°C.

The compression modulus of the scaffolds were determined with a tensile testing equipment (MINIMAT firm-ware v.3.1). Scaffold samples with length of 1 cm and width of 1 cm were compressed until their deformation. The used speed of testing was 1 $mm.min^{-1}$. A full scale load of 20 N was used. The compression modulus was calculated from the slope of the linear portion of the stress-strain curve. All samples were tested in dry state at room temperature. Load compression graphs were obtained during testing and converted to stress strain curves applying two equations. Stress (σ, N/m^2) is calculated by dividing the applied force (F, N) per cross sectional area (A, m^2) and Strain (ε) by dividing the change in length (Δl, m) per the length between clamps (L, m).

Scaffolds porosity and pore size distribution were determined by mercury porosimetry (micromeritics, autopore IV).

The water fluxes were determined at 37 ºC and 1 atm. Due to the high porosity of the scaffold network no pressure was applied. Thus, Varian columns (with a capacity of 3 mL and an effective volume of 1.2 cm^3) were packed with antimicrobial scaffolds and charged with 1 mL of distilled water. The run time was registered and at least three measurements of distilled water flux were recorded.

Scaffolds stability in PBS solution (pH 7.4) was also evaluated by gravimetric analysis. Scaffolds samples were immersed in 10 mL of PBS at 37 ºC during 15 days. Samples were removed from the medium periodically, freeze dried for 24 hours and then weighted. A new PBS solution was always used after each freeze-drying step.

Scaffolds morphology before and after grafting was recorded using scanning electron microscopy (SEM) in a Hitachi S-2400 equipment, with an accelerating voltage set to 15 kV. The scaffold samples were frozen and fractured in liquid nitrogen for cross-section analysis. All samples were coated with gold before analysis.

5.3.6. Antimicrobial testing

S. aureus NCTC8325-4 and *E. coli AB1157* bacterial strains were grown in Mueller-Hinton broth medium (Oxoid). Cultures were grown overnight in broth at 37 ºC. Native CHT scaffold and coated CHT scaffolds were placed in 24-well plates containing, in each well, a volume of 1 mL of medium with a scaffold sample of approximately 1 cm^2 of surface area. Each well was inoculated with 5 µL of bacterial culture (approximately $5x10^5$ cells) and plates were incubated at 37 ºC to assess the viability of bacterial cells. After incubation (3, 5 and 10 min), the medium with bacteria was plated on Muller Hinton Broth agar and incubated at 37 ºC for 24 h, and the number of bacterial colonies was determined. The ability of the materials to kill bacteria upon contact was also tested. For that, the assays were repeated but this time using a 24-well plate with Transwell inserts and a filter (with a pore size of 0.4 µm) dividing the upper part containing the polymeric material and the lower part containing the bacteria (Corning, Transwell® permeable supports). Both experiments were performed in duplicate for both *S. aureus* and *E. coli* strains. The results were normalized per surface area of scaffold (cm^2).

5.3.7. Protein adsorption and anti-biofouling testing

A scaffold sample was immersed in BSA solution (1 $mg.mL^{-1}$). Samples were withdrawn from the solution in order to evaluate the protein concentration in the medium after 48 h (loading step). At the end of the assays, the scaffolds were removed and washed with PBS in order to remove the BSA absorbed into the scaffold (recovery step). In parallel, and in order to evaluate the leaching of the antimicrobial polymer from the blend, the samples were placed in PBS solution (control). The absorbance at 280 nm was measured periodically. The protein percentage was normalized to the scaffolds weight.

After the direct contact with bacteria during 18 h, scaffolds samples were washed with phosphate buffered saline (PBS) and fixed with glutaraldehyde 2.5 % (v/v) during 10 minutes. After 10 minutes, scaffolds sample were washed with distilled water and dehydrated with aqueous solutions with increasing concentration of ethanol (ranging from 70 to 100 %). The presence of bacterial cells at the surface of CHT native scaffolds and OOXs-grafted scaffolds after 18 h of contact was recorded using scanning electron microscopy (SEM) in a Hitachi S-2400 equipment, with an accelerating voltage set to 15 kV. All samples were coated with gold before analysis.

5.3.8. Purification of contaminated water from environmental samples

Two different water samples were collected in the Barlavento region of the Algarve, in southern Portugal: one sample from a well (an underground source) and another one from a dam (surface water). Samples were collected to sterilized bottles and analyzed within 24 h after sampling, using the pour plate method. Samples were shaken vigorously in order to assure a homogeneous distribution of microorganisms and 1 mL of the sample (10^0) and of serial dilutions (10^{-2}, 10^{-4}, 10^{-6}) were added into a sterile Petri dish. 15 mL of the Yeast Extract molten agar (BD) at 45°C was poured, into the Petri dish containing the sample and the petri dish was gently swirled to mix evenly. After this, each petri dish was incubated at 36 °C and 20 – 22 °C for the appropriate incubation time, 48 h and 72 h, respectively. The number of total culturable microorganisms per mL was assessed in duplicate for each temperature. In parallel, water samples were incubated in direct contact with a scaffold sample of CHT-OMetOx-DDA with an approximate surface area of 1-1.5 cm^2 during 10 cycles of 5 min each cycle. The number of total colonies per mL was assessed in duplicate for each temperature and for cycles n=1, 5, 10. The reduction in viability of culturable microorganisms was normalized to the scaffold's surface area.

Yeast Extract Agar and the procedure complies with the recommendation of ISO 6222:1999.[163]

5.4. Results and Discussion

5.4.1. Chitosan scaffolds preparation

CHT scaffold surface was grafted with antimicrobial oligo(2-oxazoline)s combining two green technologies: plasma surface activation and further oligomerization and functionalization in supercritical carbon dioxide. Following our previous work,[48] three different oligooxazolines (oligo(2-methyl-2-oxazoline), oligo(2-ethyl-2-oxazoline) and oligo(2-bisoxazoline)) quaternized with *N,N*-dimethyldodecylamine were selected to be attached to CHT polymeric surface. The CHT structures were prepared by freeze-drying using a 3 % (w/v) casting solution containing *N,N'*-methylenebisacrylamide as crosslinker. After this step, the surface of CHT native scaffolds was activated using a plasma technology, with argon as an inert gas. Immediately after, activated scaffolds, the monomer 2-isopropenyl-2-oxazoline (IsoOx) and carbon dioxide were added into a high pressure cell (Figure 5.3). IsoOx reacted with radicals at the materials surface, with $scCO_2$ used as a solvent. This monomer has the peculiar feature of having two polymerizable groups, as

it is able to react with radicals and initiate a radical polymerization, but also to polymerize by cationic ring opening polymerization (CROP) mechanism, therefore being a good linker molecule to attain our goal of grafting OOX not through the reactive end-chain, enabling the posterior OOXs end-chain functionalization. After this step, a different monomer (2-methyl-2-oxazoline, 2-ethyl-2-oxazoline or 2-bisoxazoline) and an initiator (boron trifluoride diethyl etherate) were added to the high pressure cell and a cationic ring opening polymerization took place. At the end of the reaction, a grafted *living* oligomer was obtained and was quaternized by adding a tertiary amine. Fresh CO_2 was then added in a continuous way to vent the unreacted monomer, initiator and tertiary amine from the reactor and the final products were purified. The grafted 3D materials were further characterized to evaluate the morphology as well as the mechanical, protein-repellent and antimicrobial properties.

This supercritical-based procedure has several advantages when compared to more conventional grafting procedures, where the surface is soaked in an organic solution containing the solubilized monomer and initiator molecules, which have solvent diffusion limitations and require extensive purification steps in the end.

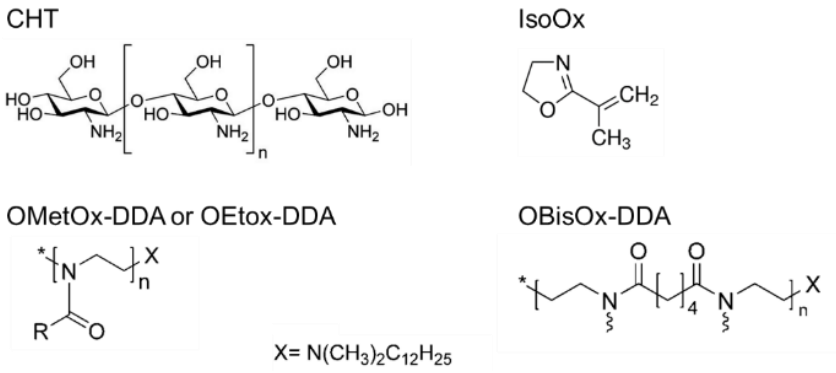

Figure 5.3 - Chemical structures of chitosan (CHT), 2-isopropenyl-2-oxazoline (IsoOx) and grafted oligomers: a) linear oligomers: R=CH_3: OMetOx-DDA- oligo(2-methyl-2-oxazoline) quaternized with *N*,*N*-dimethyldodecylamine; R= C_2H_5: OEtOx-DDA- oligo(2-methyl-2-oxazoline) quaternized with *N*,*N*-dimethyldodecylamine; and b) branched oligomer : OBisOx-DDA- oligo(2-bisoxazoline) quaternized with *N*,*N*-dimethyldodecylamine.

CHT native scaffold stands for the nongrafted scaffold. The OOXs grafted scaffolds will be described hereinafter as CHT-OMetOx-DDA as CHT grafted with oligomer OMetOx-DDA; CHT-OEtOx-DDA as CHT grafted with oligomer OEtOx-DDA; and CHT-OBisOx-DDA as CHT grafted with oligomer OBisOx-DDA.

5.4.2. Chitosan scaffolds characterization

FTIR-ATR data (Figure 5.4A) showed a large band around 1 636 cm^{-1} (amide groups from oligo-2-oxazolines) present in all grafted scaffolds, which indicates the success of the grafting procedure. A weak band around 1738 cm^{-1} (carbamate group from CO_2 insertion in oligo-2-oxazoline chain) was observed for the CHT-OBisOx-DDA scaffold. Under $scCO_2$ synthesis conditions, CO_2 is partially incorporated in the oligomer chain in the starting end.[29] OMetOx-DDA and OEtOx-DDA were grafted to the CHT scaffold by the starting end and, consequently, the grafting procedure must have impaired this incorporation in both scaffolds. On the other hand, OBisOx-DDA is a branched oligomer and the carbamic acid incorporation could occur in one starting end of the branches. In OMetOx-DDA, the sharp bands centred at 1245 and 1430 cm^{-1}, corresponded to, respectively, CH_2 wagging and/or twisting vibration modes and asymmetric CH_3 deformations of the *N*,*N*-dimethyldodecylamine end groups.[164]

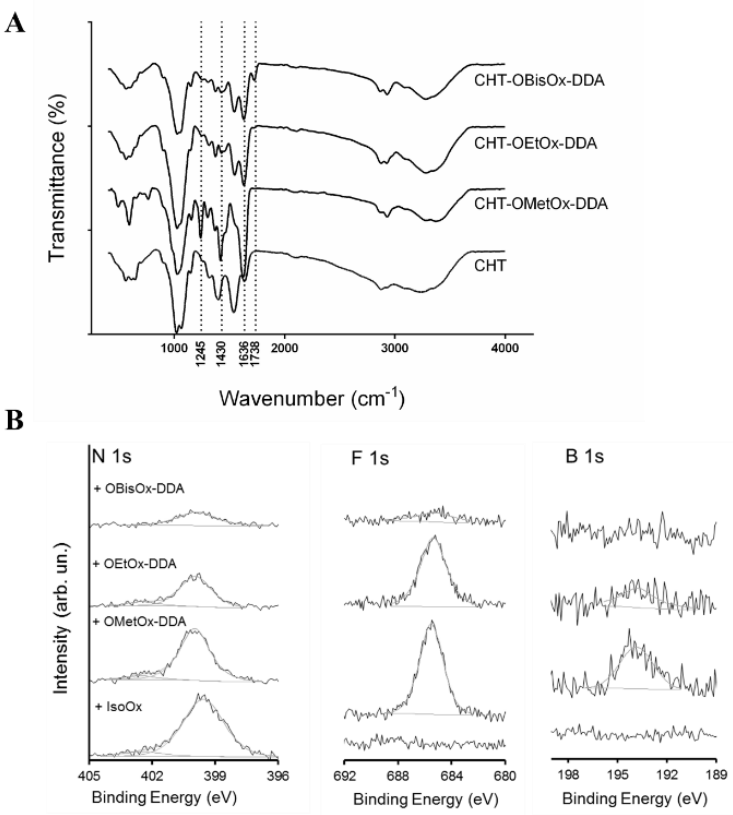

Figure 5.4 - A) FTIR-ATR spectra for CHT native scaffold and grafted CHT scaffolds; B) N 1s, F 1s and B 1s XPS regions of CHT modified scaffolds after (from bottom to top) IsoOx activation for 30 minutes and grafted with OMetOx-DDA, OEtOx-DDA and OBisOx-DDA.

Scaffolds surface elemental composition was analyzed by X-ray photoelectron spectroscopy (XPS) technique. Firstly, the efficiency of 2-isopropenyl-2-oxazoline grafting was studied after different times of CHT surface plasma activation (10, 20 and 30 min) and data is described in detail in the supporting information. Secondly, the different OOXs-grafted CHT scaffolds were analyzed to confirm the success of the immobilization and quaternization at surface of the polymeric supports.

Table 5.1 - Binding energy (eV), [At. Conc.] (%), atomic ratios and assignments. [162]

	CHT+IsoOx (30 min)			
	+OMetOx-DDA	+OEtOx-DDA	+OBisOx	
C 1s	285.0 [33.9]	285.0 [47.2]	285.0 [54.8]	sp^3
	286.1 [23.9]	286.1 [18.0]	286.6 [13.9]	C-N and C-O
	288.0 [9.8]	287.8 [7.4]	288.4 [4.8]	N-C=O
O 1s	531.3 [11.7]	531.2 [9.7]	531.5 [8.2]	C=O
	533.0 [3.4]	533.2 [2.4]	532.8 [11.6]	C-O
N 1s	400.0 [10.0]	399.9 [7.5]	399.9 [5.3]	N-C=O, NH_2
	402.5 [0.7]	402.5 [0.9]		N^+
F 1s	685.5 [4.9]	685.4 [5.5]	685.2 [1.5]	BF_4^-
B 1s	193.8 [1.6]	193.7 [1.3]		BF_4^-
F/B	3.0	4.3		
F/C	0.07	0.08	0.02	
O/C	0.22	0.17	0.27	
N/C	0.16	0.12	0.07	
O/N	1.40	1.42	3.74	

The functionalization with the different oligomers was attested not only by C 1s and N 1s regions, but also by the presence of fluorine and boron: peaks centered at 685.4 ± 0.2 eV and 193.9 ± 0.2 eV were assigned, respectively, to fluorine and boron in BF_4^- (Figure 5.4). The absence or residual relative amount of the counter ion BF_4^- showed that the functionalization with *N*,*N*-dimethyldodecylamine was not effective in the OBisOx-grafted CHT scaffolds. Most likely,

OBisOx was end-capped with OH groups by air exposure. The experimental O/C ratio, computed for OBisOx-grafted CHT, was compatible with this hypothesis: while for OMetOx-DDA and OEtOx-DDA ratios, the experimental O/C were lower but close to the stoichiometric ones for MetOx and EtOx monomers (respectively: 0.25 and 0.20), the O/C = 0.27 of OBisOx revealed an excess of oxygen which was not expected for the *living* polymer (that would be 0.20 per monomer) (Table 5.1).[162] Henceforward, this scaffold will be referred to as CHT-OBisOx.

Based on the F/C ratio, the sequence from the less to the more functionalized CHT is OBisOx < OMetOx-DDA ≈ OEtOx-DDA (Table 5.1). The atomic ratio F/B also gives some insight on the DDA alkylic chains organization. Stoichiometrically, this ratio should be 4, but for OMetOx-DDA, it was clearly lower than 4: this would only be possible if the BF_4^- counter-ions were covered by a well-organized, brush-like, overlayer of DDA aliphatic chains, which could be achieved by an ion location within pores; since the kinetic energy (KE ≈ hν-BE) of F 1s photoelectrons is much lower than the one for B 1s photoelectrons, the intensity of F 1s photoelectrons was much more attenuated than the B 1s photoelectrons intensity and the apparent atomic ratio becomes lower than its real value. For OEtOx-DDA, F/B ratio was, within the experimental error, equal to 4, which is compatible with the presence of more randomly tilted chains, that is, a less dense overlayer, which does not have a significant effect on the attenuation of F 1s photoelectrons, leading to a F/B ratio closer to the real one (Table 5.1).

It is interesting to notice, that such difference between these two samples can also be inferred from the FTIR-ATR spectra (Figure 5.4A): the DDA vibration modes, identified at 1245 and 1430 cm^{-1}, were strongly active for OMetOx-DDA, presenting very weak intensities for OEtOx-DDA, which is consistent (regarding selection rules) with the DDA chains being mainly oriented perpendicular to the surface in OMetOx-DDA.

The poor signal/noise ratio of B 1s in OBisOx (Figure 5.4B) is due to its very low sensitivity factor, ~1/8 of the F 1s factor, and to the fact that B:F = 1:4. Thence, at least a sum of 32 acquisition sweeps would be needed to obtain a "readable" B 1s signal. However, such an extended irradiation would inevitably degrade the samples. Another sign of the poor functionalization of the OBisOx sample and even poor covering of chitosan by the polymer is the ratio O/N which should be 1 if just the covering oligomer was "seen" by XPS and 4 if the chitosan was uncovered: atomic O/N ratio was 1.4 for the OMetOx-DDA and OEtOx-DDA samples and 3.7 for OBisOx (Table 5.1). As the functionalization of CHT-OBisOx with DDA was not attained successfully, this scaffold was not considered for the later antimicrobial assays.

CHT native scaffold and OOXs-grafted CHT scaffolds were also characterized to assess the mechanical and morphological properties as well as water permeability. Data showed variations

in materials stiffness, average pore size diameter, porosity and water fluxes, depending on the grafted oligo(2-substituted-2-oxazoline)s. The obtained data was summarized in Table 5.2.

Table 5.2 - Compression modulus, porosity, average pore size diameter and water permeability of the produced scaffolds.

Scaffold	Compression modulus (kPa)	Porosity (%)	Average pore size diameter (μm)	Water flux ($L.m^{-2}.h^{-1}$)
CHT	0.36±0.05	93±5	21±5	(14±4) x 10
CHT-OMetOx-DDA	0.7±0.2	86±5	22±5	21±4
CHT-OEtOx-DDA	1.5±0.3	80±5	29±5	52±5
CHT-OBisOx	0.77±0.01	90±5	25±5	(13±2) x 10^2

The mechanical properties of the scaffolds were slightly influenced by the antimicrobial oligo(2-oxazoline)s grafted at the 3D surface. The grafting increased the compression modulus values and, therefore, the stiffness of the material. All the produced scaffolds were highly porous (more than 80 % of porosity) with a variation in the average pore size diameter between 21 and 29 μm. CHT native scaffold had an average pore size diameter of 21 μm which was maintained almost unaltered when OOXs were grafted to the native scaffold. The porosity of all grafted scaffolds decreased slightly relatively to the porosity of CHT native scaffold. Also, the OOX grafting significantly altered the water flux. The water flux increased for the CHT-OBisOx scaffold, relative to the CHT scaffold. All the oligo(2-substituted-2-oxazoline) used in this work are hydrophilic polymers and, as a result of the surface grafting, water flux permeability was expected to increase.[133] In our previous work, the scaffold containing the oligomer OBisOx-DDA in the physical blend was also the scaffold with highest water flux value, probably due to the huge hidrophilicity of this oligomer and also to the endcapping with –OH groups.[81] CHT-OMetOx-DDA and CHT-OEtOx-DDA had lower water permeability, which can be justified by the decrease in the overall porosity of the 3D porous network for both scaffolds relatively to CHT native scaffold porosity. Moreover, the lowest value for water permeability was observed for CHT-OMetOx-DDA indicating that the immobilization took place, to some extent, within the pores and not only at the surface, as it was already suggested from the XPS results concerning the F/B ratio.

In order to test scaffolds structural integrity over long periods of time in solution, scaffolds were incubated in PBS during 15 days at 37 ºC. Figure 5.5A shows that the grafting of oligo(2-oxazoline)s to the surface did not change the stability of the materials, when compared to a CHT native scaffold. The CHT native scaffold presented a higher swelling ratio than the antimicrobial oligo(2-oxazoline)s enriched CHT scaffolds, and its expanded 3D structure was the most fragile. After 15 days at 37 ºC, all antimicrobial oligo(2-oxazoline)s-grafted CHT scaffolds proved to be highly stable, suggesting that the scaffolds can be reused for some cycles. These results also show that the materials were successfully crosslinked and that the CHT scaffold was a stable polymeric network. Effective and stable platforms are needed to anchor the antimicrobial compounds, in order to reduce costs associated with early material loss and to prevent detrimental effects on human health and the environment, triggered by leaching (e.g. the use of nanoparticles for disinfection has significant limitations due to unsuccessful permanent immobilization technologies).[141]

Scaffolds morphology was evaluated by scanning electron microscopy (SEM). SEM micrographs (Figure 5.5B) showed that scaffolds have elongated pores with high interconnectivity and porosity and that the surface was successfully coated (see cross-sections). The presence of the coating can also be observed in Figure 5.5C that clearly shows the immobilization of yellowish 2-oxazoline-based oligomers at the scaffolds surface.

CHT-OMetOx-DDA and CHT-OEtOx-DDA, combining high porosity and a large surface area, should be suitable for applications that require the development of materials with strong biocidal activity and the ability to kill upon contact.

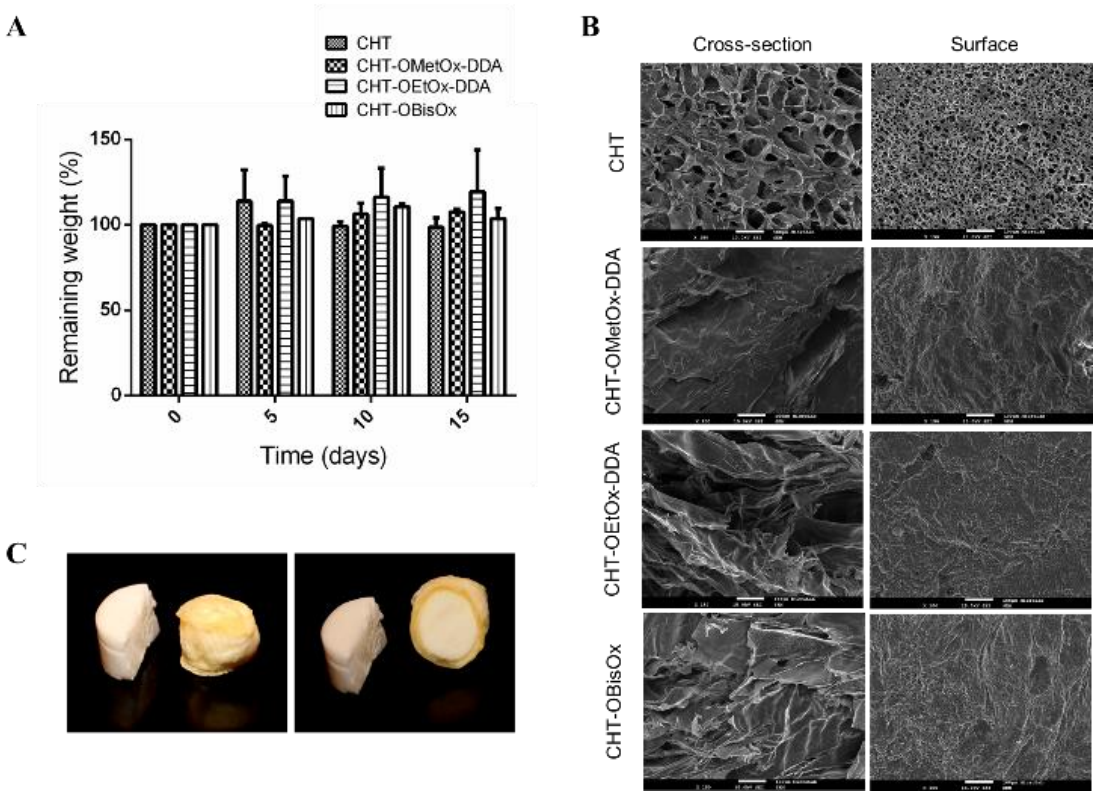

Figure 5.5 - A) CHT native scaffold and antimicrobial oligo(2-oxazoline)s-grafted CHT scaffolds are stable in PBS solution (pH 7.4) during 15 days as measured by gravimetric analysis; B) SEM micrographs of surface and cross-section of CHT native scaffold and different antimicrobial oligo(2-oxazoline)s-grafted CHT scaffolds show elongated pores and dense surface coating on OOXs-grafted scaffolds; C) Photographs of the same CHT native scaffold (white) and OOXs grafted scaffold (yellow) showing the OOXs immobilization at the top and lateral side of the scaffold (left) and the OOXs immobilization at the surface but not in the interior of the scaffold after cross-section (right).

5.4.3. Antimicrobial testing

The antimicrobial activity of OOXs-grafted CHT-scaffolds was tested using Gram-positive and Gram-negative bacteria, namely *S. aureus* and *E. coli*, respectively.

Biocidal antimicrobial surfaces can be classified as contact-active or releasing systems. One approach to distinguish between both systems consists in testing for the presence of an inhibition zone of microbial growth, which occurs near the material if a biocidal compound is released and diffuses through an agar plate.[165] However, the size and presence of an inhibition zone depends on many factors, including the quantity of released compound or release kinetics, and therefore the lack of a visible inhibition zone is not a conclusive proof for a contact-active mechanism of the antimicrobial. Another commonly performed assay consists in the measurement of microbial viability (by colony forming units, CFUs) in the surroundings of the material, assuming that, if the antimicrobial surface effectively kills bacteria, the CFUs will decrease.[166,167] Alternatively,

loss of biocidal activity upon removal of the sample from the medium can be used as an indicator of a contact-active killing mechanism.[168] Actually, previous research has shown that there is no assay that can clearly tell the difference between a contact-active and a release system.[169] In this study we have developed a simple and direct method that clearly distinguishes between these two mechanisms.

The bacteriocidal activity of the OOXs-grafted scaffolds was studied, using a 24-well plate, by determining the viability of bacterial cells after incubation, with stirring, of approximately 10^5 cells in medium with the materials. After incubation (3, 5 and 10 min), the medium was plated and the number of colony forming units (CFU) was counted. The assays were done, in parallel, using a 24-well plate with Transwell inserts with a filter (with a pore size of 0.4 μm) dividing the upper part containing the OOXs-grafted scaffold and the lower part containing the bacteria (Figure 5.6A). If the scaffolds kill only on contact with bacteria, as we expect, they should not be active in this assay, given that the direct contact between the material and bacteria is prevented. On the contrary, reduction of bacterial viability would indicate leaching of the antimicrobial oligomer from the scaffold. Leached biocide would lead to a loss of the materials` antimicrobial activity over time, to chemical contamination related to the release of biocidal agent, and could also lead to the development of bacterial resistance in the presence of sub-inhibitory concentrations of biocide. In the literature, a recent work from *Zeng et al.* highlighted the development of a hydrogel with dispersed silver nanoparticles with fast killing times for water disinfection (killed 97 % of *E. coli* cells in 60 seconds). However, leaching of silver nanoparticles from the filter was always observed although in lower levels than the drinking water standards.[147] Also, the production of contact-active antimicrobial POXs coatings on glass slides by simple solution spreading and solvent air drying was previously described. The reported procedure involved several purification steps to produce a material able to kill *S. aureus* cells that was deactivated after usage, although the antimicrobial activity could be recovered by a self-polishing event in the presence of an enzyme. Moreover, this report does not rely in POXs grafting and, therefore, still meets significant limitations.[59]

To ensure that the scaffolds were not previously colonized with bacteria, the CHT native and OOXs-grafted scaffolds were placed in medium at 37 ºC and no visible bacterial growth was observed after 24 hours, meaning that they were ready-to-use for bacterial assays after the production procedure.

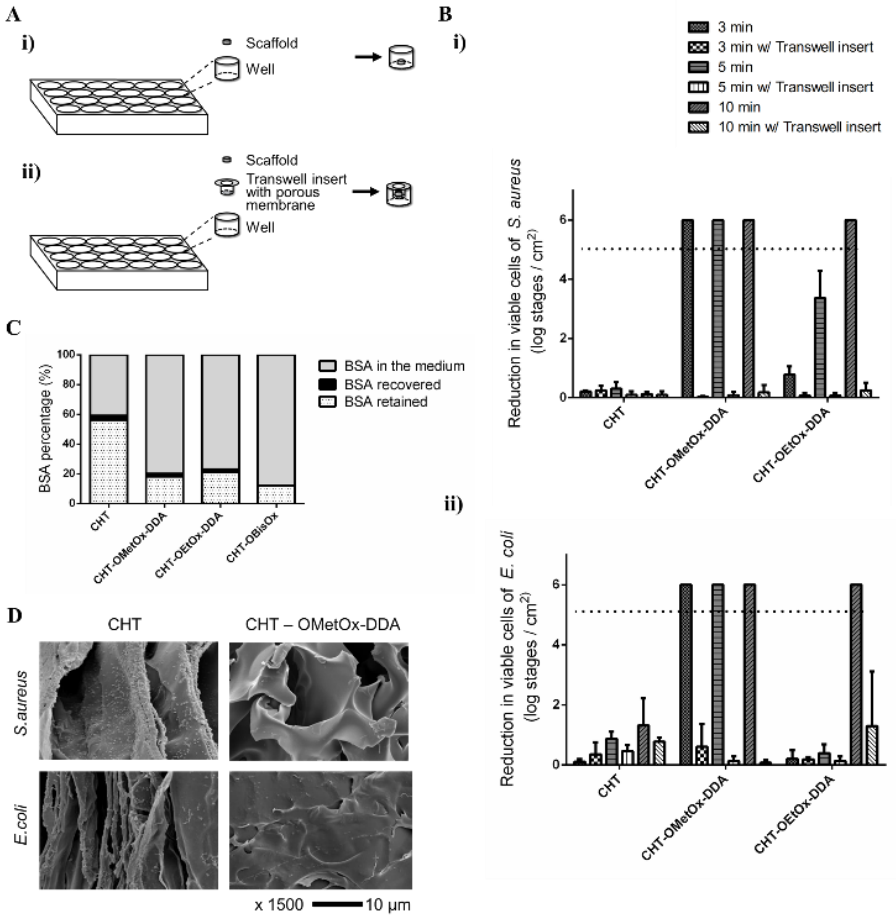

Figure 5.6 - A) Schematic representation of the methodology used to assess scaffolds killing activity upon contact: (i) test for bacteria viability after direct exposure to the scaffolds – the well containing scaffold and culture medium was inoculated with bacteria (10^5 cells); (ii) test for bacteria viability after non-direct exposure to the scaffolds – the upper part in the well contains the scaffold and culture medium and the lower part with medium was inoculated with bacteria (10^5 cells), separated by a filter with a pore size of 0.4 µm. B) Killing of (i) *S. aureus* and (ii) *E. coli* by direct exposure to OOXs-grafted scaffolds or non-direct exposure using an insert in the well. The results are presented in a logarithmic scale as the reduction in number of viable cells per surface area of used scaffold (cm^2) (1 log stage means a reduction of 90 %, 2 log stages means reduction of 99 %, 3 log stages means reduction of 99.9 %). Data above the threshold (dashed line) was not subjected to area normalization since killing percentage was higher than 99.999 % in all assays, independently of the used surface area. C) BSA adhesion profiles (percentage of BSA in the medium, recovered and retained) for CHT native scaffold and different antimicrobial oligo(2-oxazoline)s grafted CHT scaffolds. All protein percentage values were normalized to the scaffolds weight. D) SEM micrographs of CHT native scaffold and CHT-OMetOx-DDA after 18h of direct contact with *S. aureus* and *E. coli* cells.

Incubation of *S. aureus* cells in direct contact with CHT native scaffold did not cause a reduction of bacterial viability, as expected. However, grafting of oligomer OMetOx-DDA to the CHT native scaffold surface resulted in a reduction in bacterial viability of more than 99.999 % after only 3 minutes of contact. The immobilization of OEtOx-DDA in the CHT native scaffold also highly reduced *S. aureus* viability, but only after 10 minutes of contact. In contrast, no reduction

in *S. aureus* CFUs was observed for both scaffolds in the assays containing the Transwell Inserts. The fact that killing was only observed in the absence of the Transwell insert, *i.e.*, when OOXs-grafted scaffolds were in direct contact with cells, indicates that there was no significant leaching of the immobilized oligomers, OMetOx-DDA and OEtOx-DDA, to the medium. Therefore, the OOXs-grafted scaffolds kill *S. aureus* cells upon contact (Figure 5.6B).

Incubation of *E. coli* cells with the CHT native and the OOXs-grafted scaffolds showed the same trend of results as for *S. aureus*. OOXs-grafted scaffolds kill *E. coli* cells upon contact and CHT-OMetOx-DDA drastically reduced cells viability in less than 3 minutes, while CHT native scaffold did not greatly influence *E. coli* viability (Figure 5.6B).

XPS data indicated that the grafting efficiency was similar for both OMetOx-DDA and OEtOx-DDA, but CHT-OMetOx-DDA surface seems to be denser than that of CHT-OEtOx-DDA sample, presenting, most probably, brush-like alkylic chains, which are, in this way, more available to interact with bacteria. In fact, these oligomers, while grafted, showed to require different killing times for *S. aureus* and *E. coli* cells. Such a difference must also be related to the different minimum inhibitory concentration values (MIC) observed for both oligomers, where OMetOx-DDA required slightly less quantity then OEtOx-DDA to kill both bacteria. Therefore, CHT-OMetOx-DDA was more effective in reducing bacterial viability with the same amount of oligomer grafted at the surface, justifying the need of less time of contact to achieve the same reduction in the viability.

In a previous work,[81] it was hypothesized that antimicrobial oligo(2-oxazoline)s can inhibit the growth of the gram-negative bacteria *E. coli*, by acting at the outer membrane while for *S. aureus* the antimicrobial oligomer needs firstly to diffuse through the thicker peptidoglycan layer to be effective in the cell membrane. Also, when antimicrobial oligo(2-oxazoline)s were physically immobilized into a CHT native scaffold it was suggested that the diffusion through the peptidoglycan could be impaired when the antimicrobial oligo(2-oxazoline)s were immobilized by physical mixture in the blended scaffolds. To overcome this problem, it was suggested that the oligo(2-oxazoline)s should be grafted to the scaffold surface so that the antimicrobial group at the chain end could easily kill bacteria while covalently immobilized in the structure. The strategy presented in this paper was efficient to produce 3D matrixes with antibacterial activity against both Gram positive and Gram negative bacteria, after brief minutes upon contact.

Additionally, it can be concluded that this type of chain grafting does not influence the broad spectrum antimicrobial activity of the quaternized oligomers and that the oligomer chain length is enough to act as a spacer to enable the antimicrobial quaternary ammonium compound to be active against both Gram-positive and Gram-negative bacteria.

5.4.4. Protein adsorption and anti-biofouling testing

Protein adsorptions assays can be used to give a preliminary insight about the efficacy of the materials antifouling properties. Protein adsorption is one of the first steps in biofilm formation. Therefore the ability of a surface to repel protein can be used as an indicator for suitability of a material for anti-biofouling applications.[134] Previously, poly(L-lysine)-*graft*-poly(methyloxazoline) copolymers, PLL-*g*-PMOXA, were deposited onto silicon wafers by a simple dip-and-rinse procedure.[58] These bioinert coatings were able to successful and quantitatively prevent protein adsorption. This result, together with the unique versatility of POXs, highlighted the possibility to develop nonfouling coatings presenting bioactive functionalities.

Protein adsorption assays were performed using bovine serum albumin (BSA) as model protein. The BSA retained in the scaffold was calculated through the difference between BSA concentration in the initial solution and BSA quantified in both loading (BSA in the medium) and recovery step (BSA recovered – reversible fouling). Figure 5.6C shows that the grafting of oligomers OMetOx-DDA, OEtOx-DDA and OBisOx to the CHT scaffold led to an increase of BSA in the medium, *i.e.*, the incorporation of oligo(2-oxazoline)s on the CHT surface improved the protein repellent properties of the scaffold. Given its capacity to decrease protein adsorption, the grafting of a material with antimicrobial OOXs is a promising strategy for antifouling applications.

To assess the ability of the materials surface to repel bacteria and to resist cell adhesion, the presence of bacterial cells at the surface of CHT native and CHT-MetOx-DDA scaffolds was assessed by SEM micrographs after the direct contact with bacteria overnight (during 18 h). CHT-OMetOx-DDA was selected as the scaffold with the most promising contact-active antimicrobial properties. By the analysis of the SEM micrographs, it can be observed that OMeOx-DDA grafting effectively avoided bacterial adhesion at the scaffold surface enabling its reuse (Figure 5.6D).

5.4.5. Purification of contaminated water from environmental samples

Samples from underground and superficial waters were collected and the number of total culturable microorganisms was determined at two different temperatures, 20-22 ºC and 36 ºC (in accordance with the recommendation of ISO 6222:1999).[163] Given that microbiological viability can be influenced by several parameters as pH, hardness and dissolved salts, as well as the variety

of bacterial species present in the water samples, both water samples were characterized in terms of physicochemical characteristics which are detailed in the supporting information.

The reduction in the number of CFUs present in the aqueous samples was assessed using CHT-OMetOx-DDA during 10 cycles. Each cycle consists of direct contact for 5 min between an immersed scaffold sample and sequentially new samples of contaminated water – static assay. After 1, 5 and 10 cycles, contamination of water samples was evaluated by pour plate microbial counts (Figure 5.7).

Both water samples were contaminated with a variety of microorganisms, either bacteria or fungi. The sample from the underground water, a well, had 204 ± 12 culturable microorganisms per mL at 20-22 ºC after 72 h and 129 ± 30 culturable microorganisms per mL at 36 ºC after 48 h of incubation. The sample from the superficial water, a dam, had 741 ± 55 culturable microorganisms per mL at 20-22 ºC after 72 h and 396 ± 9 culturable microorganisms per mL at 36 ºC after 48 h of incubation.

Scaffold CHT-OMetOx-DDA highly reduced the variety and number of microorganisms present in both water samples, after brief times of contact. This scaffold was able to reduce > 87 % CFUs present in the well and > 74 % CFUs present in the dam. The scaffold slightly lost its ability to reduce the microorganisms viability after 10 cycles probably due to unspecific adsorption of molecules at the surface that could impair OOXs action (OOXs grafted scaffolds were able to shut down protein adsorption up to 20 % but did not avoid it completely). As a result, CHT-OMetOx-DDA represents an excellent solution for water purification for 10 cycles through a simple static procedure where the scaffold is immersed in the water to be decontaminated.

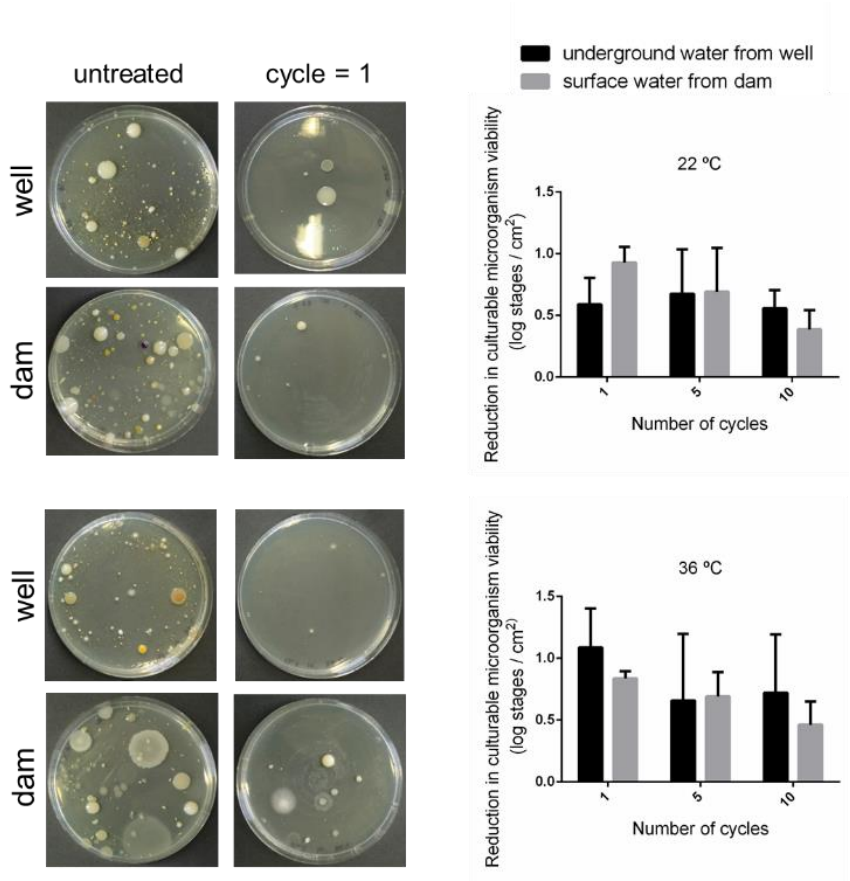

Figure 5.7 - Reduction in microorganism viability for two different environmental water samples (a well, an underground source, and another one from a dam, surface water) after direct contact with CHT-OMetOx-DDA scaffold and incubation at 22 ºC or 36 ºC. Inset images show the initial variety of culturable microorganisms present in each water sample at different temperatures (plated volume: 400 µL).

5.5. Conclusions

The main objective of this work was the development of 3D shaped polymeric matrices with unique antimicrobial and antifouling properties, through eco-friendly techniques and procedures that meet the green chemistry principles.

Two different oligo(2-oxazoline)s were successfully grafted into CHT scaffolds surface. CHT native scaffolds were produced by freeze-drying technique and the grafting procedure consisted solely in the use of non-hazardous chemical procedures: plasma activation followed by a $scCO_2$-assisted process for oligomer synthesis and quaternization. This type of grafting is a general procedure that can be applied to other types of materials, regardless of their 3D shape and chemical composition.

By varying the 2-substituted-2-oxazoline monomer grafted on the CHT matrices, it was possible to tune hydrophilicity, permeability, BSA adsorption profiles, bacterial surface adhesion and bacteria killing activity. CHT-OMetOx-DDA was the 3D polymeric matrix with the most promising antimicrobial properties against *S. aureus* and *E. coli* cells, since it required less time of contact between the material and bacteria to achieve a high viability reduction (3 min to achieve more than 99.999 % of killing). Moreover, in the presented case study with environmental water samples, this scaffold was able to achieve a high antimicrobial activity against a variety of different microorganisms with brief killing times and showed to be reusable for 10 cycles.

Oxazoline-based antimicrobial oligomers, by gathering such unique and broad biocidal activity, are an excellent alternative for surface modification when aiming to develop materials for water purification or even of devices able to maintain sterility or with self-disinfecting properties in biomedical applications. Furthermore, considering an industrial application of this type of antimicrobial materials and the versatility of the involved techniques, the process can be easily scaled-up and it is only limited to the dimensions of the plasma and $scCO_2$ apparatus.

5.6. Acknowledgments

The authors would like to thank the financial support from Fundação para a Ciência e Tecnologia (FCT-Lisbon) through contracts UID/QUI/50006/2013 and doctoral grant SFRH/BD/74730/2010 (VC), Fundação Calouste Gulbenkian. We wish to thank Dr. AM Botelho do Rego for fruitful discussions on XPS results and the Analytical Services Laboratory of REQUIMTE, FCT/UNL.

Chapter 6. Oxazoline based antimicrobial oligomers: mechanism of action disclosured by direct visualization

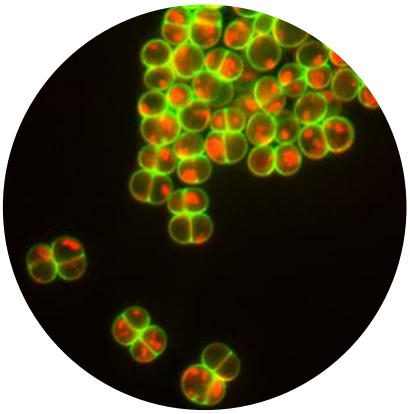

Manuscript in preparation

2015
VG Correia, JM Monteiro, MG Pinho and A Aguiar-Ricardo
Oxazoline based antimicrobial oligomers: mechanism of action disclosured by direct visualization.

Personal contribution
VGC contributed to the design of the work, performed all the experimental work with the help of JM Monteiro, interpreted the data and wrote the manuscript.

6.1. Abstract

Bacterial membrane disruption is often described by two different models, the carpet model or by the pore-forming model. In this paper, we study, for the first time, the mechanism of action of oxazoline-based antimicrobial oligomers synthesized in supercritical carbon dioxide: oligo(2-methyl-2-oxazoline), oligo(2-ethyl-2-oxazoline) and oligo(2-bisoxazoline) end-capped with *N*,*N*-dimethyldodecylamine and linear oligo(ethyleneimine) hypochloride, known by their broad spectrum of activity against several bacteria and fungi.

Large unillamelar vesicles (LUVs) composed of cardiolipin, phosphatidylglycerol and lysylphosphatidylglycerol, containing either carboxyfluorescein or a mixture of Alexa^{488}-dextran and Alexa^{633}-maleimide, were used as a model for the *S. aureus* membrane. Leakage of the incorporated dyes was followed over time after putting the LUVs into contact with each oligomer, either by fluorimetry or fluorescence microscopy. Data indicates that OMetOx-DDA and OEtOx-DDA act by a carpeting mechanism, whereas OBisOx-DDA and LPEI act by pore formation mechanism.

Additionally, *S. aureus* cells in contact with OMetOx-DDA were observed by fluorescence microscopy, showing that the oligomer caused membrane damage compromising cell viability but not cell integrity.

6.2. Introduction

The mechanisms of membrane disruption have been intensely studied in the literature. In general, membrane disruption is believed to occur mainly via a detergent-like carpet mechanism (or carpeting mechanism) or through the formation of discrete pores.[35] Different antimicrobial molecules may utilize different mechanisms to ultimately disrupt the microbial membrane.[125,170,171] Additional factors such as the lipid-to-antimicrobial molecule ratio and the target membrane composition may also have an effect on the mechanism of membrane disruption.[99]

In more detail, in the pore formation mechanism, the antimicrobial agent can form a pore that acts as a conductance channel that disrupts the transmembrane potential and its ion gradients. Consequently, it can lead to the leakage of cell components and cell death. Dissipation of the transmembrane electrochemical gradient causes a loss of the bacterial cell ability to synthesize

ATP and the increase in water and ion flow that accompanies loss of the permeability barrier leads to cell swelling and lysis.[170] This mechanism requires the antimicrobial agent to be sufficiently long to traverse the hydrophobic core of the bilayer, and implies a direct contact between the antimicrobial agent molecules upon channel formation.[172] On the other hand, in the carpeting mechanism, the antimicrobial agent accumulates at the bilayer surface like a carpet and, above a threshold concentration of the antimicrobial agent, the membrane is permeated and disintegrated in a detergent-like manner without the formation of discrete channels.[35]

Oxazoline-based polymers (POXs) have been pointed out as a more biocompatible alternative to the poly(ethylene glycol) (PEG), a polymer widely used in biomedical applications.[24,154] POXs constitute a versatile class of biocompatible polymers and have the ability to generate functional materials, characteristics that are interesting for a wide range of applications.[55] Commonly, POXs are synthesized by cationic *living* opening polymerization (CROP) which allows, by a simple manner, the functionalization of the polymeric chain with a molecule of interest.[173] Besides the control of the end-chain functionality, this synthetic route by CROP allows also an excellent control over POXs chain length, molar mass distribution, monomer composition and polymer architecture.[154]

In our group, oxazoline oligomers (OOXs) have been studied for the development of unique antimicrobial strategies using a green approach, in which the polymerization is carried out in supercritical carbon dioxide ($scCO_2$) media.[48] $scCO_2$ allows the synthesis of oligomers with defined properties such as narrow polydispersity and high purity of the final products, a constant demand in the biomedical industry.[23] Also, the screening of different potential antimicrobial end-chain molecules to functionalize oligo(2-oxazoline)s was performed. Oligomers end-capped with *N*,*N*-dimethyldodecylamine revealed to have broad spectrum activity, low minimum inhibitory concentrations (MIC) values and fast killing rates,[48] namely oligo(2-methyl-2-oxazoline), oligo(2-ethyl-2-oxazoline) and oligo(2-bisoxazoline) end-capped with *N*,*N*-dimethyldodecylamine (OMetOx-DDA, OEtOx-DDA and OBisOx-DDA) and linear oligo(ethyleneimine) hypochloride (LPEI). Frequently, the development of new antimicrobial agents requires the assessment of their mode of action in bacterial cells. The type of antimicrobial end-capping functionality used is not completely new, although reports in literature still do not provide a clear understanding of antimicrobial mechanism.[174] There are reports about the possible mechanisms of action of POXs similar to the ones synthesized in this work, suggesting that the main target of these antimicrobial agents is the membrane. It is proposed that the antimicrobial mechanism of these polymers involves interaction with the membrane surface, which causes localized disruption of the bacterial phospholipid membrane by the linear end-capper group.[54] Another interesting report used different liposomal systems as models for bacterial cell membranes that had different charge. It was described that the membrane disruption mechanism

of the polymers does not depend on the charge of the membrane and that the satellite effect of the distal nonbioactive groups is truly controlling the antimicrobial activity of the polymers.[53]

Nevertheless, as antimicrobial activity and specificity can be influenced by several parameters such as size, sequence, charge, conformation and structure, hydrophobicity and amphipathicity,[35] it was necessary to assess the mode of action of the antimicrobial oligomers synthesized in this work. Techniques used to investigate the mechanisms of action of antimicrobial peptide activity usually include microscopy, model membranes and fluorescent dyes.[35,175]

Herein, the leakage of different fluorescent markers encapsulated in large unilamelar vesicles (LUVs) after the addition of four different oligomers was followed (Scheme 6.1). Vesicles were composed by cardiolipin, phosphatidylglycerol and lysylphosphatidylglycerol in a molar proportion that mimics *S. aureus* bacterial membrane composition at the exponential phase.[176] The carboxyfluorescein leakage from LUVs experiments using fluorescence spectroscopy combined with the real-time tracking of both Alexa^{488}-dextran and Alexa^{633}-maleimide release using microscopy gave an insight of the oligomers mechanism of action.

Moreover, the direct visualization of *S. aureus* bacterial cells after addition of the compounds using wide-field and super-resolution microscopy was also performed. In combination, both can provide hints about the mechanism of action.

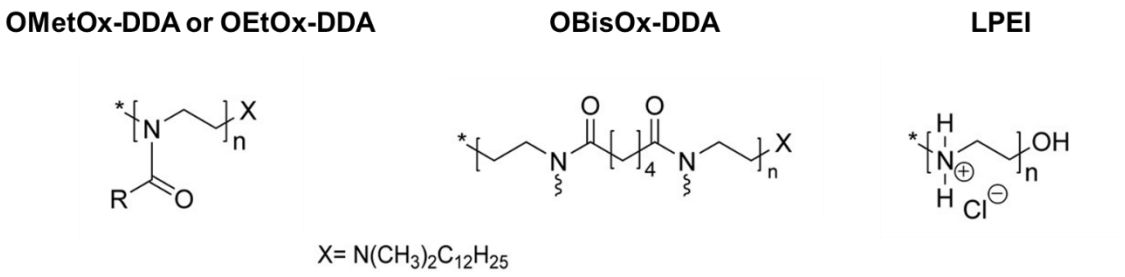

Scheme 6.1 - Chemical structure of the 4 oxazoline-based oligomers studied. R=CH_3 for OMetOx-DDA and R= C_2H_5 for OEtOx-DDA.

6.3. Experimental Section

6.3.1. Materials

Cardiolipin (CL), phosphatidylglycerol (PG) and lysylphosphatidylglycerol (LPG) were purchased from Avanti Polar Lipids and were used without further purification. Monomer 2-methyl-2-oxazoline (MeOx, purity >98 %), monomer 2-ethyl-2-oxazoline (EtOx, purity> 99%), initiator boron trifluoride diethyl etherate ($BF_3.OEt_2$, synthesis grade) and vancomycin were purchased from Sigma-Aldrich. The monomer 2-bisoxazoline (BisOx) was synthesized following a procedure already described.[95] *N*,*N*-dimethyldodecylamine was purchased from Fluka. Carbon dioxide was supplied by Air Liquide with a purity of 99.998 %. Oligo(2-methyl-2-oxazoline) quaternized with *N*,*N*-dimethyldodecylamine (M_w = 505 kg mol^{-1}) (OMetOx-DDA), Oligo(2-ethyl-2-oxazoline) quaternized with *N*,*N*-dimethyldodecylamine (M_w = 897 kg mol^{-1}) (OEtOx-DDA), oligo(2-bisoxazoline) quaternized with *N*,*N*-dimethyldodecylamine (M_w = 459 kg mol^{-1}) (OBisOx-DDA) and linear oligoethylenimine hydrochloride (Mw = 558 kg mol^{-1}) (LPEI) were synthesized as described previously.[48] 5(6)-carboxyfluorescein, Alexa^{488}-dextran and Alexa^{633}-maleimide, propidium iodide and Nile Red were purchased from Invitrogen. Tryptic Soy Broth (TSB) medium was purchased from Difco. BODIPY FL conjugate of vancomycin (Van-FL) was purchased from Molecular Probes. Agarose was purchased from Bio-rad. All materials and solvents were used as received without any further purification.

6.3.2. Preparation of carboxyfluorescein-loaded LUVs

Large unilamellar vesicles were prepared by freeze-thaw and extrusion through polycarbonate filters (pore diameter 100 nm)[177] in an extrusion device from Avanti Polar Lipids, Mini-Extruder Set and followed the procedure described by the manufacturer. Briefly, carboxyfluorescein 45 mM solution was generated by dissolving the proper amount of the fluorescent marker in Tris-HCl 20 mM, NaCl 150 mM, EDTA 1-mM buffer (pH 7.4 adjusted with NaOH 1 M). A lipid (CL/PG/LPG 0.65/1/0.36 mol ratio) solution in chloroform/methanol (2:1) was dried under a high vacuum drying overnight. This proportion mimics the *S. aureus* membrane composition at the exponential phase.[176] The lipid film was rehydrated with the carboxyfluorescein 45 mM buffer, freeze-thawed for five cycles, and extruded 19 times. The free carboxyfluorescein was removed by ultracenfrigugation (five cicles of 80000 rpm, 30 minutes at 4 ºC). To ascertain the lipid

concentration after the ultracentrifugation step, phospholipid phosphorous was measured by the modified microprocedure of Barlett.[178]

6.3.3. Measure of carboxyfluorescein leakage from LUVs

The release of carboxyfluorescein dye from the CL/PG/LPG LUVs after oligomer addition was measured using Cary Eclipse Fluorescence Spectrophotometer (Agilent Technologies, California, United States) at excitation and emission wavelengths of 480 and 510 nm, respectively. Fluorescence intensity was continuously recorded after the desired amount of peptide solution was added to a 96-well plate containing the carboxyfluorescein-loaded LUVs. Leakage is expressed as a percentage relative to the total amount of dye released by addition of 1 % (v/v) of Triton X-100, which represented 100 % leakage, as described by Weinstein et al..[179] Experiments were performed at least three times and maintaining the concentration of osmotic active particles in the same proportion inside and outside of vesicles. The time of presented release measuring was 15 min. Different molar ratio oligomer: LUVs were tested. Nisin 1mM was used as a control.

6.3.4. Preparation of Alexa^{488}-dextran/Alexa^{633}-maleimide-loaded LUVs

Large unilamellar vesicles were prepared by freeze-thaw and extrusion through polycarbonate filters (pore diameter 800 nm)[177] in an extrusion device from Avanti Polar Lipids, Mini-Extruder Set. Briefly, Alexa^{488}-dextran 1µM/Alexa^{633}-maleimide 10µM solution was generated by dissolving the proper amount of the fluorescent markers in Tris-HCl 20 mM, NaCl 150 mM, EDTA 1-mM buffer (pH 7.4 adjusted with NaOH 1 M). A lipid (CL/PG/LPG 0.65/1/0.36 mol ratio) solution in chloroform/methanol (2:1) was dried under a high vacuum drying overnight. The lipid film was rehydrated with the buffer containing the dyes, freeze-thawed for one cycle, and extruded 19 times. The free fluorescent dyes were removed by ultracenfrigugation (five cicles of 80000 rpm, 30 minutes at 4 ºC). To ascertain the lipid concentration after the ultracentrifugation step, phospholipid phosphorous was measured by the modified microprocedure of Barlett.[178]

6.3.5. Quantification of Alexa^{488}-dextran/Alexa^{633}-maleimide leakage from LUVs

The release of Alexa^{488}-dextran and Alexa^{633}-maleimide from the CL/PG/LPG LUVs after oligomer addition was quantified by fluorescence microscopy in an inverted Zeiss Axio Observer microscope equipped with a Photometrics CoolSNAP HQ2 camera (Roper Scientific). Fluorescence intensity was recorded at 0, 5, 10 and 20 min after the desired amount of peptide solution was added to the LUVs. The molar ratio oligomer:LUVs 100:1 was tested for all oligomers. Experiments were performed at least three times and maintaining the concentration of osmotic active particles in the same proportion inside and outside of vesicles. Several LUVs were followed as a function of time after peptide injection. The time of presented release measuring was 5, 10 and 20 min.

Leakage is expressed as a percentage relative to the total amount of dye initially present in each LUVs, which represented 100 %. All leakage experiments were quantitatively analyzed using ImageJ software by taking the change in fluorescence intensity as the average gray value measured for each micrograph of Alexa^{488}-dextran and Alexa^{633}-maleimide inside LUVs after oligomer addition.[180] Leakage of >= 50 % of fluorescent dye from the LUV over the course of the experiment was considered indicative of disruption and is presented in the graph. Triton X-100 1 % (v/v) and nisin 1 mM were used as controls.

6.3.6. Determination of liposomes size and zeta potential

LUVs were prepared as previously described and extruded through polycarbonate filters (pore diameter 800 nm). The size and zeta potential of the CL/PG/LPG LUVs before and after oligomer addition was determined using Zetasizer Nano (Malvern). Experiments were performed at least three times. Size and zeta potential were measured immediately after addition of the oligomer, t = 0 min, and after 15 min. The experiments were performed maintaining the concentration of osmotic active particles in the same proportion inside and outside of vesicles. The molar ratio oligomer:LUVs 100:1 was tested for all oligomers. Triton X-100 1 % (v/v) and nisin 1 mM were used as controls.

6.3.7. Direct visualization of *S. aureus* viability and integrity after contact with OMetOx-DDA

A 2 µl aliquot of an exponentially growing culture of *S. aureus NCTC8325-4* was placed on an agarose pad of PBS 1 % (w/v) containing the oligomer OMetOx-DDA and propidium iodide. *S. aureus NCTC8325-4* cells viability and integrity were assessed with an inverted Zeiss Axio Observer microscope equipped with a Photometrics CoolSNAP HQ2 camera (Roper Scientific).

6.3.8. Direct visualization of cell wall and membrane integrity of *S. aureus* after contact with OMetOx-DDA in high resolution microscopy

S. aureus NCTC8325-4 cells were incubated with the membrane dye Nile Red at a final concentration of 10 µg mL^{-1}, for 5 min at 37 °C, with agitation (550 r.p.m.). *S. aureus NCTC8325-4* cell wall labelling with vancomycin was performed by incubating the cells for 2 min at room temperature with a mixture containing equal amounts of vancomycin and a BODIPY FL conjugate of vancomycin to a final concentration of 0.8 µg mL^{-1}.

A 2 µl aliquot of an exponentially growing culture of *S. aureus NCTC8325-4* stained with Van-Fl and Nile Red was placed on an agarose pad in PBS containing OMetOx-DDA. Cells were visualized by Super-resolution structured illumination microscopy, SR-SIM. SR-SIM imaging was performed using a Plan-Apochromat 63x/1.4 oil DIC M27 objective, in an Elyra PS.1 microscope (Zeiss). Images were acquired using five grid rotations, with 34 µm grating period for the 561 nm laser (100 mW), 28 µm period for 488 nm laser (100 mW). Images were acquired using a Pco.edge 5.5 camera and reconstructed using ZEN software (black edition, 2012, version 8.1.0.484) based on a structured illumination algorithm,[181] using synthetic, channel specific optical transfer functions.

6.4. Results and Discussion

6.4.1. Measure of carboxyfluorescein leakage from LUVs

In order to determine the mode of action of the oligomers under study, large unillamelar vesicles (LUVs) with encapsulated carboxyfluorescein (CF) were prepared by extrusion and film rehydration (see methods). LUVs were prepared with a composition of cardiolipin, phosphatidylglycerol and lysylphosphatidylglycerol with a molar proportion of 0.65/1/0.36 to mimic the membrane composition of *S. aureus* cells growing in exponential phase.[176] By monitoring the dynamics of CF release from the LUVs, we could infer the mechanism of action of each oligomer under study. (Figure 6.1). In the end of the assay, the addition of a detergent, Triton X-100, that completely solubilizes the membrane, allows the quantification of total amount of the entrapped dye (100 % leakage).

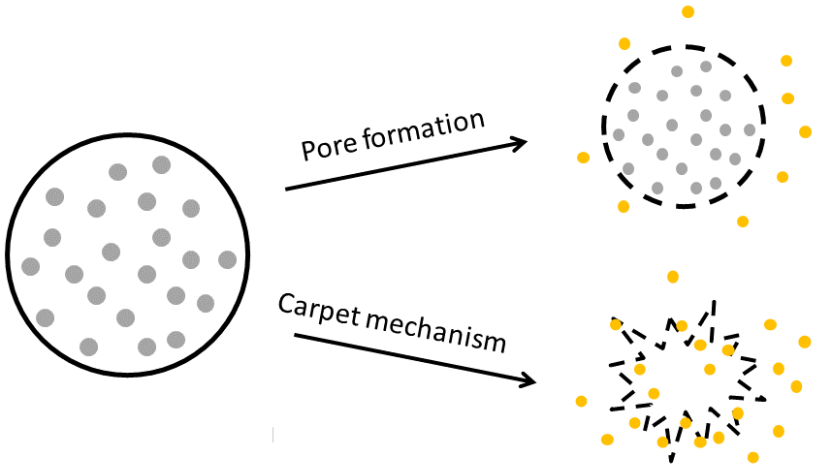

Figure 6.1 - Carboxyfluorescein leakage from LUVs as a method to study the mechanism of action of the oligomers under study. Carboxyfluorescein fluorescence is quenched above a certain concentration inside LUVs and fluorescence intensity can be measured over time when leaked and diluted in solution.[182] Slow release of carboxyfluorescein indicates pore formation, while rapid and burst release of carboxyfluorescein may indicate a carpeting mechanism.

LUVs were exposed to different molar ratios of oligomer: LUVs and carboxyfluorescein leakage was followed for 15 minutes (Figure 6.2).

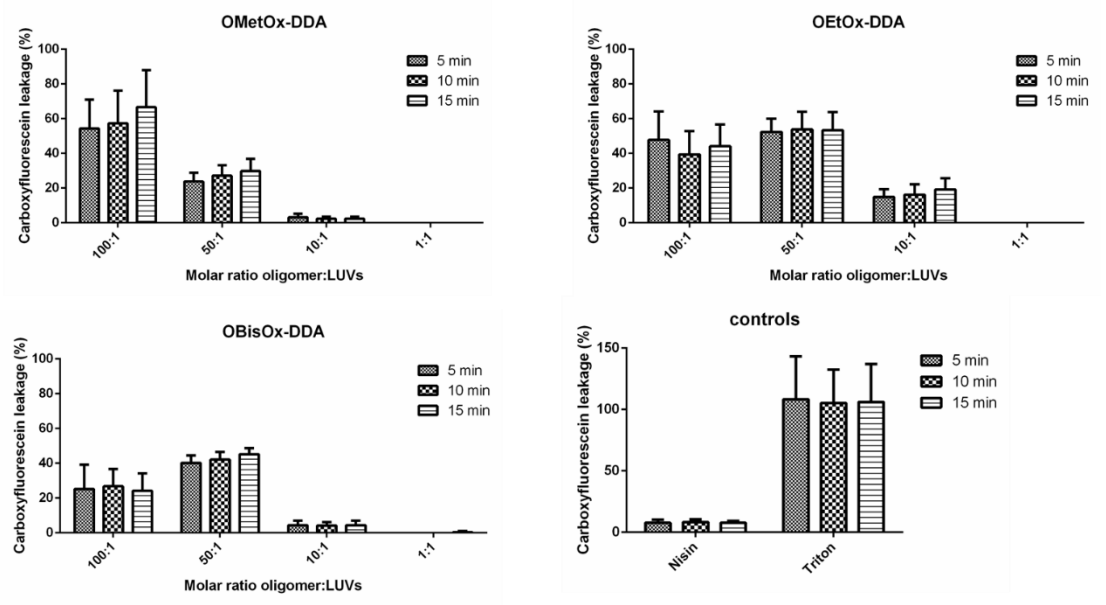

Figure 6.2 - Effect of antimicrobial oligomers on CL/PG/LPG LUVs permeability. Percentage of carboxyfluorescein release from LUVs after the addition of OMetOx-DDA, OEtOx-DDA and OBisOx-DDA over 5, 10 and 15 min. As controls, nisin 1mM (a pore forming molecule) and Triton X-100 1 % (v/v) (a detergent) were used. Results were normalized by adding triton X-100 to provoke LUVs lysis in the end of each assay (100 % leakage).

The leakage of carboxyfluorescein from CL/PG/LPG LUVs after the addition of different oligomer concentrations, is shown in Figure 2. The oligomers alter the hydrophobic/hydrophilic seal of LUV membranes allowing permeation of carboxyfluorescein. Also, the LUVs permeation is highly dependent on the used molecular ratio. OMetOx-DDA and OEtOx-DDA result in nearly 50 % carboxyfluorescein leakage at the molar ratio of 100:1. A slightly higher leakage is observed for OEtOx-DDA for the molar ratio 50:1 and 10:1 when compared to OMetOx-DDA. OBisOx-DDA also led to carboxyfluorescein leakage although in a lower percentage than the other oligomers. The leakage of carboxyfluorescein after LPEI addition was not evident during the time range of the assay, even when the assay time was extended to 240 min. In both tests, Triton X-100 1 % (v/v) was added in the end to cause LUVs lysis, allowing quantification of the total amount of dye. Interestingly, carboxyfluorescein leakage was not detected suggesting that LPEI may strongly interact with LUVs, protecting them from Triton X-100 action and from lysis.

Triton X-100 and nisin were used as controls. The addition of Triton X-100 to LUVs solution results in a burst leakage of carboxyfluorescein and proves its action as a detergent that solubilizes a lipidic vesicle.[183] On the other hand, nisin is known to act by forming pores in the bacterial cell membrane[184] leading to a slow release of carboxyfluorescein from the LUVs.

6.4.2. Quantification of Alexa^{488}-dextran/Alexa^{633}-maleimide leakage from LUVs

Data obtained in the carboxyfluorescein assay gave us an insight on the mechanism of action but not a direct and clear information about it. With that purpose, an assay that allowed tracking of the oligomer-induced leakage of two co-encapsulated fluorescent dyes with different molecular weights from LUVs was performed. Ideally, differential release among different oligomers would be observed.

The incorporation of both fluorophores, Alexa^{488}-dextran (M_w 10,000) and Alexa^{633}-maleimide (M_w ~ 1300), inside the LUVs is useful to directly observe the time course of any effect on membrane permeability (Figure 6.3).[175]

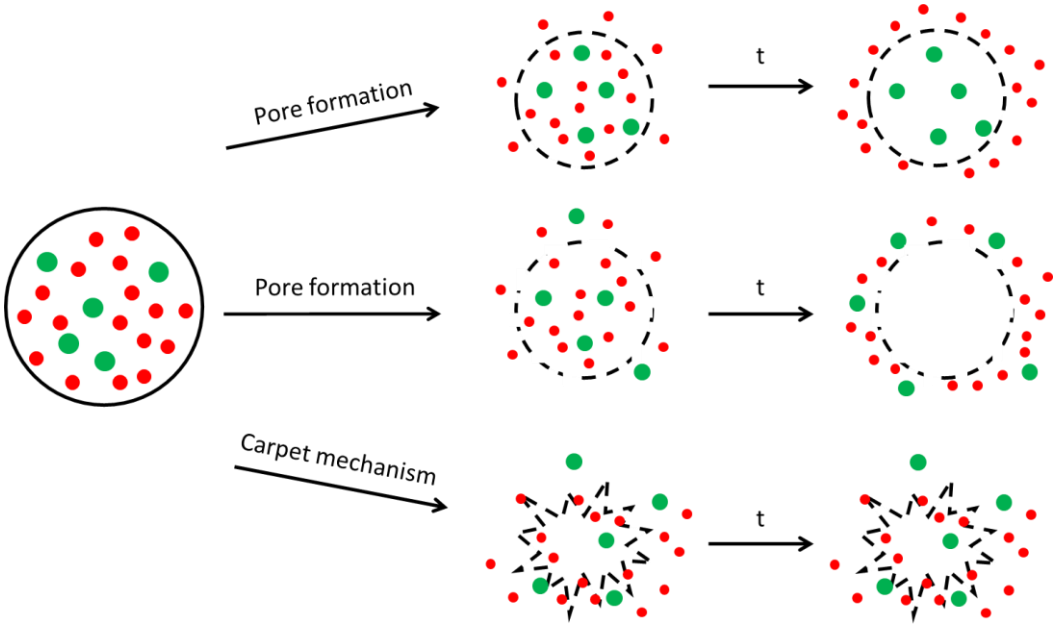

Figure 6.3 - Alexa^{488}-dextran (green, M_w 10 000) and Alexa^{633}-maleimide (red, M_w ~1300) leakage from LUVs. Red fluorophore release can indicate that the oligomer acts by forming pores in the membrane. Release of both fluorophores can indicate a formation of a big pore, if LUVs integrity is maintained, or a mode of action by carpeting if LUVs integrity is not maintained. Fluorophores different molecular weights indicate the size of the pore: if pores are formed, Alexa^{488}-dextran will only leak through the large pores while Alexa^{633}-maleimide is also able to leak from small pores. Release rates can also give an insight of the mechanism of action: slow release of both fluorophores – pore formation mechanism; fast release of both fluorophores – carpeting mechanism.

All the experiments were carried out at with a solution containing a peptide/lipid molar ratio of 100:1 where it was observed the highest percentage value of carboxyfluorescein leakage. As control, in the absence of peptide, the fluorescent dyes were not released spontaneously in a significant manner in the time frame of the assay. 20 LUVs were analysed after 5, 10 and 20 minutes of contact with each oligomer. Oligomers where added to the LUVs solution immediately

before microscope quantification. It is necessary to remark that the time of analysis was obtained from experiments performed at the microscope in solid medium, where stirring was not possible.

The effects of OMetOx-DDA, OEtOx-DDA, OBisOx-DDA and OEI on LUVs encapsulating the two fluorescent markers are shown in Figure 6.4.

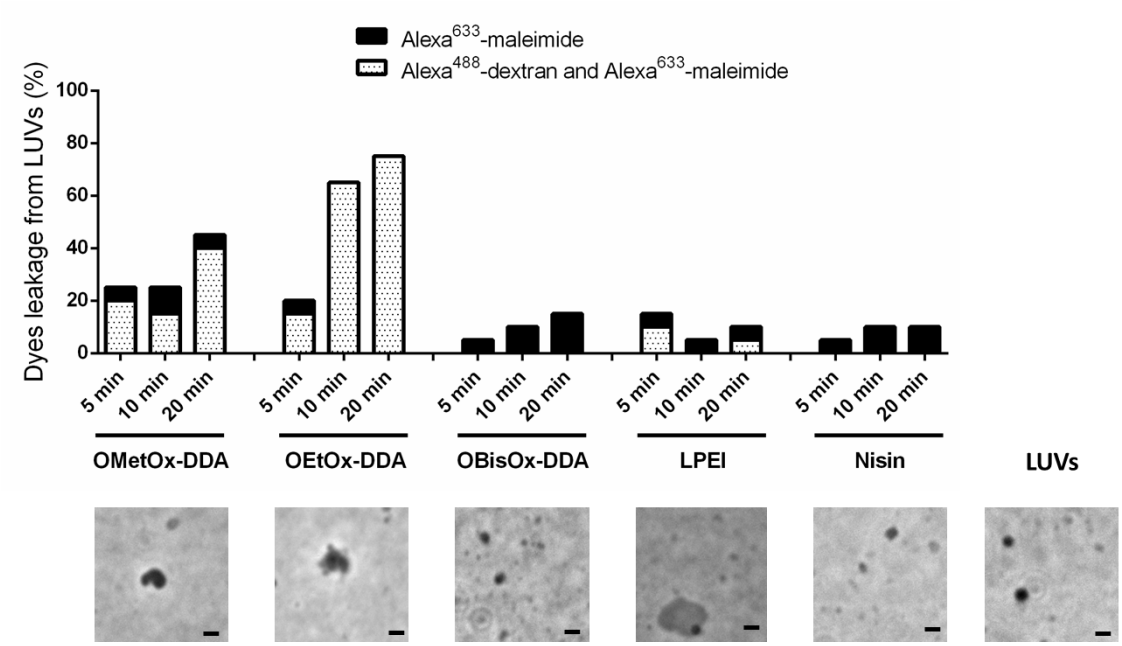

Figure 6.4 - Release of Alexa^{488}-dextran (M_w 10,000) and Alexa^{633}-maleimide (M_w ~ 1300), inside the LUVs after addition of oligomers (t = 5, 10 and 20 min). Data obtained after nisin (1mM) addition is also shown for comparison. At the bottom, is shown the LUVs morphology after 20 min of exposure to each oligomer; LUVs in the absence of oligomer is also shown as control. Scale bar, 1 µm.

After being exposed to OMetOx-DDA and OEtOx-DDA, LUVs leaked both fluorescent dyes in a similar manner and the leakage increased over time. This can indicate that these oligomers act by creating large pores in the membrane or by a carpeting mechanism. By analyzing the LUVs morphology, the mechanism of action is by carpeting mechanism as the LUVs have their integrity affected in the time range of the assay and in the tested molar ratio. It is important to mention that the immobilization of the LUVs in an agarose pad could slightly change the diffusion rate of the oligomers (when compared to the diffusion rate in solution) and could have impaired a faster action of OMetOx-DDA, justifying the difference observed when comparing to OEtOx-DDA.

After addition of OBisOx-DDA, only the low molecular weight dye leaked from the LUVs. As the fluorescence intensity of the high molecular weight dye trapped inside the LUVs did not change, these results strongly suggest that this oligomer act by the formation of pores in the time

range of the assay and in the tested molar ratio. After addition of LPEI, both dyes leaked from the LUVs. The release of both dyes occurred in a smaller percentage when comparing to OMetOx-DDA and OEtOx-DDA suggesting a slower release rate that could indicate a pore formation mechanism with big pores. No visual change in the LUVs morphology was observed for both OBisOx-DDA and LPEI in the time range of the assay and in the tested molar ratio, confirming that the mechanism of action is by pore formation.

A control performed with the pore-forming peptide nisin[184] showed a similar behavior to OBisOx-DDA. A control using Triton X-100 was also done but no LUVs were detected at the microscope, indicating that LUVs lysed immediately. Control experiments in the absence of the oligomers and in the time range of the assay (t = 20min) were performed and no change in the fluorescence intensity was observed, showing that the decrease in the fluorescence intensity is triggered by the action of the oligomers and not from dye photobleaching. Additionaly, LUVs maintained their morphology intact during the time range of the assay.

6.4.3. Determination of liposomes size and zeta potential

In order to assess the changes occurred in the LUVs size and surface, LUVs were characterized, using a Zetasizer equipment, before and after the addition of the oligomers. The experiments were carried out at a peptide/lipid molar ratio of 100:1, keeping in line with the observed highest percentage value of carboxyfluorescein leakage.

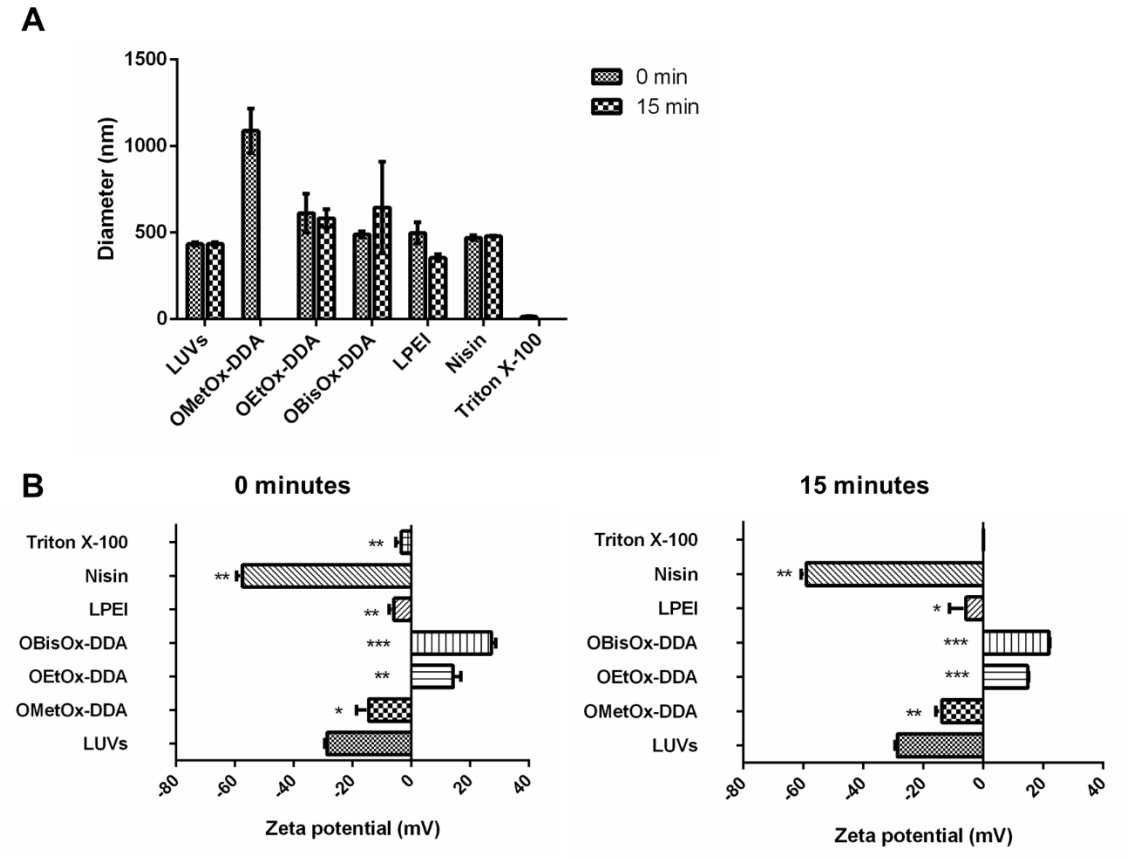

Figure 6.5 - LUVs (A) diameter (nm) and (B) zeta potential (mV) immediately after oligomers addition (t = 0min) and after 15 minutes. LUVs diameter and zeta potential in the absence of oligomer are shown as a control at both t = 0 min and t = 15 min. Nisin 1mM and Triton X-100 1 % (v/v) were used as controls.

LUVs had a mean diameter of 430 nm and maintained the diameter during the time range of the assay, 15 minutes. Immediately after the addition of OMetOx-DDA, the LUVs size increased to approximately 1µm. After 15 min, LUVs size could not be measured indicating that LUVs dissolved. Immediately after the addition of the oligomers OEtOx-DDA, OBisOx-DDA and LPEI, LUVs slightly increased in size. After 15 minutes, the same result was observed. As a control, nisin also caused a slight increase in the LUVs size at t = 0 and t = 15 min. LUVs size could not be measured after addition of Triton X-100, in accordance with previous results.

LUVs surface charge was altered after addition of the oligomers. In all oligomers, the change in the charge occurred immediately after the contact with the oligomer, indicating that their action is really fast, and the result was maintained until t = 15min. LUVs not exposed to oligomers, maintained their surface charge (approximately, -30mV) showing that changes were exclusively caused by the action of the oligomers. All oligomers caused an increase in the surface charge, which was expected since oligomers are positively charge molecules. The contribution of all oligomers charge in solution was taken into account and subtracted to obtain the final value of

LUVs zeta potential. OMetOx-DDA and LPEI increased slightly the zeta potential value, and LUVs still presented a negative value. On the other hand, OEtOx-DDA and OBisOx-DDA altered the zeta potential to a positive value, which indicates a strong interaction with the negative charge of the LUVs. The decrease in the zeta potential after addition of nisin can be justified with the nisin negative charge in solution. Additionally, it was only possible to measure LUVs zeta potential immediately after Triton X-100 addition as it dissolves the LUVs rapidly.

Both size and zeta potential values remained unaltered from t = 0 min to t = 15 min, showing that the action of the oligomers was extremely rapid and that it occurred during the early seconds of contact.

6.4.4. Direct visualization of *S. aureus* viability and integrity after contact with OMetOx-DDA

To assess *S. aureus* cell viability after oligomer action, cells were stained with propidium iodide that only enters cells if the membrane has been permeabilized.[185]

S. aureus NCTC8325-4 cells were placed on an agarose pad containing OMetOx-DDA oligomer and propidium iodide (Figure 6.6). OMetOx-DDA was chosen to perform the later assays because it revealed to be one of the oligomers that caused the more drastic and faster effects on LUVs integrity.

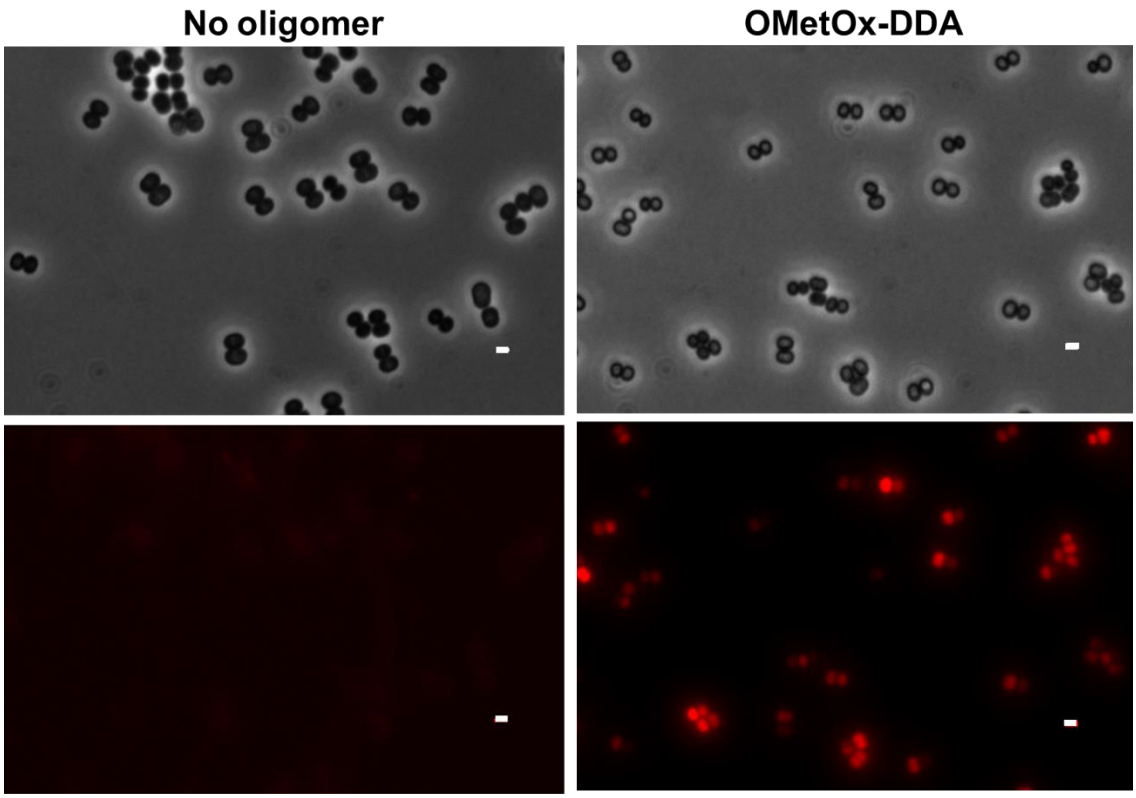

Figure 6.6 - Labelling of cells with propidium iodide (PI) to assess *S. aureus NCTC8325-4* viability after addition of OMetOx-DDA. The cells are not viable 2 min after addition but maintain cell integrity. As a control, cells were exposed to PI in the absence of oligomer. Scale bar, 1 µm.

Immediately after the addition of OMetOx-DDA, *S. aureus* cells appeared labeled with propidium iodide but maintained their normal shape. Therefore, cells lost their viability but maintained their overall integrity showing that OMetOx-DDA targets the membrane, apparently without compromising the cell wall.

6.4.5. Direct visualization of cell wall and membrane integrity of *S. aureus* after contact with OMetOx-DDA in super resolution microscopy

To directly visualize the target of OMetOx-DDA, the bacterial cell membrane, *S. aureus NCTC8325-4* was labelled with Van-FL to stain the bacterial cell wall and Nile Red to stain the bacterial cell membrane. *S. aureus* cells were then placed on an agarose pad containing OMetOx-DDA oligomer and visualized by super-resolution structured illumination microscopy, SR-SIM (Figure 6.7).

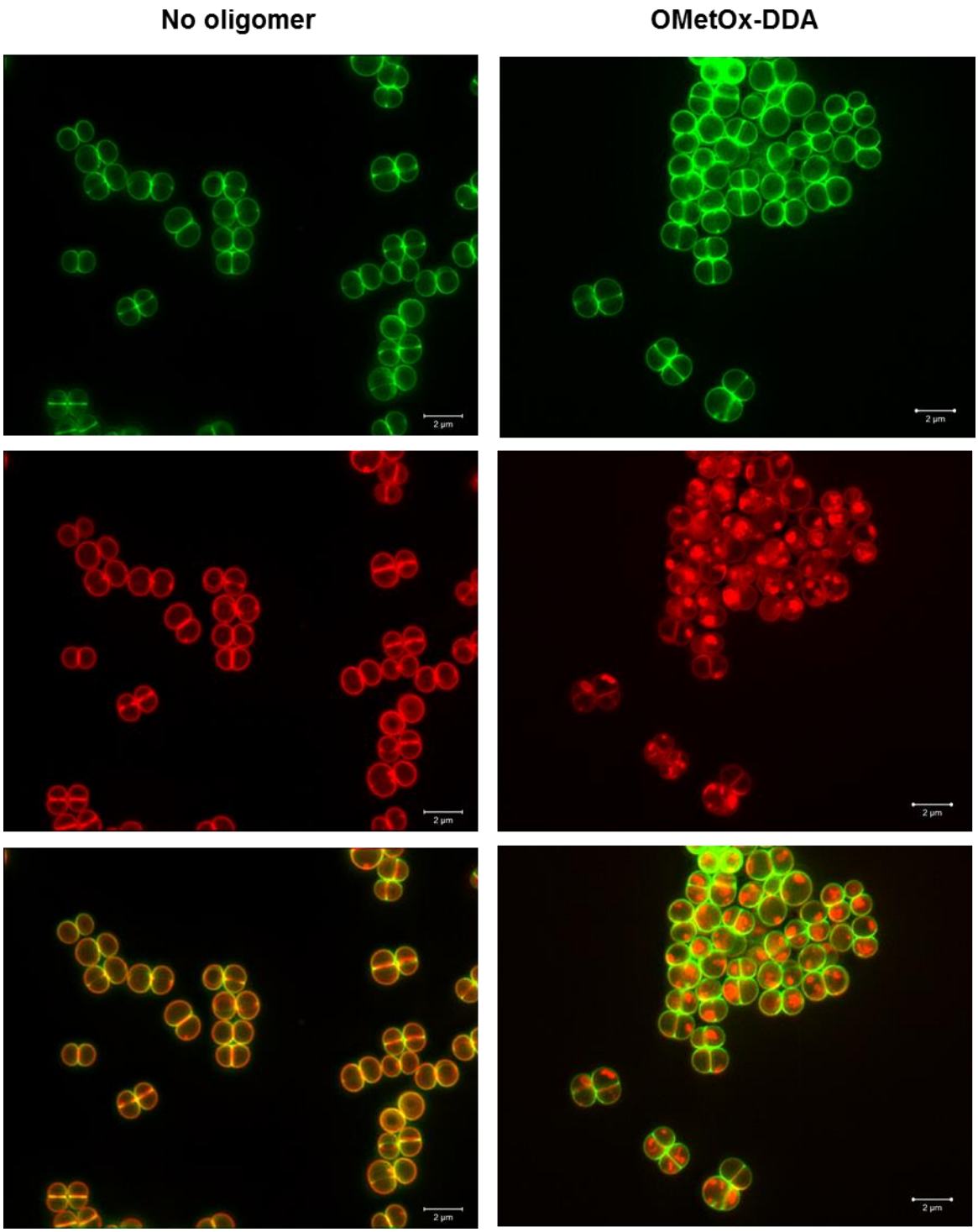

Figure 6.7 - *S. aureus NCTC8325-4* cell wall and membrane integrity was assessed by direct visualization. Cells were labeled with Van-FL (green panel, labels cell wall) and Nile red (red panel, labels membrane). At the bottom, channels were merged. Left panels show *S. aureus* cells and right panels show the effect of OMetOx-DDA on *S. aureus* cell wall and membrane integrity. Cell wall maintained the integrity while membrane was damage in the presence of OMetOx-DDA. Scale bar, 2 µm.

The action of OMetOx-DDA was observed immediately at the microscope just after the contact with the cells. SR-SIM images supports the theory that OMetOx-DDA acts in the membrane of *S. aureus* cells by disrupting it through a carpeting mechanism.

6.5. Conclusions

Experiments comprising dye encapsulation in *S. aureus* model membranes, LUVs, in association with the direct visualization of cells at the microscope represent a good method to disclosure oligomers mechanism of action.

Carboxyfluorescein leakage from LUVs allows to quantitatively measure if LUVs permeability is being affected in the presence of the oligomers. On the other hand, burst or sequential leaching of fluorescence dyes with different molecular weights by wide-field microscopy, gives further information about how oligomers act in bacterial cells. Results showed that OMetOx-DDA and OEtOx-DDA act, most likely, by a carpeting mechanism while OBisOx-DDA and LPEI seem to act by a pore formation mechanism.

Additionally, OMetOx-DDA showed to affect cell viability as it permeabilized *S. aureus* membrane to propidium iodide, without altering cells normal shape. Also, by fluorescent microscopy using SR-SIM, it was possible to observe that *S. aureus* cell wall seemed intact in the presence of OMetOx-DDA whereas the membrane was damaged.

Further work is required, namely by performing wide-field microscopy to visualize cell viability and by SR-SIM to assess the cell wall and membrane integrity for OEtOx-DDA, OBisOx-DDA and LPEI. Additionally, assays using different molecular weight fluorescent dyes co-encapsulated inside LUVs could elucidate the size of the pore formed in the presence of OBisOx-DDA and LPEI oligomers.

6.6. Acknowledgments

The authors would like to thank the financial support from Fundação para a Ciência e Tecnologia (FCT—Lisbon) and COMPETE through Contracts UID/QUI/50006/2013 and SFRH/BD/74730/2010 (VGC) and SFRH/BD/71993/2010 (JMM).

Chapter 7. Conclusions and future prospects

Microbial infection remains one of the most serious problems in different areas, particularly in medical devices and hospital equipment, drugs, health care and hygienic applications, water purification systems and food packaging. In the last years, academic research and industry have focused in the study of alternative antimicrobial agents to improve materials quality and safety and also on the development of more green and sustainable processes.

As this PhD thesis was developed in the framework of a Sustainable Chemistry doctoral program, some green chemistry principles[186] were followed:

- Prevention: by the use of supercritical carbon dioxide the formation of waste is prevented. Unreacted monomer and initiator can be recovered and extensive purification steps in the end of the reactions are avoided;

- Less Hazardous Chemical Syntheses: the synthesized antimicrobial oligomers are biocompatible and do not represent toxicity to human health and to the environment;

- Safer Solvents and Auxiliaries: by the use of supercritical carbon dioxide and plasma technology, the use of hazardous solvents is avoided. Carbon dioxide is a gas at atmospheric conditions and, therefore, the final products can be easily obtained without any traces of solvent and plasma technology is known to be a solvent free technique;

- Reduce Derivatives: both oligomerization reactions and surface grafting of oxazoline-based oligomers were performed without the use of derivatization steps;

- Design for Degradation: platforms of a natural product, chitosan, were used in order to minimize the formation of toxic byproducts after degradation.

The above mentioned green chemistry principles were used as decision tools since the conceptual design of this work: i) selecting less toxic solvents and natural materials, ii) choosing the strategy to synthesize the oligomers, and iii) the route to confer antimicrobial activity to platforms; until the application of the antimicrobial platforms for water treatment.

Polymers or oligomers are extremely versatile molecules. Their properties, like functional groups, molecular weight, biocompatibility, efficiency, selectivity and lifetime, can be easily tuned. Therefore, research developed within this topic is very challenging. In this work, it was successfully synthesized a library of 2-oxazoline-based oligomers in supercritical carbon dioxide ($scCO_2$), a class of compound known for its biocompatibility. Type of monomer, end-capping molecule and oligomer architecture was varied and their impact on the antimicrobial activity was assessed. Oligomers with low minimum inhibitory concentrations (MIC), fast killing rates, broad-spectrum activity and low cytotoxicity were selected as the most promising oligomers for antimicrobial applications.

3D porous scaffolds are known for the well organized and interconnected porous network which provides a material with high surface area. Scaffolds have been prepared, so far, mainly by conventional synthetic procedures and scaffolds functionalization strategies employed until today required several steps, use of organic solvents and, therefore, extensive purification steps in the end. In order to obtain a scaffold with unique antimicrobial properties and to minimize the impact of its production in the environment, surface modification by plasma technology was combined with oligomerization in supercritical carbon dioxide. Plasma technology, known as a solvent free technique, has demonstrated to be an alternative and powerful strategy to compete with the traditional organic functionalization routes. By this green route it was produced a scaffold with brief times of contact (3 minutes) that was able to kill > 99.999 % of *E. coli* and *S. aureus* cells without promoting, at the same time, bacterial adhesion to the material. Additionally, this scaffold was tested for its ability to purify water using two different environmental water samples and revealed to be able to efficiently kill bacteria within minutes of contact without leaching to the water and can be reused for 10 cycles.

Although these are encouraging results, more studies have to be done and industries have also to change their mentalities before this strategy can reach a commercial application. Future work involves the characterization of biocompatibility against other cell lines (mainly against red blood cells), the development of materials with different antimicrobial OOXs surface density and the further elucidation and characterization of oligomers mode of action. Also, it would be interesting to immobilize antimicrobial OOXs into completely different 3D materials, namely medical devices, to assess immobilization efficiency as well as materials self-disinfection properties.

References

(1) Ashbolt, N. J. Microbial Contamination of Drinking Water and Disease Outcomes in Developing Regions. *Toxicology* **2004**, *198*, 229–238.

(2) Zularisam, A. W.; Ismail, A. F.; Salim, R. Behaviours of Natural Organic Matter in Membrane Filtration for Surface Water Treatment - a Review. *Desalination* **2006**, *194*, 211–231.

(3) LeChevallier, M. W.; Au, K.-K. *World Health OrganizationWater Treatment and Pathogen Control: Process Efficiency in Achieving Safe Drinking-Water*; 2004.

(4) Kenawy, E.-R.; Worley, S. D.; Broughton, R. The Chemistry and Applications of Antimicrobial Polymers: A State-of-the-Art Review. *Biomacromolecules* **2007**, *8*, 1359–1384.

(5) Pintar, K. D. M.; Slawson, R. M. Effect of Temperature and Disinfection Strategies on Ammonia-Oxidizing Bacteria in a Bench-Scale Drinking Water Distribution System. *Water Res.* **2003**, *37*, 1805–1817.

(6) Pianta, R.; Boller, M.; Urfer, D.; Chappaz, A.; Gmünder, A. Costs of Conventional vs. Membrane Treatment for Karstic Spring Water. *Desalination* **2000**, *131*, 245–255.

(7) Mansouri, J.; Harrisson, S.; Chen, V. Strategies for Controlling Biofouling in Membrane Filtration Systems: Challenges and Opportunities. *J. Mater. Chem.* **2010**, *20*, 4567–4586.

(8) Bixler, G. D.; Bhushan, B. Biofouling: Lessons from Nature. *Philos. Trans. R. Soc. A* **2012**, *370*, 2381–2417.

(9) Hilal, N.; Ogunbiyi, O. O.; Miles, N. J.; Nigmatullin, R. Methods Employed for Control of Fouling in MF and UF Membranes: A Comprehensive Review. *Sep. Sci. Technol.* **2005**, *40*, 1957–2005.

(10) Vainrot, N.; Eisen, M. S.; Semiat, R. Membranes in Desalination and Water Treatment. *MRS Bull.* **2008**, *33*, 16–20.

(11) van de Witte, P.; Dijkstra, P. J.; van den Berg, J. W. A.; Feijen, J. Phase Separation Processes in Polymer Solutions in Relation to Membrane Formation. *J. Memb. Sci.* **1996**, *117*, 1–31.

(12) Matsuyama, H.; Yano, H.; Maki, T.; Teramoto, M.; Mishima, K.; Matsuyama, K. Formation of Porous Flat Membrane by Phase Separation with Supercritical CO2. *J. Memb. Sci.* **2001**, *194*, 157–163.

(13) Reverchon, E.; Cardea, S. Formation of Cellulose Acetate Membranes Using a Supercritical Fluid Assisted Process. *J. Memb. Sci.* **2004**, *240*, 187–195.

(14) Temtem, M.; Casimiro, T.; Aguiar-Ricardo, A. Solvent Power and Depressurization Rate Effects in the Formation of Polysulfone Membranes with CO2-Assisted Phase Inversion Method. *J. Memb. Sci.* **2006**, *283*, 244–252.

(15) Kemmere, M. F.; Meyer, T. *Supercritical Carbon Dioxide: In Polymer Reaction Engineering*; Wiley-VCH Verlag GmbH & Co. KGaA, 2006.

(16) Hyde, J. R.; Licence, P.; Carter, D.; Poliakoff, M. Continuous Catalytic Reactions in Supercritical Fluids. *Appl. Catal. A Gen.* **2001**, *222*, 119–131.

(17) Leitner, W. Supercritical Carbon Dioxide as a Green Reaction Medium for Catalysis. *Acc. Chem. Res.* **2002**, *35*, 746–756.

(18) Sheldon, R. A. Green Solvents for Sustainable Organic Synthesis: State of the Art. *Green Chem.* **2005**, *7*, 267–278.

(19) Beckman, E. J. Supercritical and near-Critical CO2 in Green Chemical Synthesis and Processing. *J. Supercrit. Fluids* **2004**, *28*, 121–191.

(20) Kendall, J. L.; Canelas, D. A.; Young, J. L.; DeSimone, J. M. Polymerizations in Liquid and Supercritical Carbon Dioxide. *Chem. Rev.* **1999**, *99*, 543–563.

(21) Cooper, A. I. Polymer Synthesis and Processing Using Supercritical Carbon Dioxide. *J. Mater. Chem.* **2000**, *10*, 207–234.

(22) Mingotaud, A.-F.; Dargelas, F.; Cansell, F. Cationic and Anionic Ring-Opening Polymerization in Supercritical CO2. *Macromol. Symp.* **2000**, *153*, 77–86.

(23) de Macedo, C. V.; da Silva, M. S.; Casimiro, T.; Cabrita, E. J.; Aguiar-Ricardo, A. Boron Trifluoride Catalyzed Polymerisation of 2-Substituted-2-Oxazolines in Supercritical Carbon Dioxide. *Green Chem.* **2007**, *9*, 948–953.

(24) Adams, N.; Schubert, U. S. Poly(2-Oxazolines) in Biological and Biomedical Application Contexts. *Adv. Drug Deliv. Rev.* **2007**, *59*, 1504–1520.

(25) Lobert, M.; Köhn, U.; Hoogenboom, R.; Schubert, U. S. Synthesis and Microwave Assisted Polymerization of Fluorinated 2-Phenyl-2-Oxazolines: The Fastest 2-Oxazoline Monomer to Date. *Chem. Commun.* **2008**, 1458–1460.

(26) Aoi, K.; Okada, M. Polymerization of Oxazolines. *Prog. Polym. Sci.* **1996**, *21*, 151–208.

(27) Wiesbrock, F.; Hoogenboom, R.; Leenen, M. A. M.; Meier, M. A. R.; Schubert, U. S. Investigation of the Living Cationic Ring-Opening Polymerization of 2-Methyl- , 2-Ethyl- , 2-Nonyl- , and 2-Phenyl-2-Oxazoline in a Single-Mode Microwave Reactor. *Macromolecules* **2005**, *38*, 5025–5034.

(28) Zhang, C.; Liao, L.; Gong, S. S. Recent Developments in Microwave-Assisted Polymerization with a Focus on Ring-Opening Polymerization. *Green Chem.* **2007**, *9*, 303–314.

(29) Bonifácio, V. D. B.; Correia, V. G.; Pinho, M. G.; Lima, J. C.; Aguiar-Ricardo, A. Blue Emission of Carbamic Acid Oligooxazoline Biotags. *Mater. Lett.* **2012**, *81*, 205–208.

(30) Mero, A.; Pasut, G.; Via, L. D.; Fijten, M. W. M.; Schubert, U. S.; Hoogenboom, R.; Veronese, F. M. Synthesis and Characterization of poly(2-Ethyl 2-Oxazoline)-Conjugates with Proteins and Drugs: Suitable Alternatives to PEG-Conjugates? *J. Control. Release* **2008**, *125*, 87–95.

(31) Siedenbiedel, F.; Tiller, J. C. Antimicrobial Polymers in Solution and on Surfaces: Overview and Functional Principles. *Polymers (Basel).* **2012**, *4*, 46–71.

(32) Ikeda, T.; Ledwith, A.; Bamford, C. H.; Hann, R. A. Interaction of a Polymeric Biguanide Biocide with Phospholipid Membranes. *Biochim. Biophys. Acta - Biomembr.* **1984**, *769*, 57–66.

(33) Madkour, A. E.; Dabkowski, J. M.; Nüsslein, K.; Tew, G. N. Fast Disinfecting Antimicrobial Surfaces. *Langmuir* **2012**, *25*, 1060–1067.

(34) Cornell, R. J.; Donaruma, L. G. 2-Methacryloxytroponones. Intermediates for Synthesis of Biologically Active Polymers. *J. Med. Chem* **1965**, *8*, 388–390.

(35) Brogden, K. A. Antimicrobial Peptides: Pore Formers or Metabolic Inhibitors in Bacteria? *Nat. Rev. Microbiol.* **2005**, *3*, 238–250.

(36) De Souza, A. C.; Dias, A. M. a; Sousa, H. C.; Tadini, C. C. Impregnation of Cinnamaldehyde into Cassava Starch Biocomposite Films Using Supercritical Fluid Technology for the Development of Food Active Packaging. *Carbohydr. Polym.* **2014**, *102*, 830–837.

(37) Furno, F.; Morley, K. S.; Wong, B.; Sharp, B. L.; Arnold, P. L.; Howdle, S. M.; Bayston, R.; Brown, P. D.; Winship, P. D.; Reid, H. J. Silver Nanoparticles and Polymeric Medical Devices: A New Approach to Prevention of Infection? *J. Antimicrob. Chemother.* **2004**, *54*, 1019–1024.

(38) Kumar, R.; Howdle, S.; Münstedt, H. Polyamide/silver Antimicrobials: Effect of Filler Types on the Silver Ion Release. *J. Biomed. Mater. Res. - Part B Appl. Biomater.* **2005**, *75*, 311–319.

(39) Nguyen, V. H.; Kim, B. K.; Jo, Y. L.; Shim, J. J. Preparation and Antibacterial Activity of Silver Nanoparticles-Decorated Graphene Composites. *J. Supercrit. Fluids* **2012**, *72*, 28–35.

(40) Milovanovic, S.; Stamenic, M.; Markovic, D.; Radetic, M.; Zizovic, I. Solubility of Thymol in Supercritical Carbon Dioxide and Its Impregnation on Cotton Gauze. *J. Supercrit. Fluids* **2013**, *84*, 173–181.

(41) Torres, A.; Romero, J.; Macan, A.; Guarda, A.; Galotto, M. J. Near Critical and Supercritical Impregnation and Kinetic Release of Thymol in LLDPE Films Used for Food Packaging. *J. Supercrit. Fluids* **2014**, *85*, 41–48.

(42) Milovanovic, S.; Stamenic, M.; Markovic, D.; Ivanovic, J.; Zizovic, I. Supercritical Impregnation of Cellulose Acetate with Thymol. *J. Supercrit. Fluids* **2015**, *97*, 107–115.

(43) Markovic, D.; Milovanovic, S.; Radetic, M.; Jokic, B.; Zizovic, I. Impregnation of Corona Modified Polypropylene Non-Woven Material with Thymol in Supercritical Carbon Dioxide for Antimicrobial Application. *J. Supercrit. Fluids* **2015**, *101*, 215–221.

(44) Baldino, L.; Cardea, S.; Reverchon, E. Supercritical Assisted Enzymatic Membranes Preparation, for Active Packaging Applications. *J. Memb. Sci.* **2014**, *453*, 409–418.

(45) Chen, Y.; Niu, M.; Yuan, S.; Teng, H. Durable Antimicrobial Finishing of Cellulose with QSA Silicone by Supercritical Adsorption. *Appl. Surf. Sci.* **2013**, *264*, 171–175.

(46) Kamrupi, I. R.; Dolui, S. K. Synthesis of Copper–polystyrene Nanocomposite Particles Using Water in Supercritical Carbon Dioxide Medium and Its Antimicrobial Activity. *J. Appl. Polym. Sci.* **2011**, *120*, 1027–1033.

(47) Habulin, M.; Šabeder, S.; Knez, Ž. Enzymatic Synthesis of Sugar Fatty Acid Esters in Organic Solvent and in Supercritical Carbon Dioxide and Their Antimicrobial Activity. *J. Supercrit. Fluids* **2008**, *45*, 338–345.

(48) Correia, V. G.; Bonifácio, V. D. B.; Raje, V. P.; Casimiro, T.; Moutinho, G.; da Silva, C. L.; Pinho, M. G.; Aguiar-Ricardo, A. Oxazoline-Based Antimicrobial Oligomers: Synthesis by CROP Using Supercritical CO2. *Macromol. Biosci.* **2011**, *11*, 1128–1137.

(49) Xue, Y.; Xiao, H.; Zhang, Y. Antimicrobial Polymeric Materials with Quaternary Ammonium and Phosphonium Salts. *Int. J. Mol. Sci.* **2015**, *16*, 3626–3655.

(50) Yuan, J. J.; Jin, R. H. Multiply Shaped Silica Mediated by Aggregates of Linear Poly(ethyleneimine). *Adv. Mater.* **2005**, *17*, 885–888.

(51) Luxenhofer, R.; Han, Y.; Schulz, A.; Tong, J.; He, Z.; Kabanov, A. V; Jordan, R. Poly(2-Oxazoline)s as Polymer Therapeutics. *Macromol. Rapid Commun. Rapid Commun* **2012**, *33*, 1613–1631.

(52) Waschinski, C. J.; Tiller, J. C. Poly (oxazoline)s with Telechelic Antimicrobial Functions. *Biomacromolecules* **2005**, *6*, 235–243.

(53) Waschinski, C. J.; Barnert, S.; Theobald, A.; Schubert, R.; Kleinschmidt, F.; Hoffmann, A.; Saalwächter, K.; Tiller, J. C. Insights in the Antibacterial Action of Poly(methyloxazoline)s with a Biocidal End Group and Varying Satellite Groups. *Biomacromolecules* **2008**, *9*, 1764–1771.

(54) Waschinski, C. J.; Herdes, V.; Schueler, F.; Tiller, J. C. Influence of Satellite Groups on Telechelic Antimicrobial Functions of Polyoxazolines. *Macromol. Biosci.* **2005**, *5*, 149–156.

(55) Hoogenboom, R. Poly(2-Oxazoline)s: A Polymer Class with Numerous Potential Applications. *Angew. Chemie - Int. Ed.* **2009**, *48*, 7978–7994.

(56) Ho, C. H.; Tobis, J.; Sprich, C.; Thomann, R.; Tiller, J. C. Nanoseparated Polymeric Networks with Multiple Antimicrobial Properties. *Adv. Mater.* **2004**, *16*, 957–961.

(57) Ferreira, L.; Zumbuehl, A. Non-Leaching Surfaces Capable of Killing Microorganisms on

Contact. *J. Mater. Chem.* **2009**, *19*, 7796–7806.

(58) Konradi, R.; Pidhatika, B.; Mühlebach, A.; Textor, M. Poly-2-Methyl-2-Oxazoline: A Peptide-like Polymer for Protein-Repellent Surfaces. *Langmuir* **2008**, *24*, 613–616.

(59) Bieser, A. M.; Thomann, Y.; Tiller, J. C. Contact-Active Antimicrobial and Potentially Self-Polishing Coatings Based on Cellulose. *Macromol. Biosci.* **2011**, *11*, 111–121.

(60) Majumdar, P.; Lee, E.; Gubbins, N.; Stafslien, S. J.; Daniels, J.; Thorson, C. J.; Chisholm, B. J. Synthesis and Antimicrobial Activity of Quaternary Ammonium-Functionalized POSS (Q-POSS) and Polysiloxane Coatings Containing Q-POSS. *Polymer (Guildf).* **2009**, *50*, 1124–1133.

(61) Rehfeldt, F.; Tanaka, M.; Pagnoni, L.; Jordan, R. Static and Dynamic Swelling of Grafted Poly(2-Alkyl-2-Oxazoline)s. *Langmuir* **2002**, *18*, 4908–4914.

(62) Loontjens, T.; Rique-Lurbet, L. Synthesis of α-Alkyl ω-Trimethoxysilane Polyoxazolines and Their Application as Coatings on Glass Fibres. *Des. Monomers Polym.* **1999**, *2*, 217–229.

(63) Yoshikawa, S.; Tsubokawa, N.; Fujiki, K.; Sakamoto, M. Grafting of Polymers with Controlled Molecular Weight onto Inorganic Fiber Surface by Termination of Living Polymer Cation with Amino Group on the Surface. *Compos. Interfaces* **1999**, *6*, 395–407.

(64) Yoshikawa, S.; Tsubokawa, N. Grafting of Polymers with Controlled Molecular Weight onto Carbon Black Surface. *J. Polym. Sci. Part A Polym. Chem.* **1995**, *33*, 581–586.

(65) Yoshikawa, S.; Tsubokawa, N. Grafting of Polymers with Controlled Molecular Weight onto Carbon Black Surface. *Polymer Journal*. 1996, pp 317–322.

(66) Yoshikawa, S.; Satoh, T.; Tsubokawa, N. Post-Grafting of Polymer with Controlled Molecular Weight onto Silica Surface by Termination of Living Polymer Cation with Terminal Amino Groups of Dendrimer-Grafted Ultrafine Silica. *Colloids Surfaces A Physicochem. Eng. Asp.* **1999**, *153*, 395–399.

(67) Haensch, C.; Erdmenger, T.; Fijten, M. W. M.; Hoeppener, S.; Schubert, U. S. Fast Surface Modification by Microwave Assisted Click Reactions on Silicon Substrates. *Langmuir* **2009**, *25*, 8019–8024.

(68) Lehmann, T.; Rühe, J. Polyethyloxazoline Monolayers for Polymer Supported Biomembrane Models. *Macromol. Symp.* **1999**, *142*, 1–12.

(69) Yoshinaga, K.; Hidaka, Y. Cationic Graft-Polymerization of 2-Methyl-2-Oxazoline on Monodispersed Polymer-Coated Ultrafine Silica Particles. *Polym. J.* **1994**, *26*, 1070–1079.

(70) Lee, J.-H.; An, Y.-C.; Choi, D.-S.; Lee, M.-J.; Kim, K.-M.; Lim, J.-H. Fabrication of a Nano-Porous Polyoxazoline-Coated Tip for Scanning Probe Nanolithography. *Macromol. Symp.* **2007**, *249-250*, 307–311.

(71) Shin, Y. H.; Yun, S. H.; Pyo, S. H.; Lim, Y. S.; Yoon, H. J.; Kim, K. H.; Moon, S. K.; Lee, S. W.; Park, Y. G.; Chang, S. I.; et al. Polymer-Coated Tips for Patterning of Viruses by Dip-Pen Nanolithography. *Angew. Chemie - Int. Ed.* **2010**, *49*, 9689–9692.

(72) Ueda, J.; Gang, W.; Shirai, K.; Yamauchi, T.; Tsubokawa, N. Cationic Graft Polymerization onto Silica Nanoparticle Surface in a Solvent-Free Dry-System. *Polym. Bull.* **2008**, *60*, 617–624.

(73) Zhang, N.; Pompe, T.; Amin, I.; Luxenhofer, R.; Werner, C.; Jordan, R. Tailored poly(2-Oxazoline) Polymer Brushes to Control Protein Adsorption and Cell Adhesion. *Macromol. Biosci.* **2012**, *12*, 926–936.

(74) Adden, N.; Hoffmann, A.; Gross, G.; Windhagen, H.; Thorey, F.; Menzel, H. Screening of Photochemically Grafted Polymer Films for Compatibility with Osteogenic Precursor Cells. *J. Biomater. Sci. Polym. Ed.* **2007**, *18*, 303–316.

(75) Chang, B. J.; Prucker, O.; Groh, E.; Wallrath, A.; Dahm, M.; Rühe, J. Surface-Attached

Polymer Monolayers for the Control of Endothelial Cell Adhesion. *Colloids Surfaces A Physicochem. Eng. Asp.* **2002**, *198-200*, 519–526.

(76) Murata, H.; Chang, B. J.; Prucker, O.; Dahm, M.; Ruhe, J. Polymeric Coatings for Biomedical Devices. *Surf. Sci.* **2004**, *570*, 111–118.

(77) Prucker, O.; Naumann, C. A.; Rühe, J.; Knoll, W.; Frank, C. W. Photochemical Attachment of Polymer Films to Solid Surfaces via Monolayers of Benzophenone Derivatives. *J. Am. Chem. Soc.* **1999**, *121*, 8766–8770.

(78) Yan, M.; Ren, J. Covalent Immobilization of Ultrathin Polymer Films by Thermal Activation of Perfluorophenyl Azide. *Chem. Mater.* **2004**, *16*, 1627–1632.

(79) Gann, J. P.; Yan, M. A Versatile Method for Grafting Polymers on Nanoparticles. *Langmuir* **2008**, *24*, 5319–5323.

(80) Pidhatika, B.; Möller, J.; Benetti, E. M.; Konradi, R.; Rakhmatullina, E.; Mühlebach, A.; Zimmermann, R.; Werner, C.; Vogel, V.; Textor, M. The Role of the Interplay between Polymer Architecture and Bacterial Surface Properties on the Microbial Adhesion to Polyoxazoline-Based Ultrathin Films. *Biomaterials* **2010**, *31*, 9462–9472.

(81) Correia, V. G.; Coelho, M.; Barroso, T.; Raje, V. P.; Bonifácio, V. D. B.; Casimiro, T.; Pinho, M. G.; Aguiar-Ricardo, A. Anti-Biofouling 3D Porous Systems: The Blend Effect of Oxazoline-Based Oligomers on Chitosan Scaffolds. *Biofouling J. Bioadhesion Biofilm Res.* **2013**, *29*, 273–282.

(82) Desmet, T.; Morent, R.; Geyter, N. De; Leys, C.; Schacht, E.; Dubruel, P. Nonthermal Plasma Technology as a Versatile Strategy for Polymeric Biomaterials Surface Modification: A Review. *Biomacromolecules* **2009**, *10*, 2351–2378.

(83) Barroso, T.; Viveiros, R.; Temtem, M.; Casimiro, T.; Botelho Do Rego, A. M.; Aguiar-Ricardo, A. A Combined Strategy to Surface-Graft Stimuli-Responsive Hydrogels Using Plasma Activation and Supercritical Carbon Dioxide. *ACS Macro Lett.* **2012**, *1*, 356–360.

(84) Madkour, A. E.; Tew, G. N. Towards Self-Sterilizing Medical Devices: Controlling Infection. *Polym. Int.* **2008**, 6–10.

(85) Einzmann, M.; Binder, W. H. Novel Functional Initiators for Oxazoline Polymerization. *J. Polym. Sci. Part A Polym. Chem.* **2001**, *39*, 2821–2831.

(86) Hoogenboom, R. Poly(2-Oxazoline)s: Alive and Kicking. *Macromol. Chem. Phys.* **2007**, *208*, 18–25.

(87) Makino, A.; Kobayashi, S. Chemistry of 2-Oxazolines: A Crossing of Cationic Ring-Opening Polymerization and Enzymatic Ring-Opening Polyaddition. *J. Polym. Sci. Part A Polym. Chem.* **2010**, *48*, 1251–1270.

(88) Schlaad, H.; Diehl, C.; Gress, A.; Meyer, M.; Levent Demirel, a.; Nur, Y.; Bertin, A. Poly(2-Oxazoline)s as Smart Bioinspired Polymers. *Macromol. Rapid Commun.* **2010**, *31*, 511–525.

(89) Kumar, R. S.; Arunachalam, S. DNA Binding and Antimicrobial Studies of Polymer-copper(II) Complexes Containing 1,10-Phenanthroline and L-Phenylalanine Ligands. *Eur. J. Med. Chem.* **2009**, *44*, 1878–1883.

(90) Lambermont-Thijs, H. M. L.; Van Der Woerdt, F. S.; Baumgaertel, A.; Bonami, L.; Du Prez, F. E.; Schubert, U. S.; Hoogenboom, R. Linear Poly(ethylene Imine)s by Acidic Hydrolysis of poly(2-Oxazoline)s: Kinetic Screening, Thermal Properties, and Temperature-Induced Solubility Transitions. *Macromolecules* **2010**, *43*, 927–933.

(91) Shelton, R. S.; van Campen, M. G. VAN; Tilford, C. H.; Lang, H. C.; Nisonger, L.; Bandelin, F. J.; Rubenkoenig, H. L. Quaternary Ammonium Salts as Germicides. I. Non-Acylated Quaternary Ammonium Salts Derived from Aliphatic Amines. *J. Am. Chem. Soc.* **1946**, *68*, 753–755.

(92) Shelton, R. S.; van Campen, M. G. VAN; Tilford, C. H.; Lang, H. C.; Nisonger, L.; Bandelin, F. J.; Rubenkoenig, H. L. Quaternary Ammonium Salts as Germicides. III. Quaternary Ammonium Salts Derived from Cyclic Amines. *J. Am. Chem. Soc.* **1946**, *68*, 757–759.

(93) Hancock, R. E. W.; Sahl, H.-G. Antimicrobial and Host-Defense Peptides as New Anti-Infective Therapeutic Strategies. *Nat. Biotechnol.* **2006**, *24*, 1551–1557.

(94) Zasloff, M. Antimicrobial Peptides, Innate Immunity, and the Normally Sterile Urinary Tract. *J. Am. Soc. Nephrol.* **2007**, *18*, 2810–2816.

(95) Witte, H.; Seeliger, W. Cyclische Imidsaureester Aus Nitrilen Und Aminoalkoholen. *Liebigs Ann. Chem.* **1974**, *1974*, 996–1009.

(96) Beyth, N.; Houri-Haddad, Y.; Baraness-Hadar, L.; Yudovin-Farber, I.; Domb, A. J.; Weiss, E. I. Surface Antimicrobial Activity and Biocompatibility of Incorporated Polyethylenimine Nanoparticles. *Biomaterials* **2008**, *29*, 4157–4163.

(97) Beyth, N.; Yudovin-Farber, I.; Bahir, R.; Domb, A. J.; Weiss, E. I. Antibacterial Activity of Dental Composites Containing Quaternary Ammonium Polyethylenimine Nanoparticles against Streptococcus Mutans. *Biomaterials* **2006**, *27*, 3995–4002.

(98) Palermo, E. F.; Kuroda, K. Structural Determinants of Antimicrobial Activity in Polymers Which Mimic Host Defense Peptides. *Appl. Microbiol. Biotechnol.* **2010**, *87*, 1605–1615.

(99) Matsuzaki, K. Why and How Are Peptide-Lipid Interactions Utilized for Self-Defense? Magainins and Tachyplesins as Archetypes. *Biochim. Biophys. Acta - Biomembr.* **1999**, *1462*, 1–10.

(100) *Guidelines of the International Organization for Standardization. ISO 10993-5 Biological Evaluation of Medical Devices - Part 5: Tests for in Vitro Cytotoxicity, 3rd Edition, 2009.*

(101) Ivnitski, D.; Abdel-Hamid, I.; Atanasov, P.; Wilkins, E. Biosensors for Detection of Pathogenic Bacteria. *Biosens. Bioelectron.* **1999**, *14*, 599–624.

(102) Lippincott-Schwartz, J.; Patterson, G. H. Development and Use of Fluorescent Protein Markers in Living Cells. *Science (80-.).* **2003**, *300*, 87–91.

(103) Disney, M. D.; Zheng, J.; Swager, T. M.; Seeberger, P. H. Detection of Bacteria with Carbohydrate-Functionalized Fluorescent Polymers. *J. Am. Chem. Soc.* **2004**, *126*, 13343–13346.

(104) Mouffouk, F.; Rosa da Costa, A. M.; Martins, J.; Zourob, M.; Abu-Salah, K. M.; Alrokayan, S. A. Development of a Highly Sensitive Bacteria Detection Assay Using Fluorescent pH-Responsive Polymeric Micelles. *Biosens. Bioelectron.* **2011**, *26*, 3517–3523.

(105) Weber, C.; Becer, C. R.; Hoogenboom, R.; Schubert, U. S. Lower Critical Solution Temperature Behavior of Comb and Graft Shaped poly[oligo(2-Ethyl-2-Oxazoline)methacrylate]s. *Macromolecules* **2009**, *42*, 2965–2971.

(106) Hoogenboom, R.; Schlaad, H. Bioinspired poly(2-Oxazoline)s. *Polymers (Basel).* **2011**, *3*, 467–488.

(107) Lin, S. Y.; Wu, T.-H.; Jao, Y.-C.; Liu, C.-P.; Lin, H.-Y.; Lo, L.-W.; Yang, C.-S. Unraveling the Photoluminescence Puzzle of PAMAM Dendrimers. *Chem. - A Eur. J.* **2011**, *17*, 7158–7161.

(108) Arbeloa, T. L.; Arbeloa, F. L.; Tapia, M. J.; Arbeloa, I. L. Hydrogen-Bonding Effect on the Photophysical Properties of 7-Aminocoumarin Derivatives. *J. Phys. Chem.* **1993**, *97*, 4704–4707.

(109) Tauhardt, L.; Kempe, K.; Knop, K.; Altuntaş, E.; Jäger, M.; Schubert, S.; Fischer, D.; Schubert, U. S. Linear Polyethyleneimine: Optimized Synthesis and Characterization - on the Way to "Pharmagrade" Batches. *Macromol. Chem. Phys.* **2011**, *212*, 1918–1924.

(110) Yu, Q.; Zhang, Y.; Wang, H.; Brash, J.; Chen, H. Anti-Fouling Bioactive Surfaces. *Acta Biomater.* **2011**, *7*, 1550–1557.

(111) Pidhatika, B.; Möller, J.; Vogel, V.; Konradi, R. Nonfouling Surface Coatings Based on poly(2-Methyl-2-Oxazoline). *Chim. Int. J. Chem.* **2008**, *62*, 264–269.

(112) Percival, S. L.; Walker, J. T. Potable Water and Biofilms : A Review of the Public Health Implications. *Biofouling J. Bioadhesion Biofilm Res.* **1999**, *14*, 99–115.

(113) Kumar, C. G.; Anand, S. K. Significance of Microbial Biofilms in Food Industry: A Review. *Int. J. Food Microbiol.* **1998**, *42*, 9–27.

(114) Vladkova, T. Surface Modification Approach to Control Biofouling. In *Marine and Industrial Biofouling*; Flemming, H.-C., Murthy, P. S., Venkatesan, R., Cooksey, K., Eds.; Springer Berlin Heidelberg, 2009; pp 135–163.

(115) Dunne Jr., W. M. Bacterial Adhesion: Seen Any Good Biofilms Lately? *Clin. Microbiol. Rev.* **2002**, *15*, 155–166.

(116) Bridier, A.; Briandet, R.; Thomas, V.; Dubois-Brissonnet, F. Resistance of Bacterial Biofilms to Disinfectants : A Review. *Biofouling J. Bioadhesion Biofilm Res.* **2011**, *27*, 1017–1032.

(117) DeQueiroz, G. a.; Day, D. F. Antimicrobial Activity and Effectiveness of a Combination of Sodium Hypochlorite and Hydrogen Peroxide in Killing and Removing Pseudomonas Aeruginosa Biofilms from Surfaces. *J. Appl. Microbiol.* **2007**, *103*, 794–802.

(118) Rand, J. L.; Hofmann, R.; Alam, M. Z. B.; Chauret, C.; Cantwell, R.; Andrews, R. C.; Gagnon, G. A. A Field Study Evaluation for Mitigating Biofouling with Chlorine Dioxide or Chlorine Integrated with UV Disinfection. *Water Res.* **2007**, *41*, 1939–1948.

(119) Shen, Y.; Stojicic, S.; Qian, W.; Olsen, I.; Haapasalo, M. The Synergistic Antimicrobial Effect by Mechanical Agitation and Two Chlorhexidine Preparations on Biofilm Bacteria. *J. Endod.* **2010**, *36*, 100–104.

(120) Rivardo, F.; Martinotti, M. G.; Turner, R. J.; Ceri, H. The Activity of Silver against Escherichia Coli Biofilm Is Increased by a Lipopeptide Biosurfactant. *Can. J. Microbiol.* **2010**, *56*, 272–278.

(121) Charnley, M.; Textor, M.; Acikgoz, C. Designed Polymer Structures with Antifouling-Antimicrobial Properties. *React. Funct. Polym.* **2011**, *71*, 329–334.

(122) Gelman, M. A.; Weisblum, B.; Lynn, D. M.; Gellman, S. H. Biocidal Activity of Polystyrenes That Are Cationic by Virtue of Protonation. *Org. Lett.* **2004**, *6*, 557–560.

(123) Palermo, E. F.; Kuroda, K. Chemical Structure of Cationic Groups in Amphiphilic Polymethacrylates Modulates the Antimicrobial and Hemolytic Activities. *Biomacromolecules* **2009**, *10*, 1416–1428.

(124) Pasquier, N.; Keul, H.; Heine, E.; Moeller, M.; Angelov, B.; Linser, S.; Willumeit, R. Amphiphilic Branched Polymers as Antimicrobial Agents. *Macromol. Biosci.* **2008**, *8*, 903–915.

(125) Kenawy, E.-R.; Worley, S. D.; Broughton, R. The Chemistry and Applications of Antimicrobial Polymers: A State-of-the-Art Review. *Biomacromolecules* **2007**, *8*, 1359–1384.

(126) Rabea, E. I.; Badawy, M. E.-T.; Stevens, C. V.; Smagghe, G.; Steurbaut, W. Chitosan as Antimicrobial Agent: Applications and Mode of Action. *Biomacromolecules* **2003**, *4*, 1457–1465.

(127) Elsabee, M. Z.; Naguib, H. F.; Morsi, R. E. Chitosan Based Nanofibers, Review. *Mater. Sci. Eng. C* **2012**, *32*, 1711–1726.

(128) Dash, M.; Chiellini, F.; Ottenbrite, R. M.; Chiellini, E. Chitosan - a Versatile Semi-Synthetic Polymer in Biomedical Applications. *Prog. Polym. Sci.* **2011**, *36*, 981–1014.

(129) Agnihotri, S. A.; Mallikarjuna, N. N.; Aminabhavi, T. M. Recent Advances on Chitosan-Based Micro- and Nanoparticles in Drug Delivery. *J. Control. Release* **2004**, *100*, 5–28.

(130) Zhang, C.; Liao, L.; Gong, S. (Sarah). Recent Developments in Microwave-Assisted Polymerization with a Focus on Ring-Opening Polymerization. *Green Chem.* **2007**, *9*, 303.

(131) Madihally, S. V.; Matthew, H. W. T. Porous Chitosan Scaffolds for Tissue Engineering. *Biomaterials* **1999**, *20*, 1133–1142.

(132) Temtem, M.; Barroso, T.; Casimiro, T.; Mano, J. F.; Aguiar-Ricardo, A. Dual Stimuli Responsive poly(N-Isopropylacrylamide) Coated Chitosan Scaffolds for Controlled Release Prepared from a Non Residue Technology. *J. Supercrit. Fluids* **2012**, *66*, 398–404.

(133) Wang, X.; Chen, X.; Yoon, K.; Fang, D.; Hsiao, B. S.; Chu, B. High Flux Filtration Medium Based on Nanofibrous Substrate with Hydrophilic Nanocomposite Coating. *Environ. Sci. Technol.* **2005**, *39*, 7684–7691.

(134) Gottenbos, B.; Van Der Mei, H. C.; Busscher, H. J. Models for Studying Initial Adhesion and Surface Growth in Biofilm Formation on Surfaces. *Methods Enzymol.* **1999**, *310*, 523–534.

(135) Cabral, J. P. S. Water Microbiology. Bacterial Pathogens and Water. *Int. J. Environ. Res. Public Health* **2010**, *7*, 3657–3703.

(136) CDC. *Surveillance for Waterborne Disease Outbreaks Associated with Drinking Water and Other Nonrecreational Water — United States, 2009–2010.*; 2013; Vol. 62.

(137) *Wastewater Technology Fact Sheet - Chlorine Disinfection, EPA 832-F-99-062, Office of Water, Washington D.C.*; 1999.

(138) Flemming, H.-C. Microbial Biofoulig: Unsolved Problems, Insufficient Approaches, and Possible Solutions. In *Biofilms highlights*; Springer-Verlag Berlin Heidelberg, 2011; pp 81–110.

(139) Muszanska, A. K.; Rochford, E. T. J.; Gruszka, A.; Bastian, A. A.; Busscher, H. J.; Norde, W.; Van Der Mei, H. C.; Herrmann, A. Antiadhesive Polymer Brush Coating Functionalized with Antimicrobial and RGD Peptides to Reduce Biofilm Formation and Enhance Tissue Integration. *Biomacromolecules* **2014**, *15*, 2019–2026.

(140) Cheng, W.; Yang, C.; Ding, X.; Engler, A. C.; Hedrick, J. L.; Yang, Y. Y. Broad-Spectrum Antimicrobial/antifouling Soft Material Coatings Using Poly(ethylenimine) as a Tailorable Scaffold. *Biomacromolecules* **2015**, *16*, 1967–1977.

(141) Li, Q.; Mahendra, S.; Lyon, D. Y.; Brunet, L.; Liga, M. V.; Li, D.; Alvarez, P. J. J. Antimicrobial Nanomaterials for Water Disinfection and Microbial Control: Potential Applications and Implications. *Water Res.* **2008**, *42*, 4591–4602.

(142) Campoccia, D.; Montanaro, L.; Arciola, C. R. A Review of the Biomaterials Technologies for Infection-Resistant Surfaces. *Biomaterials* **2013**, *34*, 8533–8554.

(143) Vyhnalkova, R.; Mansur-Azzam, N.; Eisenberg, A.; van de Ven, T. G. M. Ten Million Fold Reduction of Live Bacteria by Bactericidal Filter Paper. *Adv. Funct. Mater.* **2012**, *22*, 4096–4100.

(144) Noimark, S.; Weiner, J.; Noor, N.; Allan, E.; Williams, C. K.; Shaffer, M. S. P.; Parkin, I. P. Dual-Mechanism Antimicrobial Polymer-ZnO Nanoparticle and Crystal Violet-Encapsulated Silicone. *Adv. Funct. Mater.* **2015**, *25*, 1367–1373.

(145) Faure, E.; Falentin-Daudré, C.; Lanero, T. S.; Vreuls, C.; Zocchi, G.; Van De Weerdt, C.; Martial, J.; Jérôme, C.; Duwez, A. S.; Detrembleur, C. Functional Nanogels as Platforms for Imparting Antibacterial, Antibiofilm, and Antiadhesion Activities to Stainless Steel. *Adv. Funct. Mater.* **2012**, *22*, 5271–5282.

(146) Cottenye, N.; Anselme, K.; Ploux, L.; Vebert-Nardin, C. Vesicular Structures Self-

Assembled from Oligonucleotide-Polymer Hybrids: Mechanical Prevention of Bacterial Colonization upon Their Surface Tethering through Hybridization. *Adv. Funct. Mater.* **2012**, *22*, 4891–4898.

(147) Zeng, X.; McCarthy, D. T.; Deletic, A.; Zhang, X. Silver/reduced Graphene Oxide Hydrogel as Novel Bactericidal Filter for Point-of-Use Water Disinfection. *Adv. Funct. Mater.* **2015**, *25*, 4344–4351.

(148) Muñoz-Bonilla, A.; Fernández-García, M. Polymeric Materials with Antimicrobial Activity. *Prog. Polym. Sci.* **2012**, *37*, 281–339.

(149) Muñoz-Bonilla, A.; Fernández-García, M. The Roadmap of Antimicrobial Polymeric Materials in Macromolecular Nanotechnology. *Eur. Polym. J.* **2015**, *65*, 46–62.

(150) Klibanov, A. M. Permanently Microbicidal Materials Coatings. *J. Mater. Chem.* **2007**, *17*, 2479–2482.

(151) Yang, W. J.; Neoh, K. G.; Kang, E. T.; Teo, S. L. M.; Rittschof, D. Polymer Brush Coatings for Combating Marine Biofouling. *Prog. Polym. Sci.* **2014**, *39*, 1017–1042.

(152) Roberts, M. J.; Bentley, M. D.; Harris, J. M. Chemistry for Peptide and Protein PEGylation. *Adv. Drug Deliv. Rev.* **2012**, *64*, 116–127.

(153) Xu, F. J.; Neoh, K. G.; Kang, E. T. Bioactive Surfaces and Biomaterials via Atom Transfer Radical Polymerization. *Prog. Polym. Sci.* **2009**, *34*, 719–761.

(154) Sedlacek, O.; Monnery, B. D.; Filippov, S. K.; Hoogenboom, R.; Hruby, M. Poly(2-Oxazoline)s - Are They More Advantageous for Biomedical Applications than Other Polymers? *Macromol. Rapid Commun.* **2012**, *33*, 1648–1662.

(155) Kronek, J.; Paulovičová, E.; Paulovičová, L.; Kroneková, Z.; Lustoň, J. Biocompatibility and Immunocompatibility Assessment of poly(2-Oxazolines). In *Practical Applications in Biomedical Engineering*; Andrade, A. O., Ed.; InTech, 2012.

(156) Fik, C. P.; Krumm, C.; Muennig, C.; Baur, T. I.; Salz, U.; Bock, T.; Tiller, J. C. Impact of Functional Satellite Groups on the Antimicrobial Activity and Hemocompatibility of Telechelic poly(2-Methyloxazoline)s. *Biomacromolecules* **2012**, *13*, 165–172.

(157) Krumm, C.; Harmuth, S.; Hijazi, M.; Neugebauer, B.; Kampmann, A. L.; Geltenpoth, H.; Sickmann, A.; Tiller, J. C. Antimicrobial poly(2-Methyloxazoline)s with Bioswitchable Activity through Satellite Group Modification. *Angew. Chemie - Int. Ed.* **2014**, *53*, 3830–3834.

(158) Tauhardt, L.; Kempe, K.; Gottschaldt, M.; Schubert, U. S. Poly(2-Oxazoline) Functionalized Surfaces: From Modification to Application. *Chem. Soc. Rev.* **2013**, *42*, 7998–8011.

(159) Konradi, R.; Acikgoz, C.; Textor, M. Polyoxazolines for Nonfouling Surface Coatings - a Direct Comparison to the Gold Standard PEG. *Macromol. Rapid Commun.* **2012**, *33*, 1663–1676.

(160) Fernandes, C. S. M.; Gonçalves, B.; Sousa, M.; Martins, D. L.; Barroso, T.; Pina, A. S.; Peixoto, C.; Aguiar-Ricardo, A.; Roque, A. C. Biobased Monoliths for Adenovirus Purification. *ACS Appl. Mater. Interfaces* **2015**, *7*, 6605–6612.

(161) Boufi, S.; Vilar, M. R.; Ferraria, A. M.; Botelho do Rego, A. M. In Situ Photochemical Generation of Silver and Gold Nanoparticles on Chitosan. *Colloids Surfaces A Physicochem. Eng. Asp.* **2013**, *439*, 151–158.

(162) Beamson, G.; Briggs, D. *High Resolution XPS of Organic Polymers: The Scienta ESCA300 Database*; John Wiley & Sons Ltd: Chichester, 1992.

(163) International Organization for Standardization (1999) Water Quality – Enumeration of Culturable Micro-organisms – Colony Count by Inoculation in a Nutrient Agar Culture Medium. ISO 6222:1999. Geneva, ISO.

(164) Socrates, G. *Infrared and Raman Characteristic Group Frequencies, Tables and Charts*, 3rd Ed.; John Wiley & Sons Ltd, Chichester, 2001.

(165) Kugel, A.; Stafslien, S.; Chisholm, B. J. Antimicrobial Coatings Produced by "Tethering" Biocides to the Coating Matrix: A Comprehensive Review. *Prog. Org. Coatings* **2011**, *72*, 222–252.

(166) Gettings, R. L.; White, W. C. Formation of Polymeric Antimicrobial Surfaces from Organofunctional Silanes. In *Applied Bioactive Polymeric Materials*; Springer US, 1988; pp 91–95.

(167) Zumbuehl, A.; Ferreira, L.; Kuhn, D.; Astashkina, A.; Long, L.; Yeo, Y.; Iaconis, T.; Ghannoum, M.; Fink, G. R.; Langer, R.; et al. Antifungal Hydrogels. *Proc. Natl. Acad. Sci.* **2007**, *104*, 12994–12998.

(168) Kanazawa, A.; Ikeda, T.; Endo, T. Polymeric Phosphonium Salts as a Novel Class of Cationic Biocides. III. Immobilization of Phosphonium Salts by Surface Photografting and Antibacterial Activity of the Surface-Treated Polymer Films. *J. Polym. Sci. Part A Polym. Chem.* **1993**, *31*, 1467–1472.

(169) Tiller, J. C. Antimicrobial Surfaces. In *Bioactive Surfaces*; Springer Berlin Heidelberg, 2011; pp 193–217.

(170) Guilhelmelli, F.; Vilela, N.; Albuquerque, P.; Derengowski, L. D. S.; Silva-Pereira, I.; Kyaw, C. M. Antibiotic Development Challenges: The Various Mechanisms of Action of Antimicrobial Peptides and of Bacterial Resistance. *Front. Microbiol.* **2013**, *4*, 1–12.

(171) Li, Y.; Xiang, Q.; Zhang, Q.; Huang, Y.; Su, Z. Overview on the Recent Study of Antimicrobial Peptides: Origins, Functions, Relative Mechanisms and Application. *Peptides* **2012**, *37*, 207–215.

(172) Sato, H.; Feix, J. B. Peptide-Membrane Interactions and Mechanisms of Membrane Destruction by Amphipathic α-Helical Antimicrobial Peptides. *Biochim. Biophys. Acta - Biomembr.* **2006**, *1758*, 1245–1256.

(173) Jordan, R.; Ulman, A. Surface Initiated Living Cationic Polymerization of 2-Oxazolines. *J. Am. Chem. Soc.* **1998**, *120*, 243–247.

(174) Timofeeva, L.; Kleshcheva, N. Antimicrobial Polymers: Mechanism of Action, Factors of Activity, and Applications. *Appl. Microbiol. Biotechnol.* **2011**, *89*, 475–492.

(175) Ambroggio, E. E.; Separovic, F.; Bowie, J. H.; Fidelio, G. D.; Bagatolli, L. A. Direct Visualization of Membrane Leakage Induced by the Antibiotic Peptides: Maculatin, Citropin, and Aurein. *Biophys. J.* **2005**, *89*, 1874–1881.

(176) Tsai, M.; Ohniwa, R. L.; Kato, Y.; Takeshita, S. L.; Ohta, T.; Saito, S.; Hayashi, H.; Morikawa, K. Staphylococcus Aureus Requires Cardiolipin for Survival under Conditions of High Salinity. *BMC Microbiol.* **2011**, *11*, 13–24.

(177) Mayer, L. D.; Hope, M. J.; Cullis, P. R. Vesicles of Variable Sizes Produced by a Rapid Extrusion Procedure. *Biochim. Biophys. Acta - Biomembr.* **1986**, *858*, 161–168.

(178) Bartlett, G. R. Phosphorus Assay in Column Chromatography. *J. Biol. Chem.* **1958**, *234*, 466–468.

(179) Weinstein, J. N.; Klausner, R. D.; Innerarity, Y.; Ralston, E.; Blumenthal, R. Phase Transition Release, a New Approach to the Interaction of Proteins with Lipid Vesicles. *Biochim. Biophys. Acta* **1981**, *647*, 270–284.

(180) Ambroggio, E. E.; Kim, D. H.; Separovic, F.; Barrow, C. J.; Barnham, K. J.; Bagatolli, L. a; Fidelio, G. D. Surface Behavior and Lipid Interaction of Alzheimer Beta-Amyloid Peptide 1-42: A Membrane-Disrupting Peptide. *Biophys. J.* **2005**, *88*, 2706–2713.

(181) Heintzmann, R.; Cremer, C. Laterally Modulated Excitation Microscopy: Improvement of Resolution by Using a Diffraction Grating. *Proc. SPIE* **1999**, *3568*, 185–196.

(182) Chen, R. F.; Knutson, J. R. Mechanism of Fluorescence Concentration Quenching of Carboxyfluorescein in Liposomes: Energy Transfer to Nonfluorescent Dimers. *Anal. Biochem.* **1988**, *172*, 61–77.

(183) Cornett, J. B.; Shockman, G. D. Cellular Lysis of Streptococcus Faecalis Induced with Triton X-100. *J. Bacteriol.* **1978**, *135*, 153–160.

(184) Hsu, S. Te; Breukink, E.; de Kruijff, B.; Kaptein, R.; Bonvin, A. M. J. J.; van Nuland, N. A. J. Mapping the Targeted Membrane Pore Formation Mechanism by Solution NMR: The Nisin Z and Lipid II Interaction in SDS Micelles. *Biochemistry* **2002**, *41*, 7670–7676.

(185) Jones, K. H.; Senft, J. A. An Improved Method to Determine Cell Viability by Simultaneous Staining with Fluorescein Diacetate-Propidium Iodide. *J. Histochem. Cytochem.* **1985**, *33*, 77–79.

(186) Anastas, P. T.; Warner, J. C. *Green Chemistry: Theory and Practice*; Oxford University Press: New York, 1998.

(187) Fernandes, L.; Rial-Otero, R.; Temtem, M.; Veiga de Macedo, C.; Aguiar-Ricardo, a.; Capelo, J. L. Ultrasonic Energy as a Tool in the Sample Treatment for Polymer Characterization through Matrix-Assisted Laser Desorption Ionization Time-of-Flight Mass Spectrometry. *Talanta* **2008**, *77*, 882–888.

(188) Casimiro, T.; Shariati, A.; Peters, C. J.; De Ponte, M. N.; Aguiar-Ricardo, A. Phase Behavior Studies of a Perfluoropolyether in High-Pressure Carbon Dioxide. *Fluid Phase Equilib.* **2004**, *224*, 257–261.

Supporting Information

Chapter 2 - Oxazoline-Based Antimicrobial Oligomers: Synthesis by CROP Using Supercritical CO_2

Oligomers synthetic procedure

Synthesis of *Living* Oligo(2-oxazoline)s. The polymerizations were carried out in a stainless-steel reactor equipped with two aligned sapphire windows stamped in both tops with Teflon o-rings. Four different 2-substituted oxazoline monomers were studied (MeOX, EtOx, PhOx and BisOx) and boron trifluoride etherate ($BF_3.Et_2O$) was used as the initiator. The monomer/initiator ratio used to each polymerization was, respectively: [M]/[I]=15 (MetOx), [M]/[I]=12 (EtOx), [M]/[I]=10 (PhOx) and [M]/[I]=7.5 (BisOx), according to literature.[23]

The reactor cell was charged with the monomer, the initiator, a magnetic stirring bar, and then immersed in a thermostatized bath. For polymerizations performed at 60 ºC a water bath was used, for higher temperatures an oil bath was used. Carbon dioxide was introduced in the reactor in order to achieve the desired reaction pressure (from 16 to 20 MPa). After 20 hours of reaction, the pressure was slowly released and the reactor led to reach room temperature. Inside the reactor, and depending on the adopted conditions of temperature and pressure, a viscous foam or a solid was obtained.

End-capping of *Living* Oligo(2-oxazoline)s. At the end of the polymerization the *living* oligomers were end-capped with water or tertiary amines. The functionalization was achieved by the addition of a tenfold excess of the terminating agent relatively to the initiator. The mixture was kept at 70 ºC (or 90 ºC in the case of PhOx) under stirring for 24 hours. Powder oligomers were washed with diethyl ether and dried under vacuum. Oily oligomers were purified by extraction with diethyl ether and water, and the pure oligomer recovered from the aqueous phase after drying. Since these oligomers are soluble in water the final purification step (extraction with diethyl ether) can be replaced by dialysis.

Preparation of Linear Oligo(ethylenimine) Hydrochloride. Polyoxazoline **4a** was submitted to hydrolysis in a 5M HCl aqueous solution under reflux for 9 hours.[50] After this period the polymer precipitated as the hydrochloride salt. The mixture was then filtered off, washed with acetone and dried under vacuum and **6** obtained as a white solid.

Oligomers characterization

Oligo(2-methyl-2-oxazoline) End-capped with Water (1a).

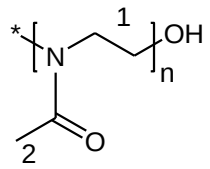

Yellow oil. Water soluble. Yield: 43 %. IR (NaCl) $\nu_{máx}$ (cm^{-1}): 3460 (OH), 1735 (NCO_2), 1634 (NCOMe). ^{1}H-NMR (400 MHz, $CDCl_3$): δ - 2.14 (bs, 3H, H-2), 3.45 (bs, 4H, H-1). ^{13}C-NMR (100 MHz, $CDCl_3$): δ - 20.54, 46.44, 104.85, 173.31. MALDI-TOF: M_n = 840 $g.mol^{-1}$.

Oligo(2-ethyl-2-oxazoline) End-capped With water (2a).

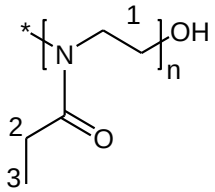

Orange oil. Water soluble. Yield: 70 %. IR (NaCl) $\nu_{máx}$ (cm^{-1}): 3418 (OH), 1738 (NCO_2), 1626 (NCOEt). ^{1}H-NMR (400 MHz, $CDCl_3$): δ - 1.08 (bs, 3H, H-3), 2.37 (bs, 2H, H-2), 3.41 (bs, 4H, H-1). ^{13}C-NMR (100 MHz, $CDCl_3$): δ - 9.40, 25.89, 44.16, 45.41, 46.46, 46.91, 174.07, 174.73. MALDI-TOF: M_n = 733 $g.mol^{-1}$.

Oligo(2-phenyl-2-oxazoline) End-capped with Water (3a).

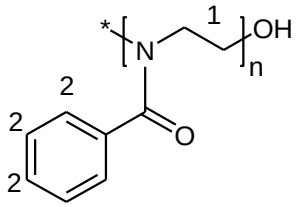

Orange oil. Yield: 99 %. IR (NaCl) $\nu_{máx}$ (cm^{-1}): 3368 (OH), 1714 (NCO_2), 1644 (NCOPh). ^{1}H-NMR (400 MHz, $CDCl_3$): δ - 3.44-3.49 (bs, 4H, H-1), 7.03-7.29 (bs, 5H, H-2). ^{13}C-NMR (100 MHz, $CDCl_3$): δ - 46.99, 126.26, 126.99, 127.83, 128.39, 128.66, 129.47, 172.28, 173.41.

Oligo(2-methyl-2-oxazoline) End-capped with *N,N*-dimethyldodecylamine (1b).

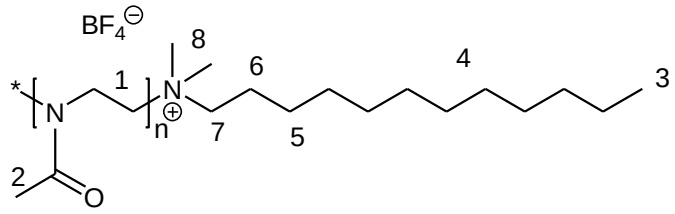

Yellow solid. Water soluble. Hygroscopic. Yield: 68 %. FTIR (KBr) $\nu_{máx}$ (cm^{-1}): 1738 (NCO_2), 1634 (NCOMe). ^{1}H-NMR (400 MHz, $CDCl_3$): δ - 0.87 (t, 3H, J= 6.3 Hz, H-3), 1.24 (bs, 16H, H-4), 1.71 (bs, 2H, H-5), 2.13 (bs, 3H, H-2), 3.01 (t, 2H, J= 8.0 Hz, H-6), 3.15 (bs, 2H, H-7), 3.44 (bs, 10H, overlapped signals, H-1 + H-8). ^{13}C-NMR (100 MHz, $CDCl_3$): δ - 14.10, 21.15, 22.65, 24.48, 26.44, 29.80, 29.35, 29.56, 31.86, 43.49, 44.95, 47.05, 47.84, 58.63, 170.88, 171.62. M_n = 1237 g.mol^{-1} (n= 12) by NMR. MALDI-TOF (after hydrolysis): M_n = 505 g.mol^{-1}.

Oligo(2-methyl-2-oxazoline) End-capped with *N*-methyldioctylamine (1c).

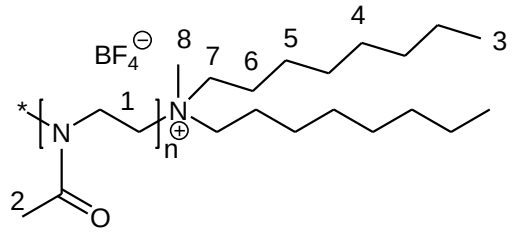

Yellow solid. Water soluble. Hygroscopic. Yield: 66 %. FTIR (KBr) $\nu_{máx}$ (cm^{-1}): 1731 (NCO_2), 1636 (NCOMe). ^{1}H-NMR (400 MHz, $(CD_3)_2SO$): δ - 0.85 (t, 6H, t, J= 6.68 Hz, H-3), 1.26 (bs, 16H, H-4), 1.54 (bs, 4H, H-5), 1.98 (bs, 3H, H-2), 2.88 (t, 4H, J= 7.6 Hz, H-6), 3.07 (s, 4H, H-7), 3.34 (bs, 7H, overlapped signals, H-1 + H-8). ^{13}C-NMR (100 MHz, $(CD_3)_2SO$): δ - 13.94, 20.84, 22.04, 23.76, 26.01, 28.46, 31.15, 42.85, 44.10, 46.01, 46.72, 55.26, 170.19. M_n = 1279 g.mol^{-1} (n= 12) by NMR. MALDI-TOF: M_n = 986 g.mol^{-1}.

Oligo(2-ethyl-2-oxazoline) End-capped with *N,N*-dimethyldodecylamine (2b).

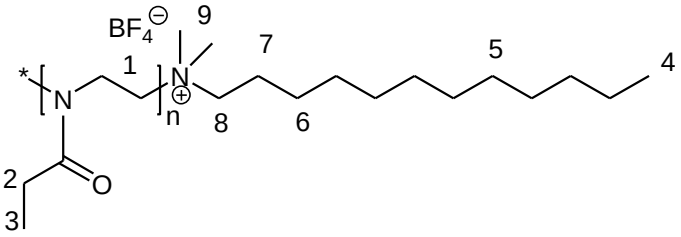

Yellow solid. Water soluble. Hygroscopic. Yield: 61 %. FTIR (KBr) $\nu_{máx}$ (cm^{-1}): 1738 (NCO_2), 1637 (NCOEt). ^{1}H-NMR (400 MHz, $CDCl_3$): δ - 0.85 (t, 3H, J= 6.6 Hz, H-4), 1.08 (bs, 3H, H-3), 1.22 (bs, 16H, H-4), 1.70 (bs, 2H, H-5), 2.27-2.38 (bs, 2H, H-6), 3.04 (t, 2H, J= 7.5 Hz, H-7), 3.14 (bs, 2H, H-8), 3.42 (bs, 10H, overlapped signals, H-1 + H-9). ^{13}C-NMR (100 MHz, $CDCl_3$): δ - 9.30, 9.42, 14.04, 22.59, 24.34, 25.87, 26.33, 27.03, 29.02, 29.29, 29.40, 29.50, 31.81, 43.45, 45.32, 45.77, 46.93, 58.59, 174.00, 174.72. M_n = 1504 g.mol^{-1} (n= 13) by NMR. MALDI-TOF: M_n = 897 g.mol^{-1}.

Oligo(2-ethyl-2-oxazoline) End-capped with *N*-methyldioctylamine (2c).

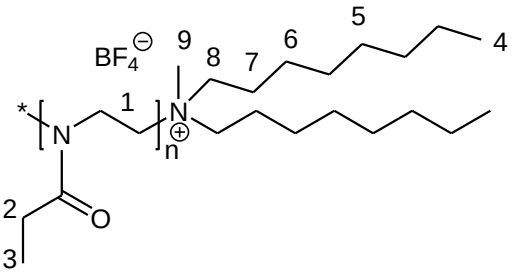

Yellow solid. Water soluble. Hygroscopic. Yield: 66 %. FTIR (KBr) $\nu_{máx}$ (cm^{-1}): 1741 (NCO_2), 1634 (NCOEt). ^{1}H-NMR (400 MHz, $(CD_3)_2SO$): δ - 0.85 (t, 6H, J= 6.68 Hz, H-4), 1.03 (bs, 3H, H-3) 1.26 (bs, 16H, H-5), 1.56 (bs, 4H, H-6), 2.30 (bs, 4H, H-2), 2.95 (t, 4H, J= 7.6 Hz, H-7), 3.07 (bs, 7H, overlapped signals, H-8 + H-9), 3.34 (bs, 4H, H-1). ^{13}C-NMR (100 MHz, $(CD_3)_2SO$): δ - 9.42, 13.94, 22.05, 23.52, 24.97, 25.96, 28.46, 31.16, 42.84, 44.45, 45.89, 55.13, 173.20. M_n = 1348 g.mol^{-1} (n= 11) by NMR. MALDI-TOF: M_n = 1237 g.mol^{-1}.

Oligo(2-ethyl-2-oxazoline) End-capped with DABCO (2d).

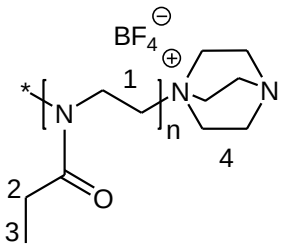

White solid. Water soluble. Yield: 79 %. FTIR (KBr) $\nu_{máx}$ (cm^{-1}): 1718 (NCO_2), 1631 (NCOEt). ^{1}H-NMR (400 MHz, $CDCl_3$): δ - 1.11 (bs, 3H, H-3), 2.29-2.41 (bs, 2H, H-2), 2.82 (s, 12H, H-4), 3.46 (bs, 4H, H-1). ^{13}C-NMR (100 MHz, $CDCl_3$): δ - 9.44, 25.91, 29.40, 29.66, 30.89, 43.65, 45.24, 46.88, 52.76, 173.93 , 174.61. M_n = 1304 g.mol^{-1} (n= 12) by NMR. MALDI-TOF: M_n = 1080 g.mol^{-1}.

Oligo(2-ethyl-2-oxazoline) End-capped with *N*-methylcyclohexylamine (2e).

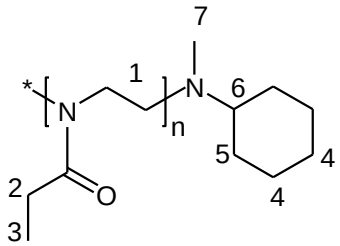

Orange oil. Water soluble. Yield: 86 %. FTIR (NaCl) $\nu_{máx}$ (cm^{-1}): 1726 (NCO_2), 1657 (NCOEt). ^{1}H-NMR (400 MHz, $CDCl_3$): δ - 0.83-1.29 (m, 6H, H-4), 1.09 (bs, 3H, H-3), 1.63-2.01 (m, 4H, H-5), 2.25-2.40 (bs, 2H, H-2), 2.58 (s, 3H, H-7), 2.70 (s, 1H, H-6), 3.43 (bs, 4H, H-1). ^{13}C-NMR (100 MHz, $CDCl_3$): δ - 9.30, 9.42, 14.04, 22.59, 24.34, 25.87, 26.33, 27.03, 29.02, 29.29, 29.40, 29.50, 31.81, 43.45, 45.32, 45.77, 46.93, 174.00, 174.72. M_n = 809 g.mol^{-1} (n= 7) by NMR.

Oligo(2-ethyl-2-oxazoline) End-capped with *N*-Methylimidazole (2f).

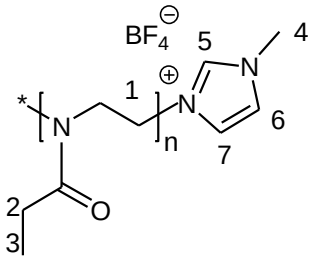

Orange oil. Water soluble. Yield: 85 %. FTIR (NaCl) $\nu_{máx}$ (cm^{-1}): 1743 (NCO_2), 1620 (NCOEt). ^{1}H-NMR (400 MHz, $CDCl_3$): δ - 1.07 (bs, 3H, H-3), 2.25-2.35 (bs, 2H, H-2), 3.41 (bs, 4H, H-1), 3.69 (s, 3H, H-4), 6.89 (bs, 1H, H-7), 7.04 (bs, 1H, H-6), 7.55 (s, 1H, H-5). ^{13}C-NMR (100 MHz, $CDCl_3$): δ - 9.37, 25.85, 33.48, 42.28, 43.71, 45.31, 120.30, 128.31, 137.54, 173.93, 174.61. M_n = 778 g.mol^{-1} (n= 7) by NMR. MALDI-TOF: M_n = 860 g.mol^{-1}.

Oligo(2-phenyl-2-oxazoline) End-capped with *N,N*-dimethyldodecylamine (3b).

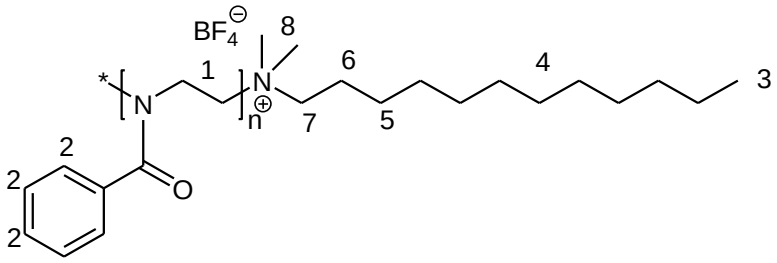

Orange solid. Yield: 99 %. FTIR (KBr) $\nu_{máx}$ (cm^{-1}): 1717 (NCO_2), 1634 (NCOPh). ^{1}H-NMR (400 MHz, $CDCl_3$): δ - 0.87 (t, 3H, J= 6.3 Hz, H-3), 1.24 (s, 16H, H-4), 1.55 (bs, 2H, H-5), 3.06 (bs, 2H, H-6), 3.10 (bs, 2H, H-7), 3.35 (bs, 10H, overlapped signals, H1 + H-8), 7.08-7.35 (bs, 5H, H-2). ^{13}C-NMR (100 MHz, $CDCl_3$): δ - 14.06, 22.63, 25.50, 26.73, 29.27, 29.39, 29.55, 31.85, 44.11, 126.29, 126.93, 128.64, 129.60, 171.74. M_n = 1097 g.mol^{-1} (n= 6) by NMR.

Oligo(2-phenyl-2-oxazoline) End-capped with *N*-methyldioctylamine (3c).

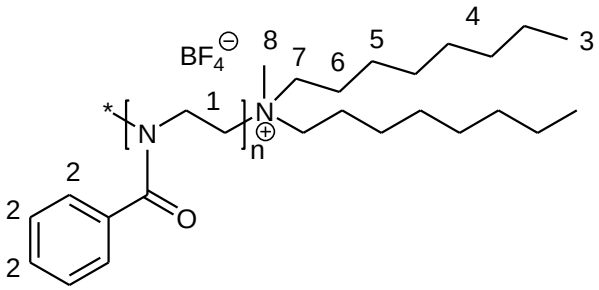

Orange solid. Yield: 88 %. FTIR (KBr) $\nu_{máx}$ (cm^{-1}): 1726 (NCO_2), 1630 (NCOPh). ^{1}H-NMR (400 MHz, $CDCl_3$): δ - 0.87 (t, 3H, J= 6.88 Hz, H-3), 1.25 (bs, 16H, H-4), 1.69 (bs, 4H, H-5), 2.99 (bs, 11H, overlapped signals, H-6 + H-7 + H-8), 2.99-3.53 (bs, 4H, H-1), 7.08-7.33 (bs, 5H, H-2). ^{13}C-NMR (100 MHz, $CDCl_3$): δ - 14.03, 22.54, 23.68, 26.39, 28.95, 31.59, 42.32, 46.25,

125.55, 126.34, 127.19, 127.85, 128.67, 129.48, 135.57, 172.13. M_n = 1287 g.mol^{-1} (n= 7) by NMR.

Oligo(2-bisoxazoline) End-capped with Water (4a).

Brown solid. Yield: 67 %. FTIR (KBr) $\nu_{máx}$ (cm^{-1}): 1737 (NCO_2), 1636 ($NCOCH_2$).

Oligo(2-bisoxazoline) End-capped with *N,N*-dimethyldodecylamine (4b).

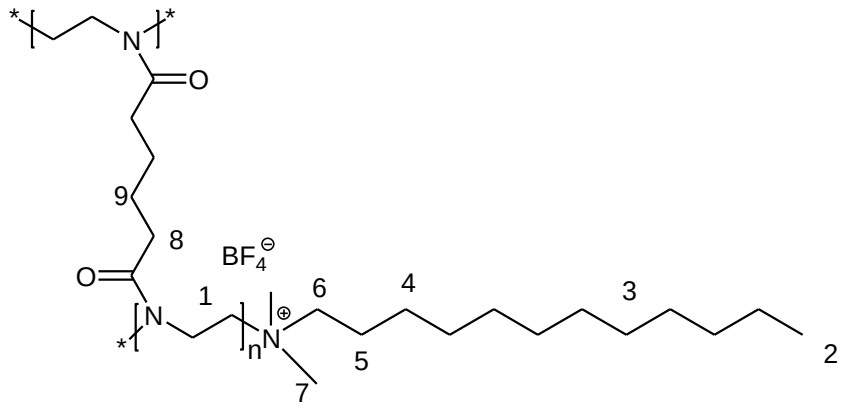

Brown solid. Water soluble. Yield: 67 %. FTIR (KBr) $\nu_{máx}$ (cm^{-1}): 1744 (NCO_2), 1652 ($NCOCH_2$). ^{1}H-NMR (400 MHz, CD_3OD): δ - 0.89 (t, 3H, J= 6.2 Hz, H-2), 1.29-1.37 (bs, 16H, H-3), 1.62 (bs, 4H, H-9), 1.70 (bs, 2H, H-4), 2.22 (bs, 4H, H-8), 3.02 (bs, 2H, H-5), 3.07-3.11 (bs, 2H, H-6), 3.26-3.30 (bs, 14H, signals overlapped with the solvent, H-1 + H-7). ^{13}C-NMR (100 MHz, CD_3OD): δ - 14.41, 17.08, 23.71, 26.63, 27.42, 30.18, 30.45, 30.47, 30.61, 30.71, 33.04, 36.66, 42.80, 42.93, 43.43, 61.60, 176.18. M_n = 812 g.mol^{-1} (n= 3) by NMR. MALDI-TOF: M_n = 459 g.mol^{-1}.

Linear Oligo(ethylenimine) Hydrochloride (5).

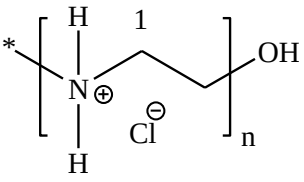

White solid. Water soluble. Yield: 74 %. FTIR (KBr) $\nu_{máx}$ (cm^{-1}): 3420 (NH). ^{1}H-NMR (400 MHz, D_2O): δ - 3.48 (s, 4H, H-1). ^{13}C-NMR (100 MHz, D_2O): δ - 43.83. MALDI-TOF: M_n = 491 $g.mol^{-1}$ (n= 11).

GPC values obtained for oligomers are not shown here due to discrepancies in the values for M_n and M_w for polymers when compared to data obtained through MALDI and NMR, techniques that tend to have better agreement.[187]

Maldi-tof spectra.

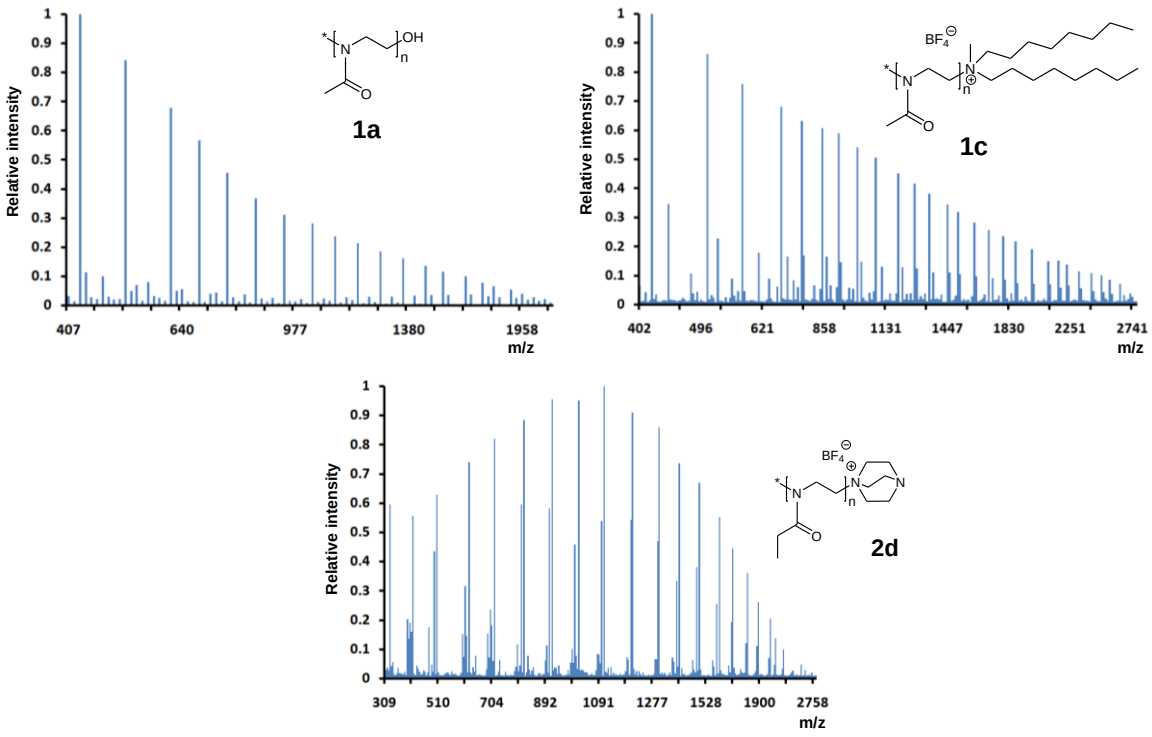

Figure S2.1 - Selected MALDI-TOF spectra of synthesized oligo(2-oxazoline)s.

Chapter 3 - Blue emission of carbamic acid oligooxazoline biotags

High-Pressure Sapphire Cylindrical Cell (HPSCC). The core of the high pressure cell is a sapphire tube with the following dimensions: height, 4.5 cm; internal diameter, 1.9 cm; external diameter, 3.2 cm. The internal diameter of the sapphire tube was chosen in order to maximize the optical path obeying the safety requirements and space available in the equipment's sample compartments. The sapphire tube is contained in a stainless steel cylindrical support where the holes for optical measurements were opened. The fluid under pressure is confined inside the sapphire tube which ends are sealed by a process identical to that developed by one of us (A.A.R.) for a similar cell used in vapor-liquid equilibrium studies.[188] It consists of a Teflon seal extruded against the sapphire tube by means of two metal pieces tightened one against the other. The cell was designed for working pressures lower than 50 MPa and temperatures under 120 ºC. The sample inside the sapphire tube can be stirred via a small Teflon coated magnetic stirring bar and magnetic stirrer near the bottom of the steel mantle. The stainless steel cover contains openings for the inlet valve, thermocouple and circulating thermostating fluid. The temperature of the cell is measured with a thermocouple T Probe, (Omega, U.S.A.) and controlled by a circulating cryostat F25-HD (Julabo Labortechnik, Seelbach, Germany) that ensures a constant water flow around the sapphire tube. Since the steel cylinder is essentially a pipe sleeve for thermostating fluid circulation, windows can be freely opened in the lateral wall as far as the axis rigidity is not compromised. Four windows were opened at right angles adequate for transmission measurements and light scattering or luminescence in 90º geometry, and closed with fused silica circular optical windows (Oriel Instruments, Stratford, U.S.A.) of 12.7 and 25.4 mm diameter and 3.2 mm thickness. The HPSCC is schematically represented in Figure S3.1 and it is also shown a photograph of the cell during an experiment showing the several connections and pipes.

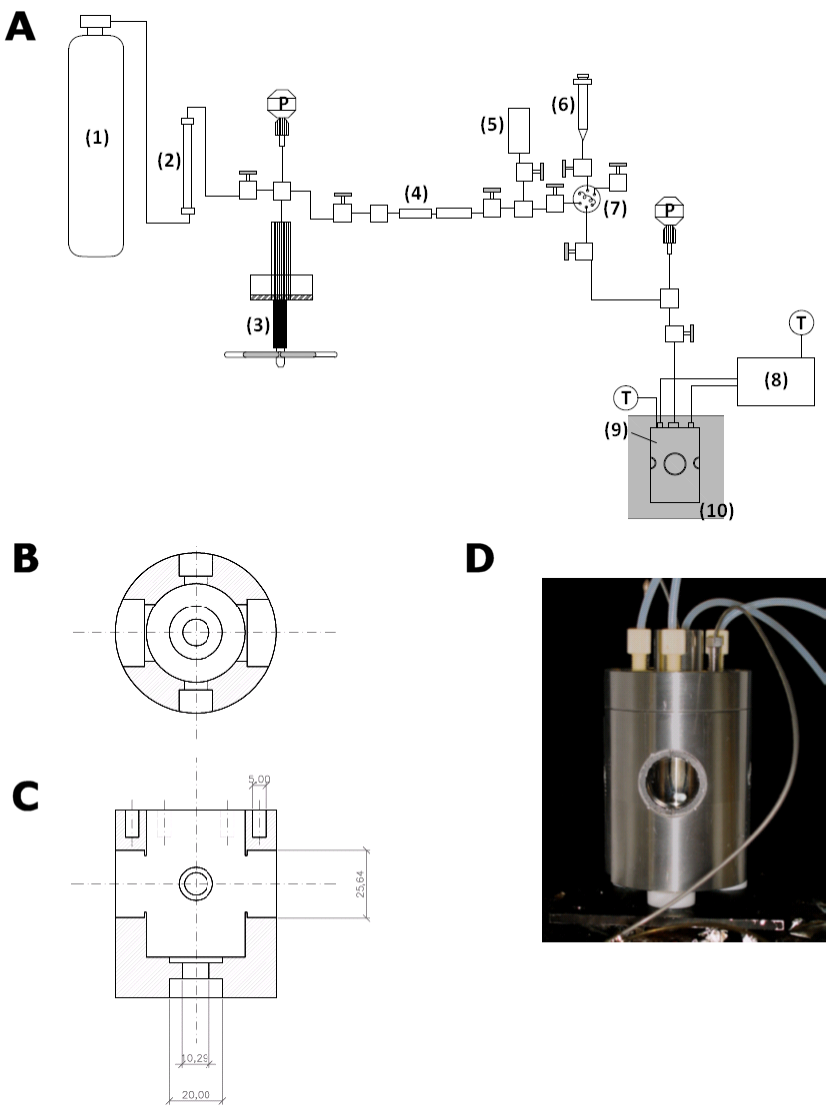

Figure S3.1 - High-pressure sapphire cylindrical cell. (A) schematic of high-pressure assembly: (1) CO_2 cylinder; (2) molecular sieves; (3) hand pump; (4) check-valve; (5) vacuum pump; (6) syringe; (7) loop; (8) thermostated bath; (9) High-pressure spectroscopic cylindrical cell; (10) sample compartment; (P) pressure sensor; (T) thermocouple. (B) Horizontal and (C) vertical cross sections of the high-pressure sapphire cylindrical cell for supercritical solutions. (D) Photo showing the cells and the connected pipes.

Chapter 5 - Antimicrobial contact-active oligo(2-oxazoline)s-grafted surfaces for fast water disinfection at the point-of-use

Scaffolds characterization. Scaffolds surface elemental composition was analyzed by X-ray photoelectron spectroscopy (XPS) technique. Firstly, the efficiency of 2-isopropenyl-2-oxazoline grafting was studied after different times of CHT surface plasma activation: 10, 20 and 30 min. Figure S5.1 shows the XPS regions N 1s and C 1s before and after activation. Table S5.1 shows the binding energies, atomic concentrations (in brackets), atomic ratios and assignments.[162]

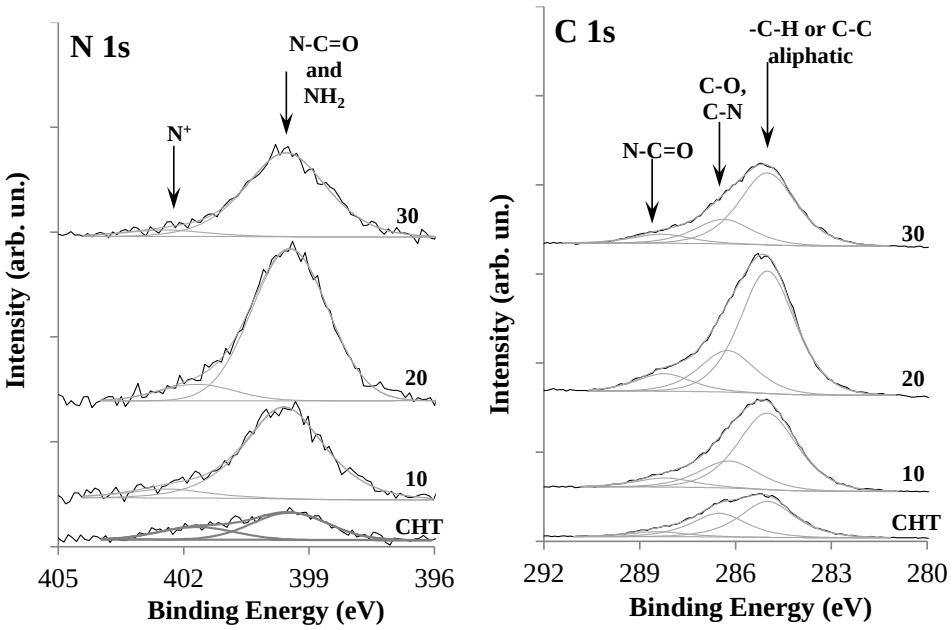

Figure S5.1 - N 1s and C 1s XPS regions of CHT before and after activation for 10, 20 and 30 minutes.

XPS N 1s regions shown in Figure S2 were composed by two peaks centred at 399.6 ± 0.1 eV (N1) and 402.0± 0.4 eV (N2). In CHT native scaffold, N1 was attributed to NH2 and N-C=O (of acetylated groups (75–85 % deacetylated) and N2 to protonated nitrogen, respectively. After interaction of chitosan with IsoOx, the N1/N2 atomic ratios increased from ~2 to ~11 for all the activation times and also N/O increases (Table S1), showing that the activation was successful. The C 1s peak assigned to N-C=O, existing in both the chitosan and in the oxazoline but in larger density in the latter one, also increased upon CHT activation, in particular, after 20 minutes of

interaction. The C 1s peak attributed to C-O and C-N (centred around 286.3 eV) decreased, while the aliphatic carbon peak increased, after 10 minutes of activation, but they both remained nearly constant with time. This is compatible with a reaction between oxazoline and chitosan C-OH and C-NH2 groups. In CHT it is expected that the peak corresponding to C-OH and C-NH2 dominates the C 1s region.

Table S5.1. BE (eV), [At. Conc.] (%), atomic ratios and assignments.[162]

	CHT	CHT + IsoOx			
Time (min)		10	20	30	
C 1s	285.0 [37.1]	285.0 [47.7]	285.0 [47.4]	285.0 [47.0]	sp^3
	286.5 [24.4]	286.2 [16.9]	286.3 [16.0]	286.4 [16.0]	C-N and C-O
	288.4 [5.1]	288.2 [5.6]	288.2 [6.8]	288.3 [5.9]	N-C=O
O 1s	530.2 [3.4]	531.5 [11.2]	531.4 [11.5]	531.2 [7.9]	C=O
	532.6 [25.0]	532.6 [10.3]	532.6 [10.2]	532.5 [15.2]	C-O
N 1s	399.5 [3.4]	399.6 [7.5]	399.5 [7.4]	399.5 [7.4]	N-C=O, NH_2
	401.7 [1.6]	402.4 [0.7]	401.7 [0.8]	402.4 [0.6]	N^+
N1/N2	2.2	10.3	9.2	13.0	
N/O	0.18	0.39	0.38	0.34	
C3/N1	1.5	0.7	0.9	0.8	
O/C	0.43	0.31	0.31	0.34	
N/C	0.08	0.12	0.12	0.12	

Purification of contaminated water from environmental samples. Reduction of microbiological viability can be influenced by several parameters as pH, hardness and dissolved salts as well as the variety of bacterial species present in the water samples. The physico-chemical characterization of collected waters was performed in order to assess the main differences between both samples.

Table S5.2. Physico-chemical characterization of collected waters.

Parameter	Well	Dam	Method
pH (22-25 ºC)	6.72	7.91	SMEWW 4500 H^+
Conductivity (µS/cm)	512	27.6	NP EN 27888:1996
Turbidity (NTU)	0.3	14	ISO 7027:1999
Total alkalinity (mg($CaCO_3$)/L)	91.8	27.6	SMEWW 2320
Hardness (mg($CaCO_3$)/L)	131	50	SMEWW 2340 B
Calcium (mg/L)	21	7.8	EPA 300.7:1986
Magnesium (mg/L)	19	7.4	EPA 300.7:1986
Total organic carbon (mg C/L)	1.3	3.5	SMEWW 5310 C